# OILFIELD SCALE MANAGEMENT BASED ON PRODUCED WATER COMPOSITION

The Thesis by

**ROBERTO MOTTA GOMES**

Submitted for the Degree of

**Master of Science in Petroleum Engineering**


Institute of Petroleum Engineering
Heriot-Watt University
Edinburgh, Scotland, UK

**April 2016**

## ABSTRACT

Evaluation of the scaling risk at production wells is generally carried out using thermodynamic prediction models. These models are generally very accurate in terms of predicting the type of scale that may form, the degree of supersaturation, and the mass of scale that will deposit when the system reaches equilibrium – provided the brine composition or compositions involved are well known, and the pressure and temperatures conditions are accurately specified. However, in performing these calculations, engineers often fail to take account of reactions occurring in the reservoir, and assume that brines reaching the production wells have not reacted in any way prior to entering the wellbore. This often leads to a significant overestimate of the scaling risk.

This work seeks to address this issue by studying field data from a variety of sources to identify what can be learnt from the produced brine compositions, and by simulating various possible scenarios using reservoir simulation calculations, and taking account of potential reservoir reactions, but also considering other factors, such as reservoir properties and architecture, fluid properties, etc., that may impact the composition of the brine by the time it reaches the production wells.

This work also provides the basic information regarding commercial reservoir simulators with a focus on reservoir scale management. Black-oil, semi-compositional and fully compositional simulators will be analysed with this purpose.

Finally, this work will present a scale management strategy based upon the use of an integrated approach, that considers both flow and thermodynamical properties of the reservoir, aided by numerical simulations. This approach can lead to a more realistic forecast of scaling potential, leading to the development of optimized scale management strategies.

## ACKNOWLEDGEMENTS

Firstly, I would like to express my sincere gratitude to my advisor Prof. Eric Mackay for the continuous support of my MSc study and related research, for his patience, motivation, and immense knowledge. His guidance helped me in all the time of research and writing of this thesis. I could not have imagined having a better advisor and mentor for my MSc study.

I am also indebted to the members of the FAST group, with whom I have interacted during the course of my MSc studies. Particularly, I would like to acknowledge Prof. Ken Sorbie, Ivan Davis, Jammal Ibrahim, Cyril Okocha, Nazia Farooqui, Debbie Ross, and Oleg Ishkov for the many valuable discussions.

Besides, I would like to thank my colleagues from PETROBRAS specially: Ricardo Huntemann, Rogério Favinha, Fábio Prais and Walter Becker for their insightful comments and encouragement, but also for the hard question which incented me to widen my research from various perspectives.

My sincere thanks also goes to Mrs. Ena Mackay, who provided me a great support during my research and also assisted me to review all the material. She was a very important person that helped me to adapt to the culture and way of life of beautiful Edinburgh.

Most importantly, none of this would have been possible without the love and patience of my family. My immediate family to whom this dissertation is dedicated to, has been a constant source of love, concern, support and strength all these years. I would like to express my heart-felt gratitude to my family.

HERIOT WATT UNIVERSITY

ACADEMIC REGISTRY
**Research Thesis Submission**

| | | | |
|---|---|---|---|
| Name: | Roberto Motta Gomes | | |
| School: | Institute of Petroleum Engineering | | |
| Version: *(i.e. First, Resubmission, Final)* | Final | Degree Sought: | MSc in Petroleum Engineering |

## Declaration

In accordance with the appropriate regulations I hereby submit my thesis and I declare that:

1) the thesis embodies the results of my own work and has been composed by myself
2) where appropriate, I have made acknowledgement of the work of others and have made reference to work carried out in collaboration with other persons
3) the thesis is the correct version of the thesis for submission and is the same version as any electronic versions submitted*.
4) my thesis for the award referred to, deposited in the Heriot-Watt University Library, should be made available for loan or photocopying and be available via the Institutional Repository, subject to such conditions as the Librarian may require
5) I understand that as a student of the University I am required to abide by the Regulations of the University and to conform to its discipline.
6) I confirm that the thesis has been verified against plagiarism via an approved plagiarism detection application e.g. Turnitin.

* *Please note that it is the responsibility of the candidate to ensure that the correct version of the thesis is submitted.*

| | | | |
|---|---|---|---|
| Signature of Candidate: |  | Date: | 24/11/2016 |

## Submission

| | |
|---|---|
| Submitted By *(name in capitals)*: | |
| Signature of Individual Submitting: | |
| Date Submitted: | |

## For Completion in the Student Service Centre (SSC)

| | | | |
|---|---|---|---|
| Received in the SSC by *(name in capitals)*: | | | |
| *Method of Submission* *(Handed in to SSC; posted through internal/external mail)*: | | | |
| *E-thesis Submitted* ***(mandatory for final theses)*** | | | |
| Signature: | | Date: | |

**Please note this form should be bound into the submitted thesis.**

# TABLE OF CONTENTS

# LIST OF TABLES

# LIST OF FIGURES

# NOMENCLATURE AND ABBREVIATIONS

## Abbreviations

| | |
|---|---|
| ESP's | Electric Submersible Pumps |
| FW | Formation Water |
| G | Gas |
| I1 | Injector Well 1 |
| IW | Injection Water |
| MIC | Minimum Inhibitor Concentration |
| P | Pressure |
| P1 | Producer Well 1 |
| PDG | Permanent Downhole Gauge |
| PI | Production Index |
| PW | Produced Water |
| PWRI | Production Water Re-Injection |
| O | Oil |
| SEM | Scanning Electron Microscope |
| SI | Saturation Index |
| Sor | Saturation Oil Residual |
| SR | Saturation Ratio |
| SRWI | Subsea raw water injection |
| Swi | Initial water saturation |
| T | Temperature |
| TST | Transition State Theory |
| TPT | Temperature and Pressure Transmitters |
| W | Water |

## Greek letters

| | |
|---|---|
| $\gamma_i$ | Activity Coefficient |
| Φ | Fugacity coefficient or porosity |
| α | Stoichiometry Coefficients |
| $\mu_o$ | Oil viscosity |
| $\mu_w$ | Water viscosity |

## Latin letters

| | |
|---|---|
| *A* | Reactive Surface Area of Mineral |
| *Ai* | *Mineral Reactive Surface Area* |
| $a_i$ | Activity of Species *i* |
| *åi* | Ion Size parameter of Species *i* |
| *Ḃ* | Debye–Hückel parameter |
| $C_i$ | Concentration ion |
| $[C]$ | Pseudo component concentration |
| $[C_{Produced}]$ | Pseudo component concentration in the produced brine |
| $[C_{Formation}]$ | Pseudo component concentration in the formation brine |
| $[C_{seawater}]$ | Pseudo component concentration in the seawater |
| dx | Cell length in x direction |
| dy | Cell length in y direction |
| dz | Cell length in z direction |
| $E_{ak}$ | Reaction Activation Energy |
| *H* | Henry'sconstant |
| Hr | Enthalpy |
| *I* | Ionic strength of the solution |
| $K_{eq}$ | Chemical Equilibrium Term |

| | |
|---|---|
| $k_i$ | Constant rate of mineral i |
| $K_{ps}$ | Solubility Product |
| Kro | Oil relative permeability |
| Krw | Water relative permeability |
| *m* | Molality |
| *m** | Total molality |
| $N_i$ | Mole number of mineral $_i$ |
| no | Corey coefficient oil |
| nw | Corey coefficient water |
| $P_g$ | Gas phase pressure |
| *Q* | Ionic Activity Product |
| *R* | Universal gas constant |
| *r* | Dissolution/precipitation rate for mineral |
| rk | Pre-exponential Factor |
| SI | Saturation Index |
| $S_k$ | stoichiometric coefficients |
| SR | Saturation Ratio |
| $y_i$ | Molar fractio of component $_i$ |
| *zi* | Ionic charge of species *i* |

# CHAPTER 1: INTRODUCTION

This chapter introduces the problem of scale occurrence in oilfields by presenting a brief historical review, basic concepts involving salt precipitation as well as the main parameters affecting scale deposition. After the introduction, the aims and objectives of the thesis are listed and a brief outline of the thesis is given.

## 1.1 HISTORY OF OCCURRENCE, PREDICTION AND PREVENTION OF OILFIELD SCALES

Human beings have had contact with aquifers and formation water since the beginnings of civilization. Where surface water supplies have been insufficient, this resource has been vital for human survival and expansion, and as a result some cities have developed in proximity to subsurface aquifers. Research related to water supply, including wells in use for cities, can be found throughout the literature. An instance of this would be London in 1869 [1] and 1889 [2].

Since the 1910s the presence of water in hydrocarbon reservoirs has been reported; chemical analysis of this water has shown considerable differences between formation water and seawater compositions [3]. In the literature there is research reported on water injection in hydrocarbon reservoirs in order to improve production and the recovery factor, since as early as the 1920s [4,5]. In the 1930s [6] the existence of water in oil reservoirs was widely accepted. The occurrence of inorganic scale in oilfields has been reported since the 1950s [7,8,9].

An important landmark related to the occurrence of scale was the beginning of offshore production. By 1897 the first offshore well started to produce off the coast of California, and after this twenty two other companies drilled over 400 wells in this area (Figure 1). The introduction of offshore fields encouraged the injection of seawater, due to its abundance in this environment. Sea water is often incompatible with the formation brine and consequently it increases the scaling tendency in oilfields, and may lead to damage in oil production wells.

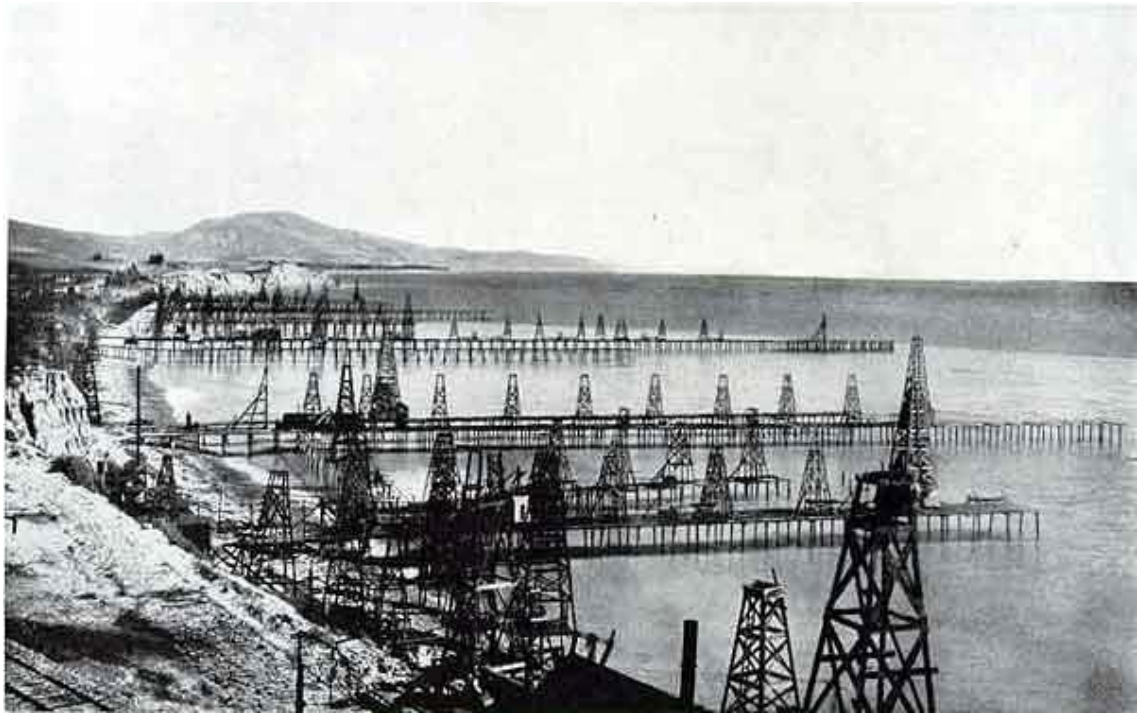

**Figure 1 - Wells off the California coast [10].**

Nowadays, around 60% of worldwide oil production comes from offshore fields [11]. Some important areas are the North Sea, the Campos Basin, the Gulf of Mexico and the West African coast.

Although the scale problem in the oil industry is a relatively new issue, man has been dealing with scale for a long time. In the 18$^{th}$ century scale was observed to grow in boilers. By this time, the first use of chemicals (inhibitors) to prevent mineral crystallization had been reported, when it was found that potato starch reduces the rate of scale accumulation [12].

Thus, since it was first observed that mineral scale started to impact well productivity, the scale phenomenon has been studied by the oil industry. In 1956, squeeze inhibitor operations were introduced as a form of protecting wells against the occurrence of scale [13]. By the 1960s [14], squeeze inhibitors had been successfully applied in hydrocarbon wells in order to prevent scale deposition. This methodology consists of injecting an inhibitor near the wellbore rock formation, and inducing it to adhere onto the rock grains (either through adsorption or precipitation). During subsequent oil and

water production, the inhibitor will return into the production water (desorption or dissolution from the rock). In this way the well will be protected for as long as the returning inhibitor concentration is above the Minimum Inhibitor Concentration (MIC). The MIC is the lowest concentration of inhibitor that can effectively inhibit the scale growth.

In squeeze treatments, the intention is to retain the maximum amount of inhibitor in the formation itself either by (i) Adsorption of the inhibitor on the rock substrate by a physicochemical process or (ii) Precipitation (or phase separation) of the inhibitor in a controlled manner, away from the near wellbore area. This is generally achieved by adjusting the solution chemistry ($[Ca^{2+}]$, pH, temperature, etc). Reactions that govern the inhibitor adsorption and release are very complicated. Several factors, such as pH, $[Ca^{2+}]$,$[Mg^{2+}]$, temperature, rock mineralogy, etc, affect the adsorption level and the shape of the adsorption isotherm [15,16].

Other options for controlling scale include the use of physical treatment methods. Surface material influences the rate of scale formation and is related to the surface free energy. The lower the surface energy, the lower the scale adhesion on the material will be. Thus, there is research carried out in order to develop materials that reduce scale adhesion in the oil industry.

Physical methods, especially magnetic treatments, have been studied and have been available for the past few decades as an alternative to chemical methods in some circumstances. Some authors [17-20] claim that the magnetic field modifies particle sizes, crystallinity, morphology, and consequently the nucleation. Interesting publications, such as by Farshad et al. [21], have shown the great potential of this technique. However, the precise mechanisms are not well understood, and there is inadequate evidence to suggest that it is effective for systems with large volume throughputs, such as wells flowing thousands of barrels of water per day.

More recently, in the 1980s, other technologies have been applied in order to avoid scale. The search for an alternative solution resulted in the development of sulphate-removal technology. This patented technology [22] uses modified reverse-osmosis

membranes to remove sulphate ions from the seawater before injection in the reservoir. This option can be very efficient in the prevention of sulphate scales, but it carries high CAPEX and moderate OPEX costs, due to the system footprint, and the need for frequent membrane replacements.

### 1.1.1 Worldwide produced water rates

According to Khatib and Verbeek [23], in 1999, 210 MM bbl of water was produced worldwide on a daily basis. This value is three times greater than the worldwide daily oil production rate, and the subsequent tendency has been for water production to increase year on year due to the use of injection water for oil recovery.

By 2007, in the United States alone, an annual 21 billion barrels of water were produced in hydrocarbon fields [24]. This represents approximately 60 million barrels per day. The total average of water-to-oil rate was 5.3 bbl/bbl and the water-to-gas ratio was 182 bbl/MMscf.

## 1.2 SCALE FORMATION BACKGROUND

Scale deposits can be of organic or inorganic origin and both of them can lead to significant production impairment. Organic scales are formed from crude oil compounds and their precipitation can be triggered by changes in temperature and pressure, causing the deposition of compounds such as asphaltenes and paraffins. Inorganic scales are mainly deposited from aqueous supersaturated solutions of oilfield waters and are the focus of this research.

Mineral scale accumulation in production wells and surface equipment is one of the main sources of increase in operational costs and production decline. Saline scale results from changes in the physicochemical properties (pH, temperature, pressure etc.) of the produced fluids and/or of the chemical incompatibility between injection and formation water. Nevertheless, the prediction of such phenomena remains a challenge, mainly due to the complexity of the precipitation kinetics.

The main types of scale deposited in oilfiels are: calcium carbonate ($CaCO_3$), calcium sulphate ($CaSO_4$), bairum sulphate ($BaSO_4$), barium carbonate ($BaCO_3$), strontium sulphate ($SrSO_4$), Siderite ($FeCO_3$), Sulphide scales (FeS, $FeS_2$, $Fe_3S_4$) and sodium chloride (NaCl).

According to Mackay et al. [25], there are three principal mechanisms by which scale is formed in an oilfield system:

1 - Decrease in pressure and/or increase in temperature of a brine, leading to reduction in the solubility of the salt. The typical case is the reaction involving the equilibrium of calcium and bicarbonate ions, carbon dioxide gas and calcium carbonate (equation 1):

$$Ca^{2+} + 2HCO_3^- \leftrightarrow CaCO_3 + CO_2 + H_2O \quad (1)$$

Figure 2 shows a pipe full of calcium carbonate scale and a scanning electron microscope (SEM) image of calcium carbonate crystals.

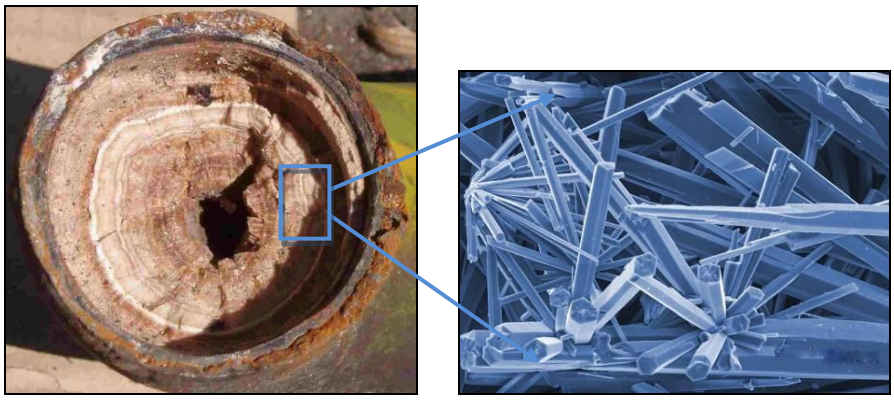

**Figure 2 - Calcium Carbonate scale and image of the crystals [26,27]**

2 - Mixing of incompatible brines, usually seawater and formation water. As already mentioned, often the formation brine is rich in some cations such as barium, strontium, and calcium; brines with these characteristics, when mixed with seawater that it is rich in sulphate, lead to the precipitation of sulphate scales (equations 2 to 4).

$$Ba^{2+} + SO_4^{2-} \leftrightarrow BaSO_4 \quad (2)$$

$$Sr^{2+} + SO_4^{2-} \leftrightarrow SrSO_4 \quad (3)$$

$$Ca^{2+} + SO_4^{2-} \leftrightarrow CaSO_4 \quad (4)$$

$$\underline{Formation\ brine + seawater \leftrightarrow precipitation}$$

Besides reactions represented with equations 2 to 4, other second order reactions, such as barium ion exchange in clay rich sandstones or sulphate adsorption in carbonate reservoirs are not considered at this work.

Figure 3 shows a scanning electron microscope (SEM) image of barium sulphate scale.

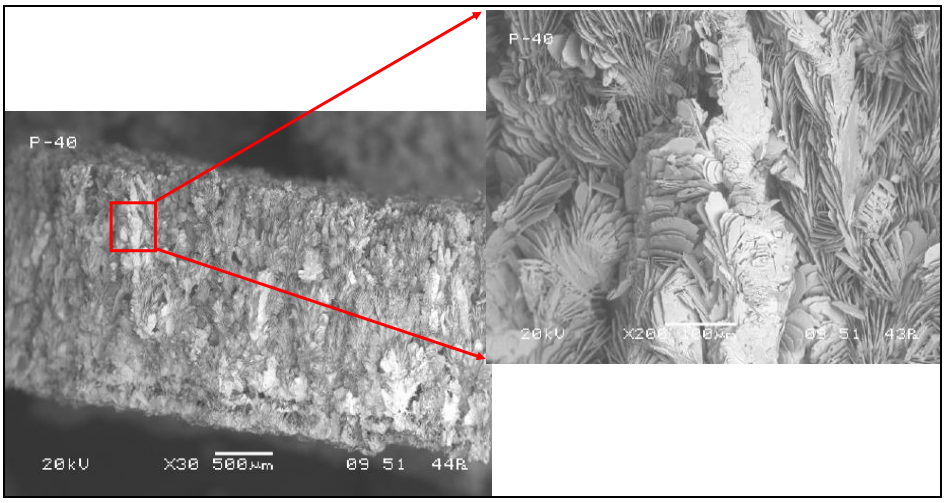


**Figure 3 - Barium sulphate scale in the scanning electron microscope (SEM) [28].**

3 - Brine evaporation, resulting in the salt concentration increasing above the solubility limit and leading to salt precipitation. The most commonly observed evaporated salt is sodium chloride precipitation (Equation 5).

$$NaCl_{(aq)} \leftrightarrow NaCl_{(s)} \quad (5)$$

However, Puntervold [29] points out that in some reservoir systems, where seawater is injected continuously, other reactions may be important for a satisfactory understanding of the scale phenomenon, such as equations 6 to 12:

Reactions linked to chalk dissolution:

$$CaCO_{3(s)} \leftrightarrow Ca^{2+} + CO_3^{2-} \quad (6)$$

$$Ca_3^{2-} + H_2O \leftrightarrow HCO_3^- + OH^- \quad (7)$$

$$HCO_3^- + H^+ \leftrightarrow H_2CO_3 \quad (8)$$

$$H_2CO_3 \leftrightarrow CO_{2(aq)} + H_2O \quad (9)$$

$$H_2O \leftrightarrow H^+ + OH^- \quad (10)$$

Substitution reactions:

$$CaCO_{3(s)} + Mg^{2+} \leftrightarrow MgCO_{3(S)} + Ca^{2+} \quad (11)$$

$$2CaCO_{3(s)} + Mg^{2+} \leftrightarrow CaMg(CO_3)_{2(s)} + Ca^{2+} \quad (12)$$

According to Collins [30], inorganic scale can occur in different parts of the oilfield production system, such as: reservoir, near wellbore region, tubing and surface facilities. Figure 4 exemplifies the places where scale can form in an oilfield. In this scenario there is seawater injection, subsea raw water injection (SRWI), production water re-injection (PWRI), aquifer water, and mixing at the manifold.

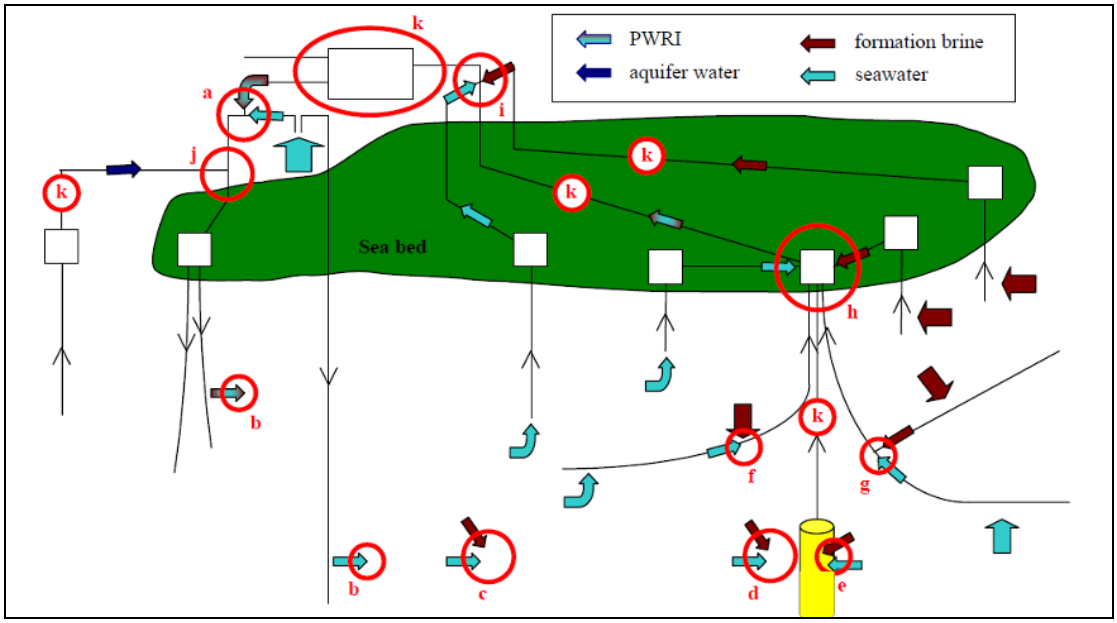


**Figure 4 - Locations throughout the flow system where scale deposition may take place, Collins *et al.*, 2006 [30].**

Where (a) to (k) refers to locations at scale may take place [30,48]:

(a) prior to injection, for example if seawater injection is supplemented by produced water re-injection(PWRI);
(b) around the injection well, as injected brine enters the reservoir, contacting formation brine;
(c) deep in the formation, caused by displacement of formation brine by injected brine, or converging flow paths;
(d) as injection brine and formation brine converge towards the production well, but beyond the radius of a squeeze treatment;
(e) as injection brine and formation brine converge towards the production well, and within the radius of a squeeze treatment;
(f) in the completed interval of a production well, as one brine enters the completion, while another brine is flowing up the tubing from a lower section;
(g) at the junction of a multilateral well, where one branch is producing one brine and the other branch is producing another brine;
(h) at a subsea manifold, where one well is producing one brine and another well is producing another brine;
(i) at the surface facilities, where one production stream is flowing one brine and another production stream is flowing another brine;
(j) where aquifer water produced to surface is mixed with produced or seawater prior to re-injection;
(k) anywhere where there is pressure decline that would lead to precipitation of pH sesntive scales, such as calcium carbonate.

### 1.2.1 Theoretical aspects of scale precipitation

A fundamental concept on the scale precipitation is the solubility, which is the capacity of a liquid (in this case, water) to keep a salt in solution, without precipitation. For the precipitation to occur, the salt concentration must be higher than the salt solubility. When this happens, it is said that the solution is supersaturated. The supersaturation represents the amount of salt present in excess of the solubility and thus represents the amount available for precipitation from solution until the solution reaches equilibrium. The solubility of a salt is not constant and varies with temperature, pH, pressure, etc.

A very important concept for analyzing the scale phenomenon is to understand saturation index (SI). The saturation index is defined as the logarithm of the saturation ratio (SR) – Equation 15. The saturation ratio of a given salt is the ratio between its constituents (ions) activity product and its solubility product $K_{ps}$. The precipitation potential of a salt can be determined by the SI, which depends on temperature, pressure, pH, and brine composition.

For a salt with ions ***i and j*** (SR) is defined by equation 13. The activity of species *i* ($a_i$) can be evaluated by equation 14, where ($\gamma_i$) is the activity coefficient and ($m_i$) is the concentration. For low salinity water $\gamma_i$ is close to one (ideal solution), and decreases with increasing salinity or charge of the ion in solution. So, for all real (non-ideal) aqueous electrolyte solutions, $\gamma_i$ is a function of temperature, pressure and ionic strength, and can be estimated by appropriate models [76, 77, 79].

$$SR = \frac{a_i \cdot a_j}{K_{ps}} \tag{13}$$

$$a_i = \gamma_i \cdot m_i \tag{14}$$

$$SI = \log(SR) = \log\left(\frac{a_i \cdot a_j}{K_{ps}}\right) \tag{15}$$

According to the saturation index of a solution, there are three direct possibilities (Table 1).

**Table 1 - Consequence of different SI of a solution**

| SR | SI | Solution | Condition of precipitation |
|---|---|---|---|
| $a_i \cdot a_j < K_{ps}$ | $SI < 0$ | Undersaturated | Dissolution if mineral present |
| $a_i \cdot a_j = K_{ps}$ | $SI = 0$ | Equilibrium | No reaction |
| $a_i \cdot a_j > K_{ps}$ | $SI > 0$ | Supersaturated | May precipitate |

Depending on the values of SR or SI, one can predict the severity and rate of the precipitation. A high value of SR, which implies that ion concentrations are much higher than the solubility, leads to an instantaneous precipitation at the point of mixing of waters. For intermediate values of SR, the crystal can undergo nucleation and precipitation, but it is less severe than the first case. Finally, small values of SR result in a slower nucleation process, reducing the speed of precipitation which is strongly influenced by changes in thermodynamic properties occurring along the tubing, for example.

There are some computer based prediction packages commercially available that can predict the supersaturation and the amount of precipitation likely to occur under specific conditions. Four examples are Multiscale® [31], ScaleUp [32], ScaleChem [74] and ScaleSoftPitzer [75]. These models are an important tool in the prediction of scale in oilfields and they are widely used. Nevertheless, there is not yet a complete tool that integrates all the oilfield system (reservoir, near wellbore area and tubing). These packages are based on thermodynamic scale model that calculates the solubilities of salts at equilibrium conditions, and uses these solubilities to calculate the scale potential for given brine compositions.

Dyer [40] has conducted some experiments with a dynamic tube blocking rig for different brines, pressures and temperatures. These experiments have shown that the effect of temperature on the scaling tendency was generally greater than the effect of pressure. Other authors obtained similar results with calcium sulphate [41,42].

Onyenezide [43] used Multscale [31] to simulate different brines for different pressures and temperatures. Figure 5 shows that the barium sulphate saturation ratio (SR) decreases as temperature increases and the SR increases as barium concentration increases. Figure 6 illustrates that the calcium sulphate SR increases as temperature increases as well as that SR increases with the calcium concentration. Figure 7 shows that strontium sulphate (celestite – $SrSO_4$) has a similar behaviour to calcium sulphate, although with less intensity.

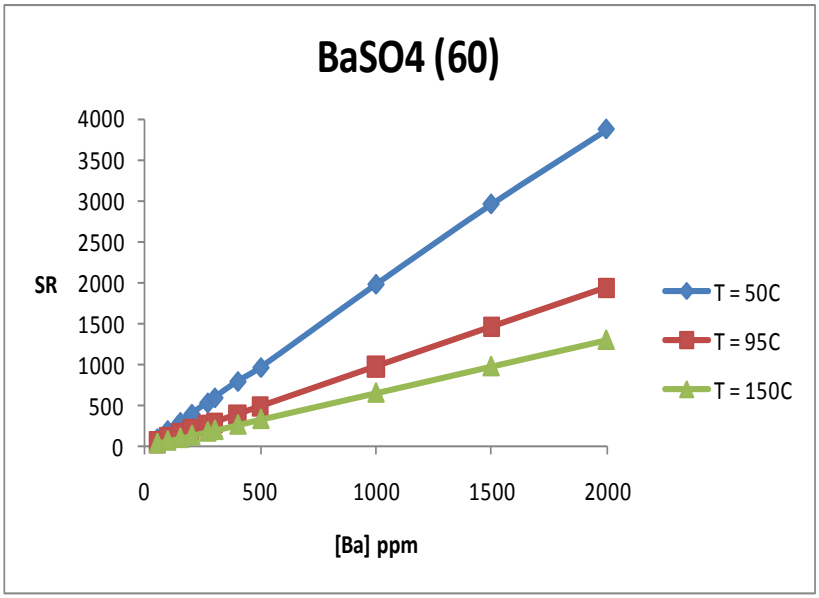


**Figure 5 - The saturation ratio of $BaSO_4$ versus barium concentration at temperatures 50, 95 and 150°C [43]**

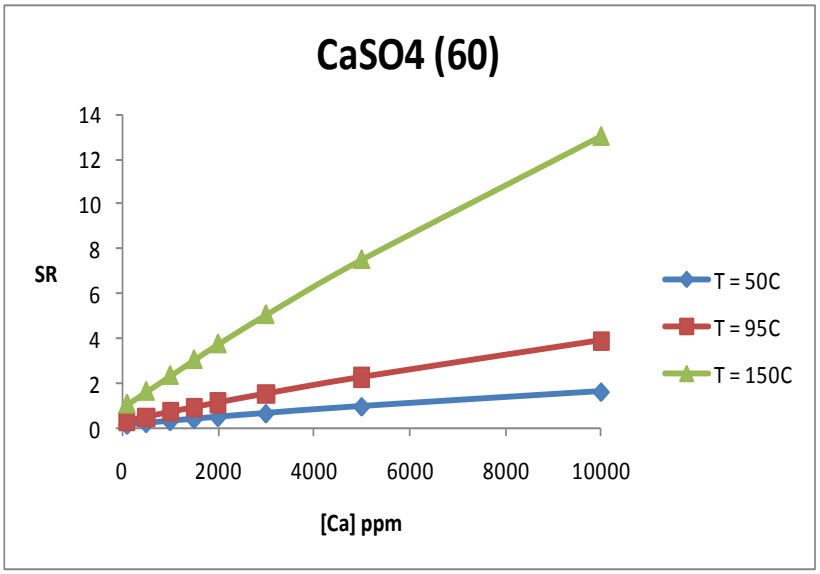


**Figure 6 - The saturation ratio of $CaSO_4$ versus calcium concentration at temperatures 50, 95 and 150°C [43]**

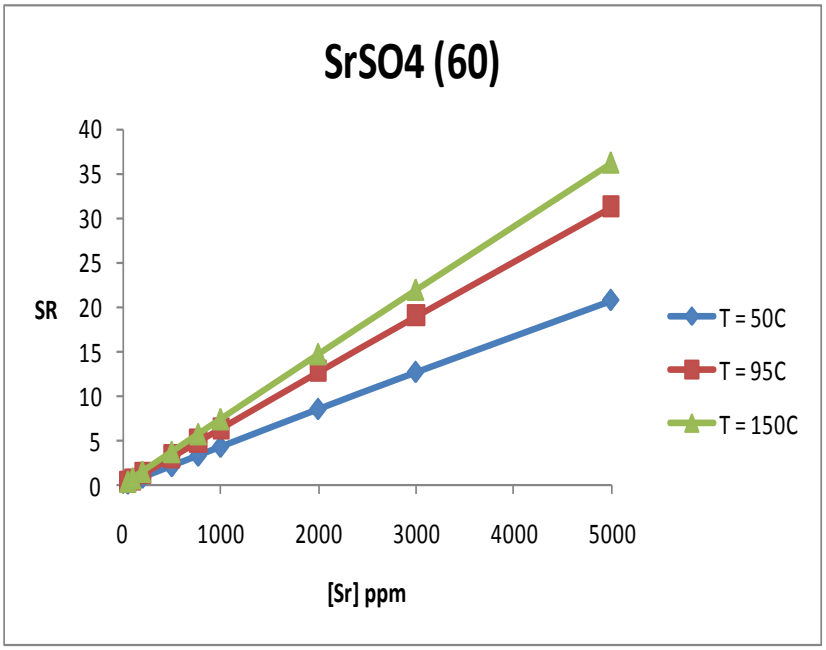


**Figure 7 - The saturation ratio of $SrSO_4$ versus strontium concentration at temperatures 50, 95 and 150°C [43]**

Based on these three figures from the Onyenezide [43] study, it is interesting to note that the temperature has a much greater impact on $CaSO_4$ than on $BaSO_4$ or $SrSO_4$. At a higher temperature (150ºC) the SR of $CaSO_4$ may be ten times bigger than for a low temperature (50ºC). As outlined above, possible mineral reaction in high temperature reservoirs undergoing seawater injection may result in the formation of calcium

sulphate scale. Temperature is a critical parameter in the precipitation of calcium sulphate.

The major cause of $BaSO_4$ or $SrSO_4$ scaling is the chemical incompatibility between the injected water, with high concentration of sulphate ion and formation waters, with high concentration of barium and strontium ions. In that case, the injected water fraction in the produced brine mix is an important parameter that determines the severity of this type of scale formations.

The percentage of seawater breakthrough can be calculated with equation 19, using conservative ions as chlorine and sodium, which are expected not to react with any ion in the formation or injection brines (except possibly by some ion exchange reactions).

A linear combination of the ions participating in reactions (mainly Ba, Sr and $SO_4$) can be used for calculating seawater percentage, according to the Reaction Ions Method [61]. The equations 16 to 20 explain the procedure. All the calculations below are in molar units.

$$[C] = [SO_4] - [Ba] - [Sr] \tag{16}$$

$$Seawater\,(\%) = \frac{[C_{Produced}] - [C_{Formation}]}{[C_{seawater}] - [C_{Formation}]} \tag{17}$$

$$[C_{Produced}] = [SO_4]_{produced} - [Ba]_{produced} - [Sr]_{produced} \tag{18}$$

$$[C_{Formation}] = [SO_4]_{Formation} - [Ba]_{Formation} - [Sr]_{Formation} \tag{19}$$

$$[C_{seawater}] = [SO_4]_{seawater} - [Ba]_{seawater} - [Sr]_{seawater} \tag{20}$$

Considering only two reactions among barium, strontium and sulphate, equation 18 defines a combination of ions for which its molar conservation equation has the reaction terms cancelled. In that case, this pseudo ion is assumed to be conservative.

### 1.2.2Chemical reaction rates

Chemical kinetics is the study of rates of chemical processes. It is related to the speed at which a chemical reaction occurs and it is fundamental for understanding how much precipitation may take place in a transient environment, such as near the wellbore. Numerous mathematical models have been developed on the basis of experiments. In 1864, Peter Waage and Cato Guldberg [44] pioneered the development of chemical kinetics by formulating the law of mass action, which states that the speed of a chemical reaction is proportional to the concentration of the reacting substances. Thus, if the reaction follows the law of mass action, its rate can be represented by the product of each of its reactants concentration raised to a power equal to their stoichiometric coefficients (elementary rate law). Other more complex reaction rate models can be used that do not obey the elementary rate law.

There are several factors that can influence the rate of a chemical reaction, such as the physical state of the reactants, the concentrations of the reactants, the temperature at which the reaction occurs, whether or not any catalysts are present in the reaction, etc. In general, a factor that increases the number of collisions between particles will increase the reaction rate and a factor that decreases the number of collisions between particles will decrease the chemical reaction rate.

The chemical reaction rate between incompatible brines (injected and formation waters) is an important parameter that determines the oilfield scaling intensity. This parameter is affected by flow velocity, diffusion/dispersion in porous media, SR, chemical rate constants, etc.

The reaction rate for barium sulphate growth has been studied for years and numerous mathematical equations have been proposed. (Table 2 is taken from SPE 81127 – Bedrikovetsky [45].)

**Table 2 - Review of BaSO4 crystal growth rate [45].**

| Reference | Equation | Comments |
|---|---|---|
| Nielsen, 1959 | $q = 630\, c_{Ba}^{\ 4}$ (mμ/s)<br>$K_a = 6.1 \cdot 10^{17} \frac{mol}{cm^2\, s}\left(\frac{cm^3}{mol}\right)^4$ | Equimolar mixture.<br>The rate is determined by a surface adsorption. |
| Nancollas and Liu, 1975 | $q = K_a A_s \left(c_{Ba} - c_{Ba}^{eq}\right)^2$<br>$K_a A_s : 150 - 1480\,(M\,min)^{-1}$<br>$A_s : 0.138 - 0.430\,(m^2\,L^{-1})$ | Equimolar mixture.<br>Precipitation is induced by solid seeds. |
| Gardner and Nancollas, 1983 | $q = K_a A_s \left(c_{Ba} - c_{Ba}^{eq}\right)^2$<br>$K_a(105^oC) = 6.33\ 10^4\ L^2 mol^{-1} min^{-1} m^{-2}$ | Provides the seed concentration instead of reaction area. |
| Goulding, 1987 | $q = K_a A_s \left(\frac{c_{Ba}}{c_{Ba}^{eq}} - 1\right)^2$ $K_a A_s \sim 1.6\ 10^5\ (M\,s)^{-1}$ | Affirms almost instantaneous heterogeneous nucleation in a reservoir environment. |
| Steefel and Cappellen, 1990 | $q = K_a A_s \left(\left(\frac{a_{Ba} a_{SO_4}}{K_{sp}}\right)^m - 1\right)^n$ m,n > 0 | Lists the value for m and n for some minerals. |
| Wat, Sorbie, *et al.*, 1992 | $q = K_a (c_{Ba} - c_{Ba}^{eq})^2\, K_a = 1.26 \cdot 10^2 (Mmin)^{-1}$ | Equimolar mixture. |
| Christy and Putnis, 1992 | $q = (162 \pm 65) A_s (c_{Ba} - c_{Ba}^{eq})^2$ | Equimolar mixture. The higher the concentrations, the higher the chemical reaction order. |
| Stumm, 1992 | $q = K_a \left(\left(\frac{a_{Ba} a_{SO_4}}{K_{sp}}\right)^{\frac{1}{2}} - 1\right)^2$ | General equation for the rate is presented, the commonly used exponent value is two. |
| Bethke, 1996 | $q = A_S K_a \left(\frac{a_{Ba} a_{SO_4}}{K_{sp}}\right)$ | Simplified general equation ignoring either inhibition or catalysis. |
| Aoun *et al.*, 1998 | $q = (2.5 \pm 0.5) 10^{-7} \left(\sqrt{c_{Ba} c_{SO_4}} - \sqrt{K_{sp}}\right)^{2.1 \pm 0.1}$ | Equimolar mixture.<br>Simultaneous measurements of nucleation and crystal growth. |
| Araque-Martinez and Lake, 1999 | $q = K_a A_s \left(a_{Ba} a_{SO_4} - K_{sp}\right)$ | Different areas for dissolution and precipitation are considered. |
| Azaroual *et al.*, 2001 | $q = K_a A_s \left(\frac{a_{Ba} a_{SO_4}}{\alpha K_{sp}} - 1\right)$, α – crit. sat. coef.<br>$K_a : 10^{-11}(600m) - 10^{-10}(3700m) \frac{mol}{s kg_{H_2O}}$ | The area coefficient $A_s$ is the total area multiplied by its reactive fraction. |
| Rocha *et al.*, 2001 | $q = 5.3 \cdot 10^{-6} \exp\left(0.011 \left(\frac{a_{Ba} a_{SO_4}}{K_{sp}} - 1\right)\right)$ | The precipitation area $A_s$ was obtained by experimental data adjustment, and is included in the rate expression. |

### 1.2.3 Diffusion and Dispersion

There are two important concepts that are intrinsically associated with precipitation deep in the reservoir because of the influence of dispersion and diffusion on miscible-displacement processes. Diffusion occurs when two miscible fluids of different concentrations are brought into contact. Initially there will be an area of separation between them. Over time, the initial surface separation between the fluids will turn into a mixing zone. In the absence of a porous medium, this phenomenon is called molecular diffusion, and in the presence of a porous medium, it is called apparent diffusion. In the diffusion mechanism the movement (convection) of fluids is not considered.

In the case of fluid flow in porous media, there will be another mechanism of mixing occurring due to a velocity gradient that forms between the various flow paths, the result of heterogeneities of the porous medium. This process is called dispersion. In other words, dispersion is the mixing of fluids caused by diffusion, local velocity gradients, locally heterogeneous streamline lengths, and mechanical mixing [47]. Several variables affect the dispersion [46], such as: edge effect in packed tubes, particle size distribution, particle shape, packing or permeability heterogeneities, viscosity ratios, gravity forces, degree of turbulence, and effect of immobile phase.

The greater the levels of dispersion and diffusion, the larger will be the mixing zone deep within the reservoir. There are studies [49, 50, 51, 52] that discusses the mixing zone in theoretical and fields examples in order to evaluate where the scale can form.

In the mixing zone deep in the reservoir, flow speeds will be low and the system will have time to reach thermodynamic equilibrium [53]. Thus, if one can estimate accurately the mixing zone in a specific reservoir, by use of a precise thermodynamic prediction model it would be possible to estimate the resulting brine composition in the near-wellbore region, and consequently the real scale potential at this point. However, as fluids approach the wellbore, the rate of convection is much higher, and equilibrium may not be achieved. In addition, increased turbulence in the near-wellbore zone would

increase reaction rates [53]. In addition, if significant evaporation of water occurs in the hydrocarbon gas phase, the scale potential may increase markedly.

### 1.2.4 Reservoir Effects

Most formations containing hydrocarbon accumulations have been deposited with water occupying the interstitial spaces (pores). Gradually, physical and geochemical processes will transform the rock strata. The co-deposited water, which may have been fresh, terrestrial water, brackish estuarine water or seawater, will also gradually transform. The transformation of the co-deposited water will be driven by pressure and temperature changes, which alter the equilibrium state of the water/rock system. In addition, water movement from different layers and subsequent water/rock interaction are also significant. During this long process it is expected that the brine in the reservoir will be in equilibrium with the rock strata. Besides that, the mineralogy of formation strata can usually give an indication of the saturation state of formation water [33].

On the other hand, the composition of the injected water – which may be out of equilibrium with the reservoir rock substrates and connate brine – may cause mineral dissolution and/or precipitation, ion exchange or other clay/fluid and fluid/fluid interactions to occur. Thus, a waterflood can alter the reservoir geochemistry. The chemistry of the formation rock/fluid interactions is complex and involves numerous chemical species and reactions paths. Transport of reactive species through permeable media further complicates the situation. The interactions cannot be easily evaluated by simple stoichiometric relationships [34].

The composition of seawater generally has a much higher Mg/Ca ratio than occurs for formation brines. This larger difference stimulates the interaction between calcium and magnesium. Thus, when the seawater is injected, the equilibrium between the rock and fluid is disturbed. If the Mg/Ca ratio for seawater is much greater than the Mg/Ca ratio in the formation brine, the system tends to re-equilibrate the Mg/Ca ratio. Therefore, an ion exchange mechanism causes magnesium to be retained from the brine phase within the rock, and in return, calcium is released from the rock into the brine phase equation (11. This behaviour has been observed in many field examples [28,35]. Korsnes et al.

[36] also verified experimentally that some substitution of $Ca^{2+}$ by $Mg^{2+}$ took place in chalk when seawater was flooded through a chalk core at 90 ºC.

Dolomitisation is defined as the process by which the calcium within the calcium carbonate is partially substituted by magnesium to give calcium, magnesium carbonate (dolomite) mineral. This is an important mechanism in certain oilfields (carbonate reservoirs) because this reaction generates reservoir porosity [37]. There is also a discussion regarding whether dolomitisation (equation 12) can happen in the production time scale. Nevertheless, some authors [38] use this phenomenon to explain the resulting brine composition produced in some fields. Water chemistry data suggest that by the time of breakthrough seawater composition has in fact been enriched in calcium and bicarbonate but become depleted in magnesium, sulphate and potassium.

The calcium magnesium exchange may stimulate the calcium sulphate reaction ($CaSO_4$) because it increases the calcium concentration in the brine composition. As a result, the brine tends to be more highly saturated. Another fundamental factor for the calcium sulphate reaction deep in the reservoir (equation 4) is the temperature. Puntervold et al. [39] shows that the total amount of scale and the SR increase as a function of the temperature for different mix between seawater and Ekofisk formation brine (Figure 8 - ). A usual software package, based on thermodynamic equilibrium conditions using published experimental data, was used for the simulations.

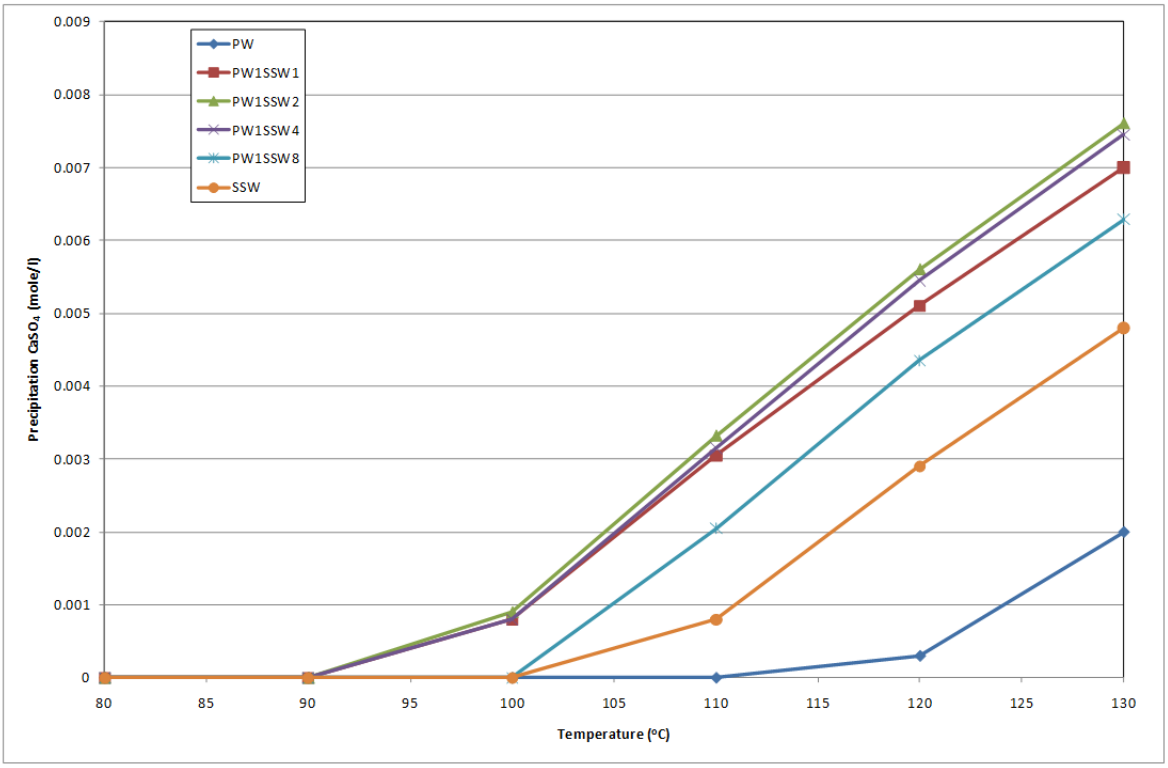


**Figure 8 - Precipitation of CaSO4 vs. temperature for mixtures of seawater and PW from Ekofisk field – Ekofisk formation, T. Puntervold et al. 2008 [39].**

Although the flow speeds deep in the reservoir are low and the brine has time enough to reach chemical equilibrium, the deposition inside the reservoir does not block the flow or cause a significant reduction in the permeability/porosity due to incompatible brines for several reasons: first, the mixing zone is always in movement along the flow path. Secondly, some experiments have shown, for instance, that in a core test in which one pore volume of formation brine ($[Ba^{2+}]$ = 240 ppm) is displaced by seawater ($[SO_4^{2-}]$ = 2,860 ppm) there was no measurable loss of permeability, even though approximately 27% of the barium ions were precipitated, based on material balance calculations [31].

In terms of stoichiometry, even in an aquifer or in a core completely saturated with a brine ($[Ba^{2+}]$ = 1000ppm) the maximum average reduction in the pore may be 0.17%, even if all the barium precipitated with sulphate from another source, such as seawater. This is strong evidence why no reduction of permeability is observed deep in the

reservoir, but damage effects are concentrated in the near-wellbore area, where there is a much higher volume throughput. Although a significant reduction in pore volume/permeability is not observed deep in the reservoir, the produced brine composition may be completely changed as a direct result of the mixing of waters.

Some authors [54] also estimate the reduction in permeability due to calcium sulphate scales. However, these analyses refer much more to the near-wellbore area than to the reservoir, because they are based on experiments that inject some pore volumes of a scaling brine in a core. Thus, it is a very good study for estimating damage in the well, where there are multiple volume throughputs, for calcium sulphate precipitation and corroborates all the studies shown here.

Although there are some papers showing evidence that scale can precipitate deep in the reservoir, most of the studies for assessing the severity of the phenomenon in the wells use calculations that do not take into account the effects occurring deep inside the reservoir. In these calculations, a direct mix of previously unreacted brines is usually considered, and most of the reservoir data is not utilized (only temperature and pressure). To the present day, there has been little work carried out to identify the location of scale formation within the reservoir [55].

Based on laboratory tests, Bedrikovetsky [45] points out that the position of the centre of the chemical reaction zone for reagents goes forward to the centre of the mixture zone. It is also shown that the reaction rate is a linear function of velocity in a core (porous medium) and the diffusion increases as a function of flow velocity.

The reaction rate is inversely proportional to the solubility product, which may be determined by a thermodynamic model based on empirical data. The reaction rate is also a function of the activation energy and the surface area of the mineral phase. However, these latter parameters are often unknown, but it may be assumed for most reservoir reactions that at sufficient distance from the wells the advection rate is low relative to the chemical reaction rate, such that the reaction effectively reaches equilibrium within the residence time of the brines. All the reactions are in principle reversible; however, in practice the solubility of minerals such as $BaSO_4$ are sufficiently

low that dissolution is unlikely to occur, particularly during water flooding with typical sulphate concentrations encountered in seawater and barium concentrations encountered in formation waters, and thus, in practice a scaling reaction such as for $BaSO_4$ may be considered to be irreversible.

Although reactions in the reservoir generally reduce the scaling tendency or the supersaturation in the produced brine, care should be taken with this. The highest scaling potential can occur at low seawater fractions or at high seawater fractions, and not necessarily as is conventionally assumed, when seawater accounts for around 50-60% of the mixture [34]. In addition, inhibitor squeezes may be required at different stages of production.

Understanding what happens deep inside the reservoir and the effects in the produced brine can influence significantly major investment decisions and the associated risk assessment process. Reservoir stripping can significantly reduce the scaling potential in the wells. As a result, the "real" MIC (minimum inhibitor concentration) values may be much lower than those calculated based on the thermodynamic prediction model evaluation, when the effect of ion depletion due to reactions deep within the reservoir is ignored [56].

In this context, knowledge of brine chemistry is not enough to calculate the real scale tendency in the near-wellbore area. Thus, a more integrated approach using reservoir data is also required [57]. The use of reservoir models has been extended to include the actual scaling reaction [54,58]. Hence, one can estimate not only the location where the brines mix as they progress through the reservoir, but also the impact on brine composition of precipitation of scale deep in the reservoir. The important information is not the loss of permeability due to scale deposition, as previously mentioned, but the removal of scaling ions from the flowing brines [55].

Analyzing the produced brine from different fields can produce an extensive and extremely useful dataset yielding information on water chemistry variations in time and space.

In order to optimize the economic value of the field, the scale control planning effort should be developed during the project stage [55]. However, during this stage, the knowledge of the reservoir is usually incipient because of the small amount of data usually available at this stage. As a consequence, the reservoir models tend to be much more homogeneous than is borne out by reality. Thus, if one uses this model directly in order to evaluate the field scale potential, the result can have a high degree of uncertainty associated with them. Thus, this begs the question how to address the scale problem in this situation?

## 1.3 MOTIVATION

Thermodynamic prediction models have been regularly used to assess scale potential in oilfields. However, other important information has been neglected, or at least has not been used appropriately (only subjectively) for an estimation of scaling tendency. As presented before, the reservoir may play an essential role in the scale process. It is not difficult to find two different fields with a similar scaling tendency (based on thermodynamic curves), but in one significant scale damage occurred, while in the other it failed to happen. The problem is exacerbated by the fact that in some cases wells from the same reservoir display a tendency to scale up, while at the same time others did not. As a result, the impact of processes occurring within the reservoir should not be neglected.

It is the case that oftentimes reactions in the reservoir are not considered, probably because it they are difficult to measure, and the finite difference models require an enormous number of cells in order to avoid numerical dispersion effects in the mix of waters *in situ*. The reservoir model may have many other uncertainties, which makes forecasting scale a complex issue.

## 1.4 RESEARCH OBJECTIVES

It has been established previously that reactions occur during flow and mixing in the reservoir, but this work extends the range of examples and shows that this behaviour has been largely neglected in scale prediction calculations used to design field scale management strategies. This work also shows that the chemical reactions deep inside

reservoir have considerable influence on potential of scale precipitation at the producer wells. Furthermore, it aims to be applicable to real field cases, thus different produced brines from several oilfields located worldwide were analyzed, aiming to establish the main factors affecting the scale potential. The establishment of such factors can be useful for scale management during project definition and scale prevention of an oilfield.

In addition to that, largely used reservoir simulation softwares will be evaluated in order to verify the results and the advantages and disadvantages of each one in terms of simulation of scaling.

## 1.5 ORGANIZATION OF THE DISSERTATION

**Chapter 1** is this introductory chapter which presents a brief overview of scale occurrence history and the introduction of basic concepts of inorganic scale precipitation in petroleum reservoirs. In addition, Chapter 1 presents the motivations and objectives of this study.

**Chapter 2** presents the analysis of field data from various oilfields, focusing on produced water composition and the informations that it provides regarding the chemical reactions occurring inside the reservoir.

**Chapter 3** presents the evaluation of reservoir simulators on the perspective of scale management. The positive and negative aspects of each simulator are discussed as well as examples of application.

**Chapter 4** introduces an alternative approach for scale management strategy. The main difference between the proposed strategy and the strategy traditionally employed is the attempt to incorporate the effect of geochemical reactions occurring inside the reservoir to evaluate scale diagnosis as well as in the scale prevention strategies.

**Chapter 5** presents the conclusions of the thesis and recommendations for further work.

# CHAPTER 2: RESERVOIR DATA

## 2.1 INTRODUCTION

This chapter contains the evaluation of the scaling behaviour of several reservoirs by means of a detailed study of the produced brine compositions. Some of the data presented are from the literature while others were generously conceded by partners of the FAST research group. In this chapter, all figures are given at reservoir conditions.

## 2.2 RESERVOIR A

This reservoir consists of high porosity (approximately 30%), high permeability, and unconsolidated sandstones. The oil density is 24º API, and the connate water saturation is around 30%. The reservoir temperature is around 78ºC and the original pressure is approximately 305 kgf/cm$^2$. Pressure support in Reservoir A is provided by water injection and the lifting method used is continuous gas-lift. The water injected is standard seawater. The formation water composition is given in Table 3. This reservoir also has an aquifer.

**Table 3 – Representative Water Reservoir A**

| Water | $Na^+$ (mg/L) | $K^+$ (mg/L) | $Mg^{2+}$ (mg/L) | $Ca^{2+}$ (mg/L) | $Sr^{2+}$ (mg/L) | $Ba^{2+}$ (mg/L) | $Cl^-$ (mg/L) | $SO_4^{2-}$ (mg/L) | Salinity (mg/L) |
|---|---|---|---|---|---|---|---|---|---|
| Reservoir A | 23600 | 141 | 338 | 1160 | 222 | 108 | 41200 | 3-4 | 67980 |

This reservoir is designed with wet completions, satellite and horizontal/vertical wells, with openhole gravel packs for sand control. All of the wells are equipped with temperature and pressure transmitters (TPT) located at the wellhead, and permanent downhole gauges (PDG) located near the completions. This equipment allows the reservoir team to monitor real-time changes in pressure, and consequently the evolution of the productive index of the wells with time. Figure 9 shows the saturation ratio values and Figure 10 the maximum predicted mass of barium sulphate for the brine in Table 3 as a function of the seawater fraction in the brine. The data used in these figures

were generated using the Multiscale® simulator [31]. Multiscale is a thermodynamic scale model that calculates the solubilities of salts at equilibrium conditions, and uses these solubilities to calculate the scale potential for given brine compositions. The Pitzer ion interaction model is used for the aqueous phase. Multiscale does not calculate any kinetic reaction rates [80]. The maximum mass precipitated is equal to mass of precipitate determined by the limiting reactant (lower molal concentration) minus the mass that will remain in solution at equilibrium conditions.

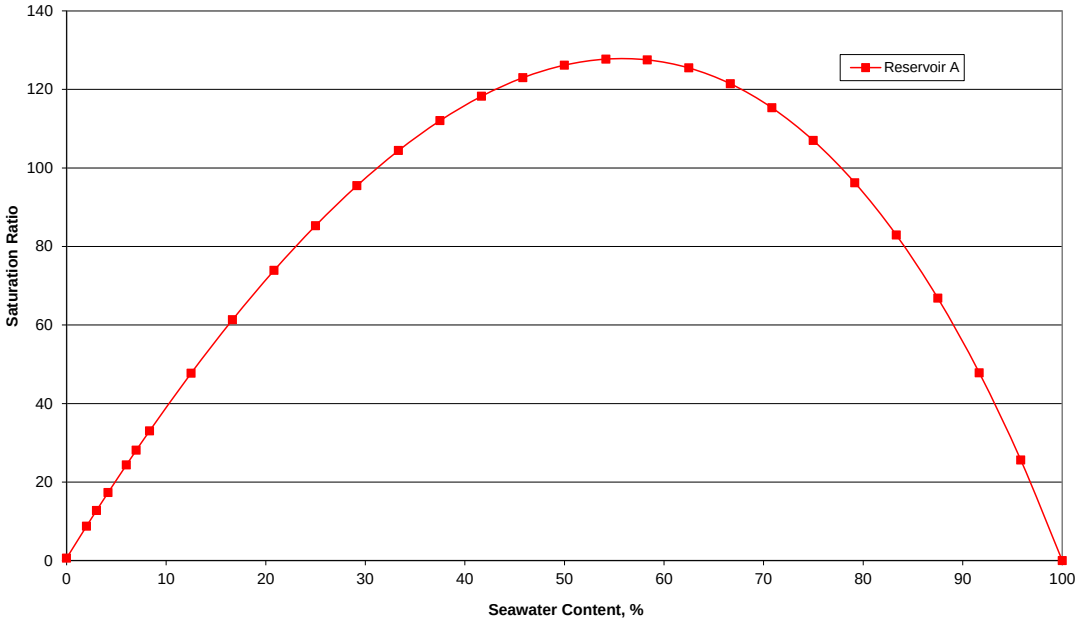


**Figure 9 - Saturation ratio values**

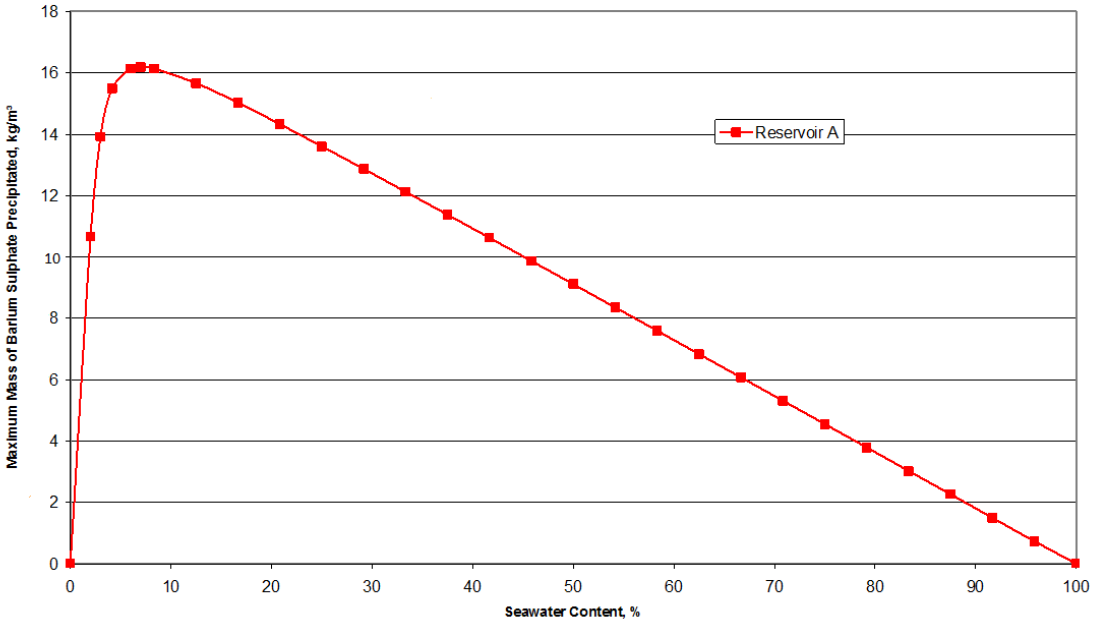


**Figure 10 - Maximum predicted mass of barium sulphate precipitated for Reservoir A**

As one can see, if the effects of processes in the reservoir were neglected, the maximum potential of scale would occur with a seawater fraction around 60%. However, due to the effect of the reservoir on the produced brine, it may be noted that at this seawater fraction in fact none of the wells in this reservoir produce more than 2 mg/l of barium. Figure 11 shows the observed barium concentration versus seawater fraction. As a consequence, the MIC (minimum inhibitor concentration) in this case is lower than expected if one just uses the thermodynamic prediction model (without reservoir effect), and naturally it is possible to prolong the life of the squeeze treatments before re-treating. Thus, the costs associated with scale management could be just a fraction of those forecast using only that model, and without analysing the reservoir effects. The plot in Figure 11 is based on 217 data samples. The dilution line is obtained calculated the barium concentration considering only mixing of injection and formation waters.

Another interesting aspect is that no increase in barium ion concentration post squeeze treatments is observed. Nevertheless, if the squeeze treatment is not applied, scale occurs in the producer well in Reservoir A, since the mixture is still supersaturated.

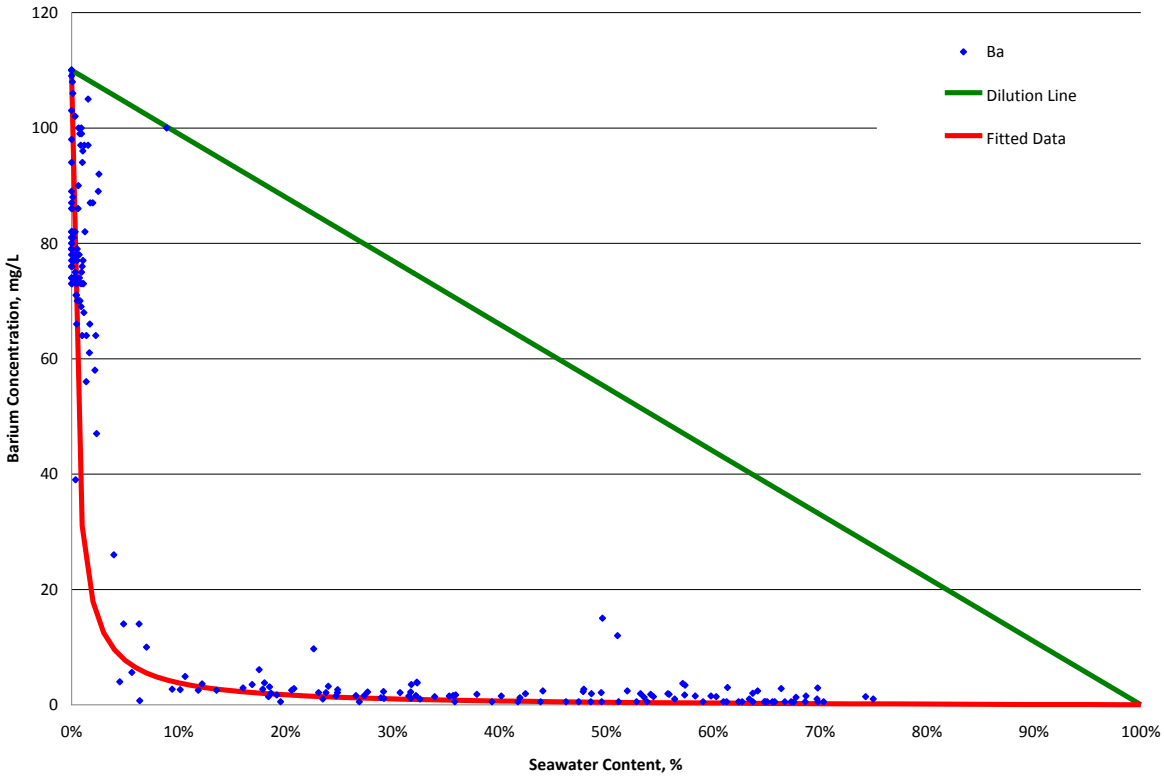


**Figure 11 - Barium concentration expected by dilution line and observed in Reservoir A**

Another excellent piece of evidence that the scaling reaction occurs deep within Reservoir A and significantly affects the produced brine is illustrated in Figure 12. It can be observed in Figure 12 that at the beginning of well production, it produced brine with high barium concentrations and low sulphate concentrations. In the course of time, the barium concentration drops without an increase in sulphate concentration, which means that the sulphate front reacted with barium inside the reservoir, as no production loss and no change in productivity index were observed. After some time, sulphate concentrations started to rise, indicating the possibility of precipitation around the wellbore.

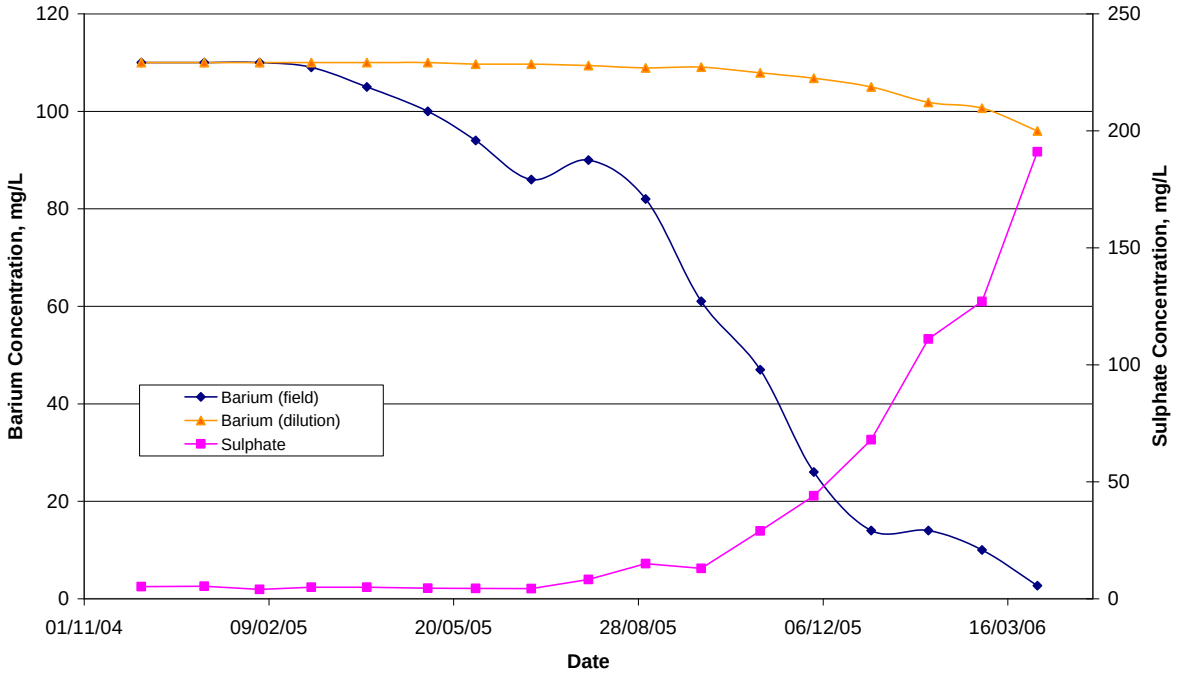


**Figure 12- Example of Barium and sulphate concentration for one well in Reservoir A**

Another important point to be noted in Figure 12 is that the barium trends inform the reservoir team, in this case six months in advance when compared to the sulphate trend, that there is a mix of brines in the produced water. This example motivates the use of pseudo-ion (sulphate corrected for the barium consumption) to estimate seawater fraction in this reservoir [59], as presented in equations 16 to 20 (chapter 1).

After analyzing the produced brine in Reservoir A, a reservoir simulator that allows chemical reactions will be applied in order to calibrate the reactions deep in the reservoir.

## 2.3 RESERVOIR B

This reservoir is composed of high porosity (approximately 30%), high permeability, unconsolidated sandstones, with an oil density of 23º API, and a connate water saturation around 15%. The reservoir temperature is around 65ºC and the original pressure is approximately 306 kgf/cm$^2$. Pressure support in Reservoir B is provided by water injection and the lifting method used is continuous gas lift. The water injected is standard seawater. The formation water composition is given in Table 4.

**Table 4 – Representative Water Reservoir B**

| Water | $Na^{+}$ (mg/L) | $K^{+}$ (mg/L) | $Mg^{2+}$ (mg/L) | $Ca^{2+}$ (mg/L) | $Sr^{2+}$ (mg/L) | $Ba^{2+}$ (mg/L) | $Cl^{-}$ (mg/L) | $SO_4^{2-}$ (mg/L) | Salinity (mg/L) |
|---|---|---|---|---|---|---|---|---|---|
| Reservoir B | 18000 | 40 | 320 | 930 | 170 | 44 | 29600 | 20 | 48842 |

This reservoir is designed with wet completions, satellite and vertical/horizontal wells, with openhole gravel packs for sand control. Most of the wells are equipped with a temperature and pressure transmitters (TPT) located at the wellhead, and permanent downhole gauges (PDG) located near the wellbore. Figure 13 shows the saturation ratio values and Figure 14 the maximum predicted mass of barium sulphate for the brine in Table 4 as a function of the seawater fraction in the brine. The data used in these figures were generated using the Multiscale® simulator [31].

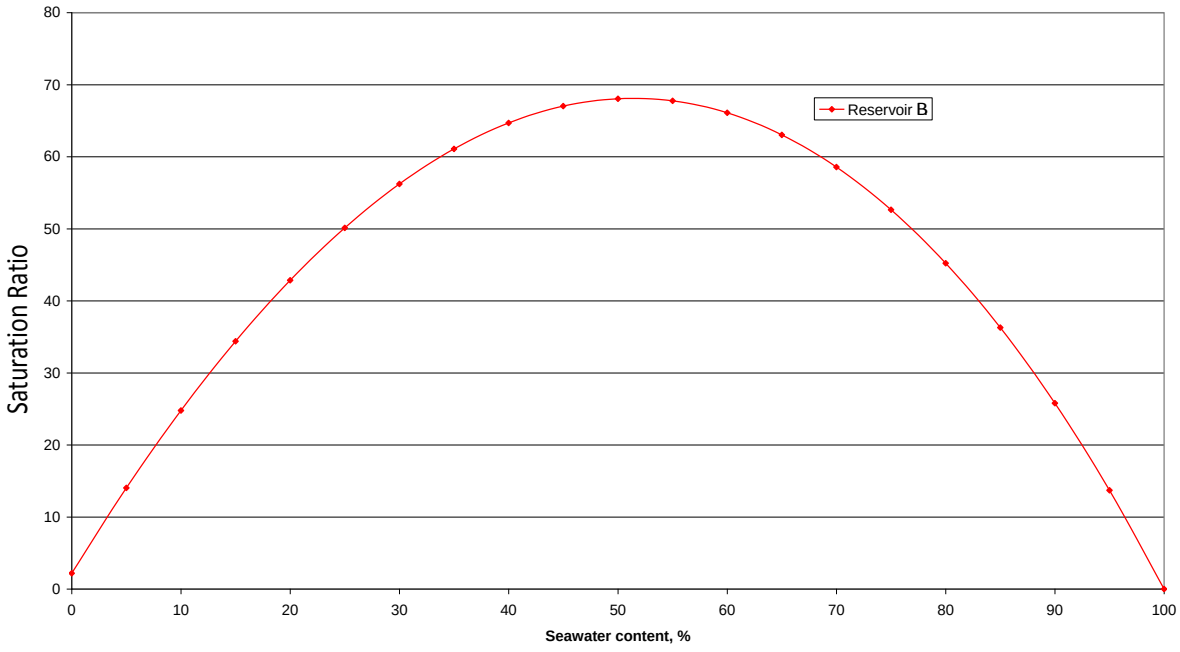


**Figure 13– Saturation ratio values for Reservoir B**

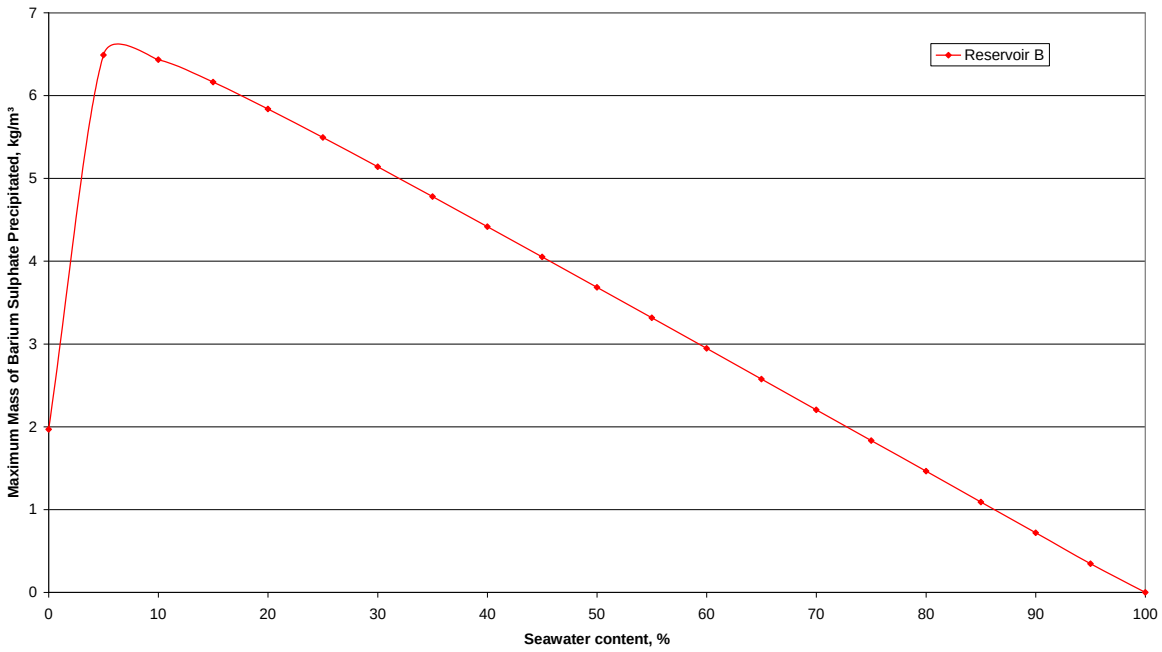


**Figure 14 – Maximum predicted mass of barium sulphate precipitated for Reservoir B**

According to the methodology widely used to evaluate scale potential, one will assume a moderate risk of scale in Reservoir B. Notwithstanding, no well in this reservoir has had any scale problem.

Therefore, let us consider the data and understand what has happened. Figure 15 shows the barium concentration versus seawater fraction. Subtracting the barium concentration expected with no precipitation by the barium concentration obtained by the adjustment of the fitted curve (Figure 15), it is possible to obtain the operational curve of barium precipitation for each seawater fraction (Figure 16). This is the mass consumed per unit volume until the sampling point (downstream of the production bean). Using the stoichiometric relationships, the reservoir team calculates the mass of barium sulphate that precipitates per unit volume. Seven hundred sample analyses were used to form Figure 15.

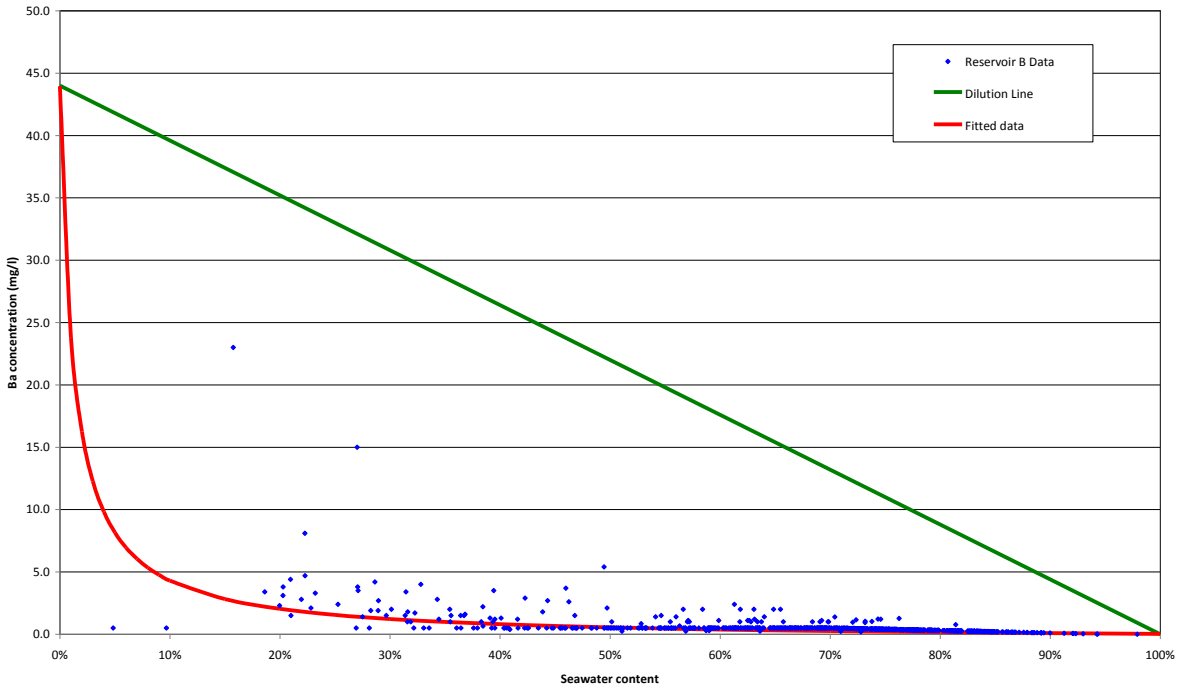


**Figure 15 – Barium concentration expected by dilution line and observed in the Reservoir B**

It is also important to note that there is a lack of data below 15% seawater fraction: the reason is that the first sample collected in all the wells of this reservoir already has a mixture of injected water and formation water, even if the watercut is approximately 1%. For some reason, the mixing zone in this reservoir is bigger, and consequently the chemical reactions deep in the reservoir are also considerable. The question is whether it is an isolated case or whether it is quite normal in reservoirs with the same characteristics. Many authors claim that the first produced water will always have the composition of formation water; this example shows that this is not always the case if one considers that the "first" water is what can be measured. Another challenge is to reproduce this phenomenon in a reservoir simulator, because the real dispersivity is bigger than in the model in this case. This is an interesting observation, since it is usually noted that models have more dispersivity than reality due to numerical dispersion. However, again, in this case it is quite difficult to fit the mixing that has occurred using a conventional black-oil model.

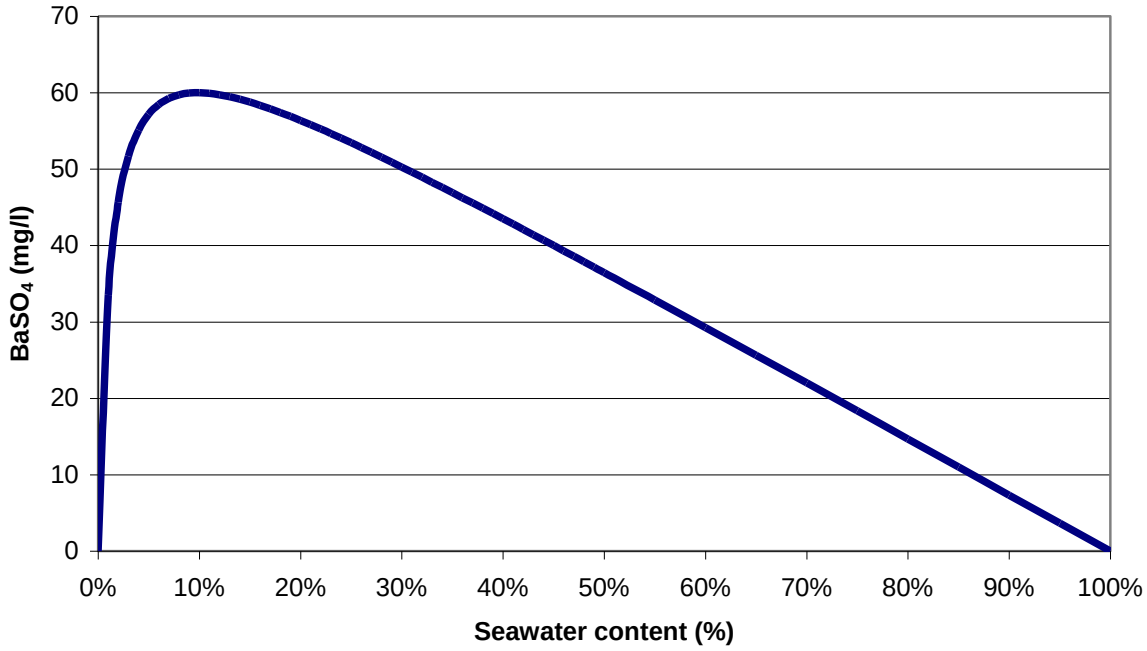


**Figure 16 – Mass of barium sulphate precipitated until the sampling point - Reservoir B**

Based on the curve of mass of barium sulphate precipitated prior to the sample point (platform manifold) and the produced water behaviour of each well, it is possible to estimate the amount of barium sulphate that precipitated from the water produced in a specific well (Equation 21).

$$TotalMassBaSO_4 = \sum Q_{wi} \times f(seawater\%) \qquad (21)$$

Where $f(seawater\%)$ is based on the curve in Figure 16. This methodology was implemented for one well in this reservoir and the result was that approximately 120 tons of barium sulphate scale had precipitated below the sample point. As mentioned before, no well in this reservoir has lost production due to scale. Hence, the only reasonable explanation is that most of this scale occurred deep in the reservoir. Obviously, if ever less than 1% of this scale had happened near the wellbore region the production would have declined. Thus, it is further strong evidence of how the reservoir can influence the produced brine.

Another interesting point is to evaluate what these 120 tons in the reservoir represent. First of all, 120 tons of barium sulphate occupies approximately 26.7 $m^3$. This is a large

volume of scale. However, when compared with the reservoir pore volume associated with this example well, it represents less than 0.001% of the total pore volume. That is why it is imperceptible in terms of reservoir volume. This simple analysis is in agreement with previous studies [60].

## 2.4 RESERVOIR C

This reservoir is composed of high porosity (approximately 30%), high permeability, unconsolidated sandstones, oil density of 24.5º API, and has a connate water saturation of around 30%. The reservoir temperature is around 75ºC and the original pressure is approximately 302 kgf/cm$^2$. Pressure support in reservoir C is provided by water injection and the lifting method used is continuous gas lift. The water injected is standard seawater. The formation water composition is given in Table 5.

**Table 5 – Representative Water Reservoir C**

| Water | $Na^+$ (mg/L) | $K^+$ (mg/L) | $Mg^{2+}$ (mg/L) | $Ca^{2+}$ (mg/L) | $Sr^{2+}$ (mg/L) | $Ba^{2+}$ (mg/L) | $Cl^-$ (mg/L) | $SO_4^{2-}$ (mg/L) | Salinity (mg/L) |
|---|---|---|---|---|---|---|---|---|---|
| Reservoir C | 27800 | 256 | 259 | 999 | 187 | 208 | 47997 | 23 | 73432 |

This reservoir is designed with wet completions, satellite and horizontal wells, with an openhole gravel pack used as the sand control system. All of the wells are equipped with temperature and pressure transmitters (TPT) located at the wellhead and permanent downhole gauges (PDG) located near the wellbore. Figure 17 shows the saturation ratio values for different barium and sulphate concentrations on a 3D view graph, considering all the possibilities of barium stripping deep in the reservoir due to chemical reactions. Figure 18 illustrates a simple mixing of waters, and is a subset of Figure 17 (red curve) assuming no reservoir stripping.

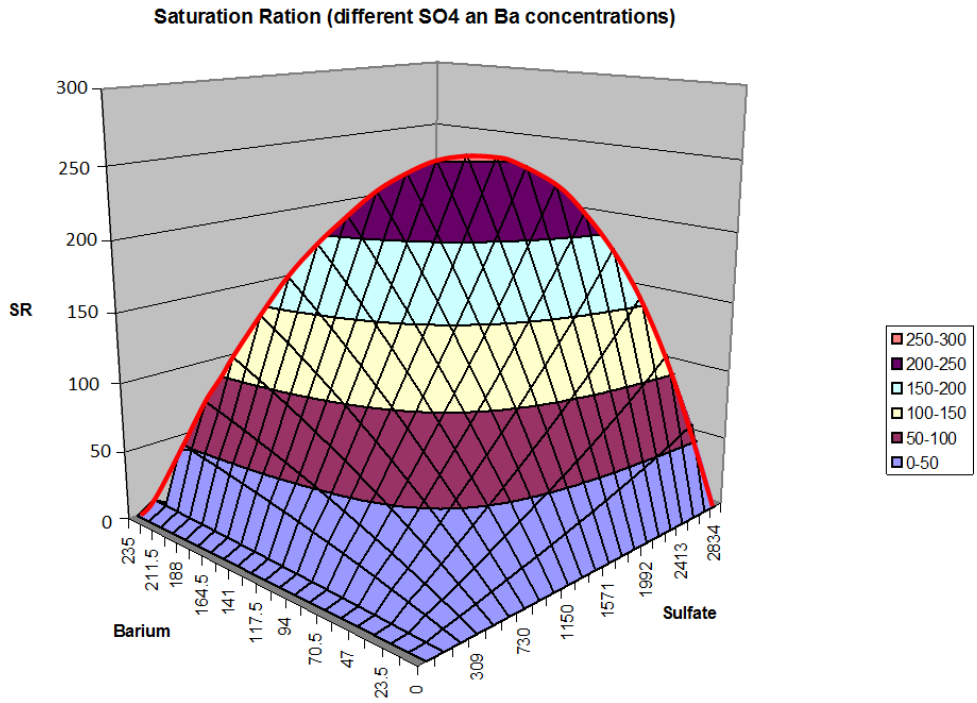


**Figure 17 - Reservoir C, Surface response of SR as function of different barium and sulphate concentrations considering reservoir stripping**

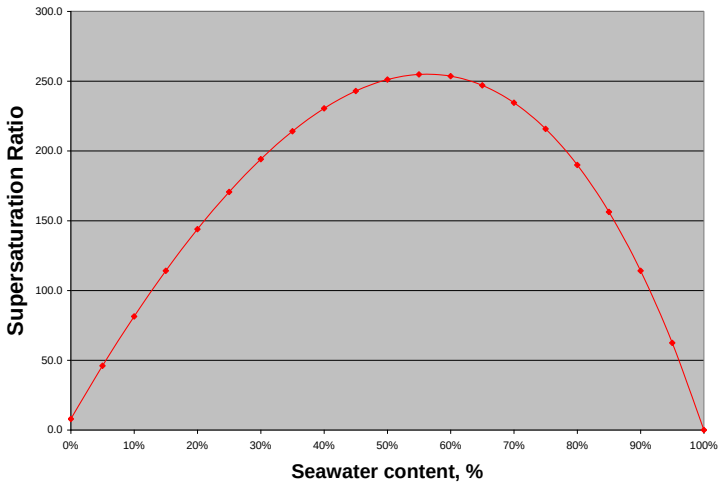


**Figure 18 - Saturation ratio values for Reservoir C**

Based on Figure 17 and the samples from Reservoir C, it is possible to estimate the real SR (saturation ratio) and mass of precipitation for a specific well in the reservoir. To do that, a well was chosen that had been squeezed since water breakthrough. It is also assumed that the chemical inhibition is 100% efficient when the inhibitor concentration is above the MIC (Minimum inhibitor concentration). Thus, samples collected on the

topsides represent the brine composition in the near wellbore. Figure 19 shows the "real" saturation ratio of a specific well in Reservoir C.

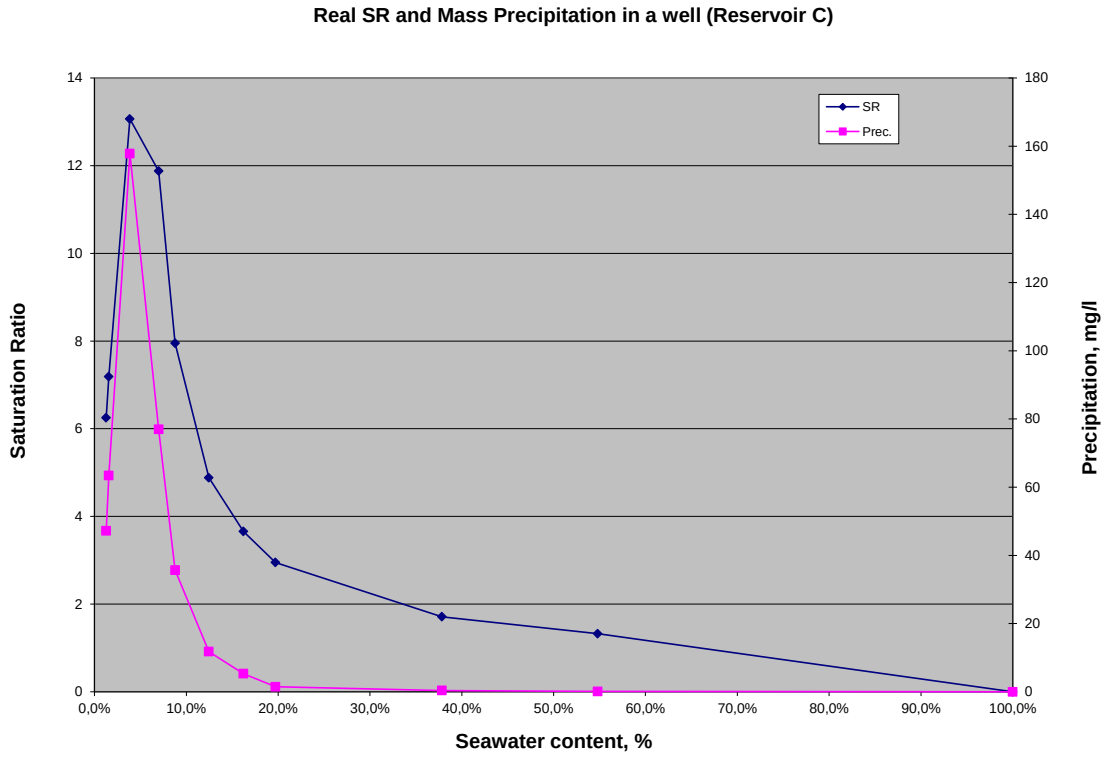


**Figure 19 - Supersaturation ratio and precipitation values for a well in Reservoir C**

Figure 19 shows how the reservoir can change the shape of the curves of saturation ratio and precipitation. When one does not consider the reservoir effect, these curves usually have the maximum saturation ratio between 50% and 60%; in this case, due to the effect of reactions in the reservoir, the maximum potential for scale occurs around 5% - 10% seawater fraction. This is even clearer when one examines the history of the other wells in this reservoir: when any well was not squeezed the worst moment in terms of scale was right after seawater breakthrough.

Although the barium concentration is very low above 20% seawater fraction, the simplistic calculation of saturation ratio shows that barium sulphate precipitation can occur at seawater contents of up to 65%-70%. Thus, this well should be squeezed until 70% of seawater content, but the MIC is quite small above 20% of seawater content.

It is important to emphasize that the brine production usually tends to increase with the seawater content. Thus, although there is more precipitation per volume at small

seawater fractions, in some cases the total precipitation can be bigger at intermediate seawater fractions. Therefore, Figure 19 has to be analyzed in conjunction with other sources of information, such as water production rates.

The observation of this specific well can be generalized for the other wells of this reservoir since a reaction model is adjusted with this example and the proprieties of the system are similar for the rest of Reservoir C.

## 2.5 RESERVOIR D

This reservoir is composed of high porosity (approximately 30%), high permeability, unconsolidated sandstones, oil density of 20º API, and very low connate water saturation (around 7%); however, it is important to note the presence of aquifers. Pressure support in Reservoir D is provided by water injection and the lifting method used is electric submersible pumps (ESP's). The water injected is standard seawater. The formation water composition is given in Table 6.

**Table 6 – Representative Water Reservoir D**

| Water | $Na^+$ (mg/L) | $K^+$ (mg/L) | $Mg^{2+}$ (mg/L) | $Ca^{2+}$ (mg/L) | $Sr^{2+}$ (mg/L) | $Ba^{2+}$ (mg/L) | $Cl^-$ (mg/L) | $SO_4^{2-}$ (mg/L) | Salinity (mg/L) |
|---|---|---|---|---|---|---|---|---|---|
| Reservoir D | 14000 | 150 | 130 | 575 | 33 | 55-80 | 22960 | 10 | 37900 |

This reservoir is more heterogeneous than the other examples, and as a consequence each well must be analyzed separately or, at least, separated into groups with similar patterns. Each well has a different scaling potential depending on some reservoir parameters, mainly related to the aquifers. Squeeze treatments have been applied in order to prevent scale in the near wellbore region.

In the group of wells more distant from the aquifers a quick increase of the watercut was observed, as well as a very significant stripping of barium, even though the wells are producing brine with inhibitor concentrations above the MIC and no production loss was noted. This is evidence that the barium is consumed somewhere far from the well bore region. On the other hand, wells closer to the aquifer can produce formation water for years until produced brine samples indicate mixing between formation and injection

water. Even in these cases, it is possible to observe in some wells a reduction of the barium concentration when compared with the dilution line. Figure 20 shows the produced brine history of one of the wells that has aquifer support. During the first months, the well produced only formation water, but eventually the seawater percentage increases (based on sulphate). After some time the sulphate concentration increases in such a way that the saturation ratio is bigger than one. At this point, it is necessary to squeeze the well in order to avoid scale in the near wellbore region, however this was not done. Some months later, scale damage occurred (highlighted region in red) and finally the well was squeezed (blue line). After that treatment the barium concentration increased to a value a little lower than the dilution line. In this case the reservoir effect is not very pronounced.

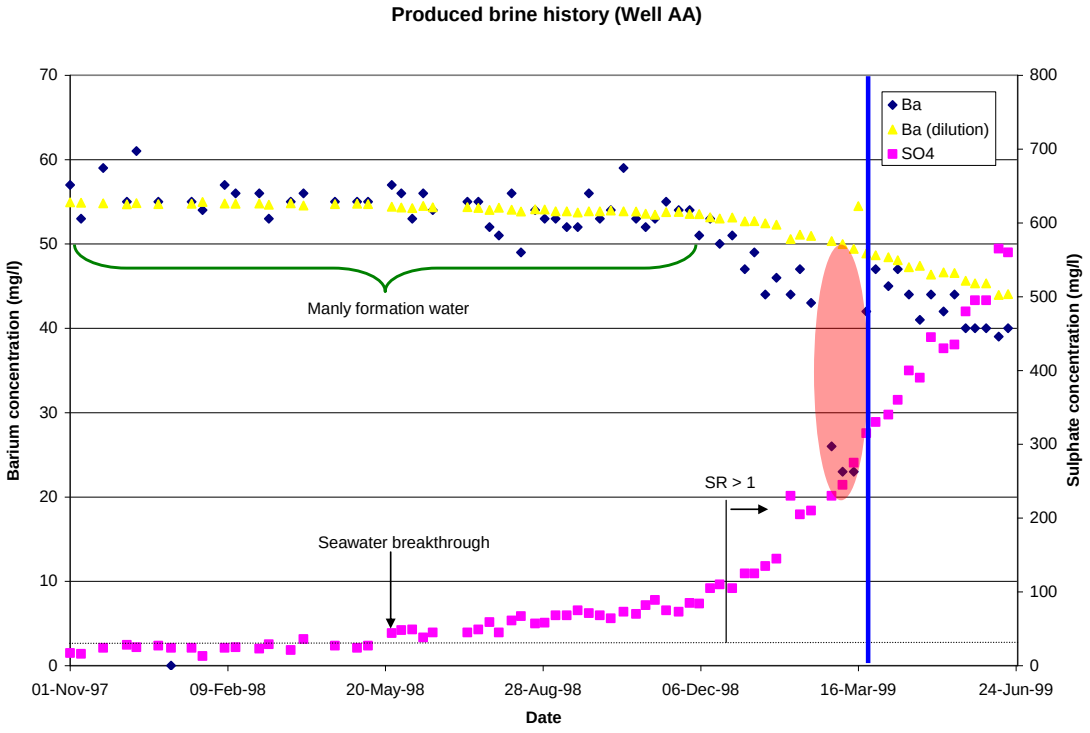


**Figure 20 - Produced brine history well AA**

Figure 21 illustrates another well where it was possible to interpret an explanation for the barium concentration along the time line. Firstly, this well produced water with formation brine characteristics (this period was not completely shown in Figure 21). Secondly, immediately after seawater breakthrough precipitation occurred in the near wellbore region, and then again nine months later (highlighted red regions). The well was squeezed on each occasion (yellow lines) and the barium concentration increased to

a value below the dilution line (the highlighted blue region represents reservoir stripping of barium). Therefore, even in this case with an aquifer present, the barium sulphate scale potential is affected by the reservoir and consequently is smaller than the direct mix of brines.

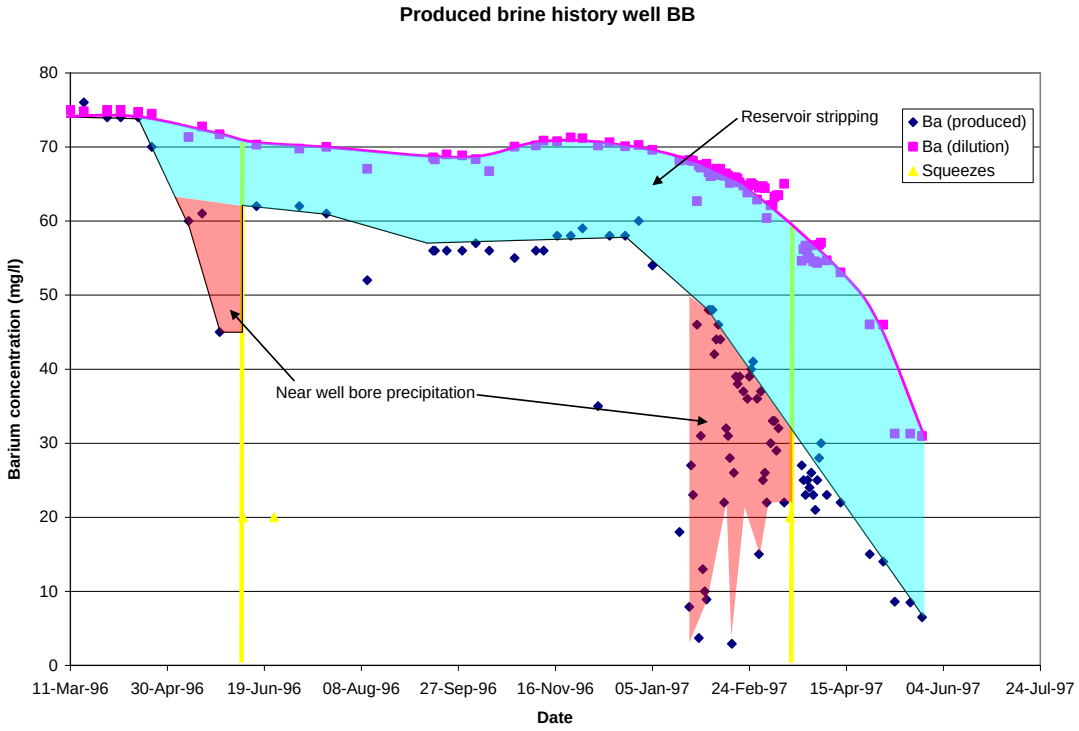


**Figure 21 - Produced brine history – well BB**

## 2.6 RESERVOIR E

This reservoir is composed of high porosity (approximately 15-25%), modest permeability (around 100md), consolidated sandstones, oil density of 20º API, and connate water saturation around 20%. The presence of a bottom aquifer is important. Pressure support in Reservoir E is given by water injection and the lifting method used is electric submersible pumps (ESP's). The water injected is standard seawater. The formation water composition is given in Table 7. The temperature of the reservoir is 124ºC and the original pressure is around 207 kgf/cm².

**Table 7 – Representative Water Reservoir E**

| Water | $Na^+$ (mg/L) | $K^+$ (mg/L) | $Mg^{2+}$ (mg/L) | $Ca^{2+}$ (mg/L) | $Sr^{2+}$ (mg/L) | $Ba^{2+}$ (mg/L) | $Cl^-$ (mg/L) | $SO_4^{2-}$ (mg/L) | Salinity (mg/L) |
|---|---|---|---|---|---|---|---|---|---|
| Reservoir E | 38500 | 840 | 130 | 9500 | 800 | 255 | 70000 | 19 | 115500 |

Although the well illustrated in Figure 22 was protected by scale inhibitor squeeze treatments during all the time shown, it is quite clear that there is a difference between the barium concentrations sampled and those estimated based only on dilution. As one can see, there is extensive stripping in the reservoir. Production losses due to scale were not observed.

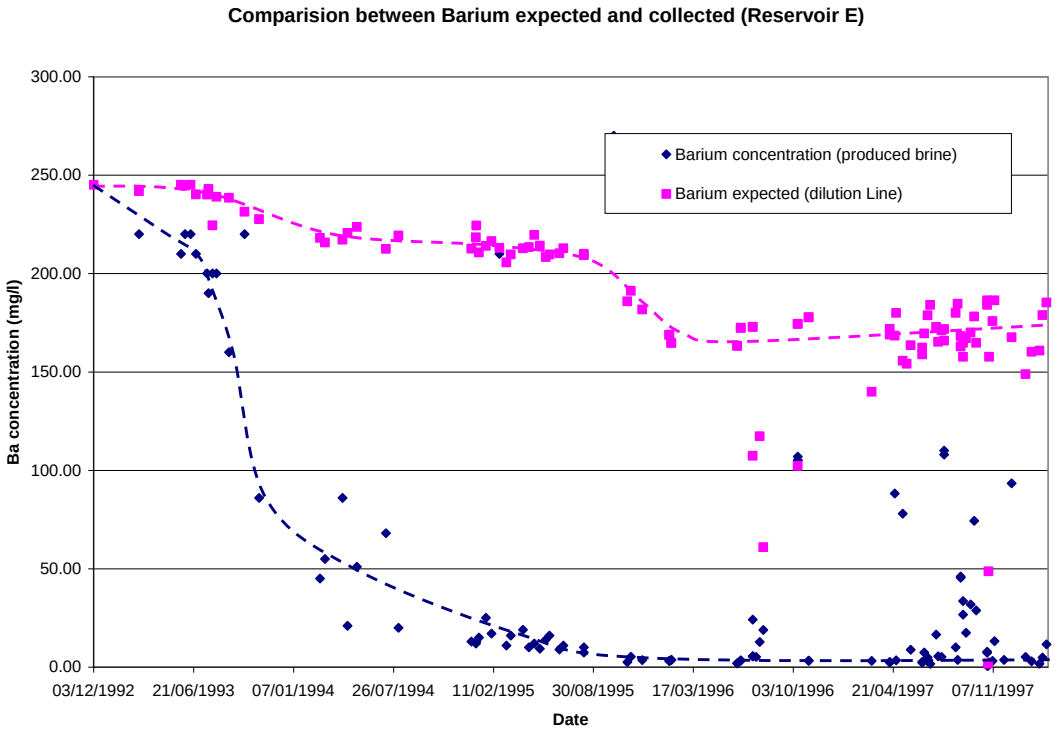


**Figure 22 – Barium production and based on the dilution line.**

Chloride was used to estimate seawater percentage in this reservoir for two reasons: firstly due to the high reservoir temperature there is the possibility of sulphate reacting with calcium in the formation brine to form anhydrite, and secondly, because there is a big difference between the chloride concentrations of the formation brine and that of the injected water. Naturally, the methodology explained in Reservoir A (equations 16 to

20) to estimate seawater percentage with sulphate, strontium and barium can also be applied, but in this case, it is necessary to exchange strontium with calcium. Calcium plays an important role in the reactions deep in the reservoir.

In summary, not only the barium stripping (reacting with sulphate) deep in the reservoir is observed, but also sulphate stripping is observed (reacting with calcium). As in the case of the Gyda field [35] when the reservoir is hot (160 ºC) there is a greater propensity for the injected sulphate to react with the calcium in the reservoir. It is also fundamental to highlight that in both cases the calcium concentration in the formation brine is high (over 9,000 mg/l). Thus, it can be said that in this type of reservoir the barium sulphate precipitation in the wells is reduced by two factors: conventional barium stripping and also sulphate stripping. In these cases the final result is quite different from the direct mix of brines. Figure 23 and Figure 24 show the thermodynamic prediction calculations.

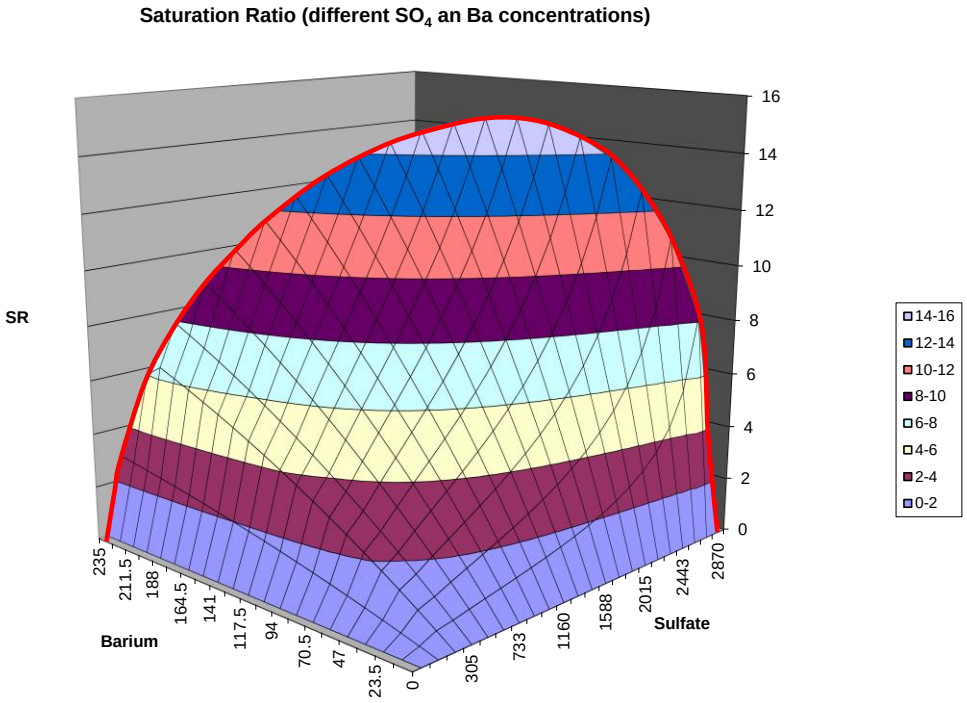


**Figure 23- Reservoir E, Surface response of SR (barium sulphate) for a mix of injected water and formation water, accounting for reservoir effects**

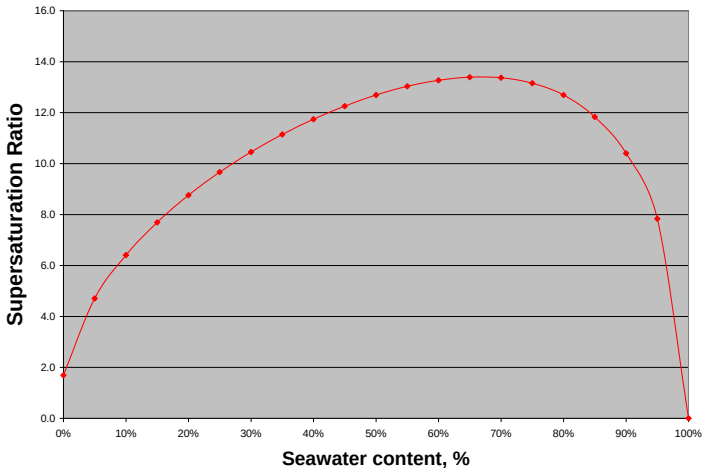


**Figure 24 – Supersaturation ratio values for Reservoir E (barium sulphate)**

It is interesting to highlight that not only in this case, but in other examples throughout this study, the formation brine is apparently supersaturated at reservoir conditions. In fact this is not possible since this brine is in equilibrium with the reservoir for millions of years. There are four possible explanations.

- Incorrect analyses;
- Brine contamination;
- Methodology – counts sulfur as a sulphate;
- Natural inhibitor in the reservoir.

Using the surface response based on barium and sulphate concentrations in Reservoir E, one can say that up for to 30% of seawater content (from the available history) the saturation ratio is below or at most 1. Thus, in fact any barium sulphate precipitation was not expected and the squeezes were unnecessary. Probably, as was the case in the Gyda [35] field, the scale risk will be greater at higher seawater content. The risk of $CaSO_4$ precipitation in the production wells should also be considered.

## 2.7 RESERVOIR F

Reservoir F is another example of a reservoir with high temperature and a high concentration of calcium in the formation brine. Exactly as expected, the sulphate reacts

deep in the reservoir with calcium and barium, and again the barite scaling tendency is considerably reduced in the producer well. The formation water composition is given in Table 8. The temperature of the reservoir is 125ºC.

**Table 8 – Representative Water Reservoir F**

| Water | $Na^+$ (mg/L) | $K^+$ (mg/L) | $Mg^{2+}$ (mg/L) | $Ca^{2+}$ (mg/L) | $Sr^{2+}$ (mg/L) | $Ba^{2+}$ (mg/L) | $Cl^-$ (mg/L) | $SO_4^{2-}$ (mg/L) | Salinity (mg/L) |
|---|---|---|---|---|---|---|---|---|---|
| Reservoir F | 26920 | 1408 | 412 | 7000 | 945 | 365 | 58000 | 20 | 96000 |

As was the case in the Gyda [35] field, the magnesium is depleted when compared with the dilution mixing line (Figure 25). This can be explained based on the interaction between calcium and magnesium. Thus, when the seawater is injected, the equilibrium between the rock and fluid is disturbed. Since the Mg/Ca ratio for seawater is much greater than Mg/Ca ratio in the formation brine, the system tends to re-equilibrate the Mg/Ca ratio. Therefore, an ion exchange mechanism causes magnesium to be retained from the brine phase within the rock, and in return, calcium is released from the rock into the brine phase. Naturally, this effect in Reservoir F is less pronounced than in the Gyda [35] field since the magnesium concentration is lower.

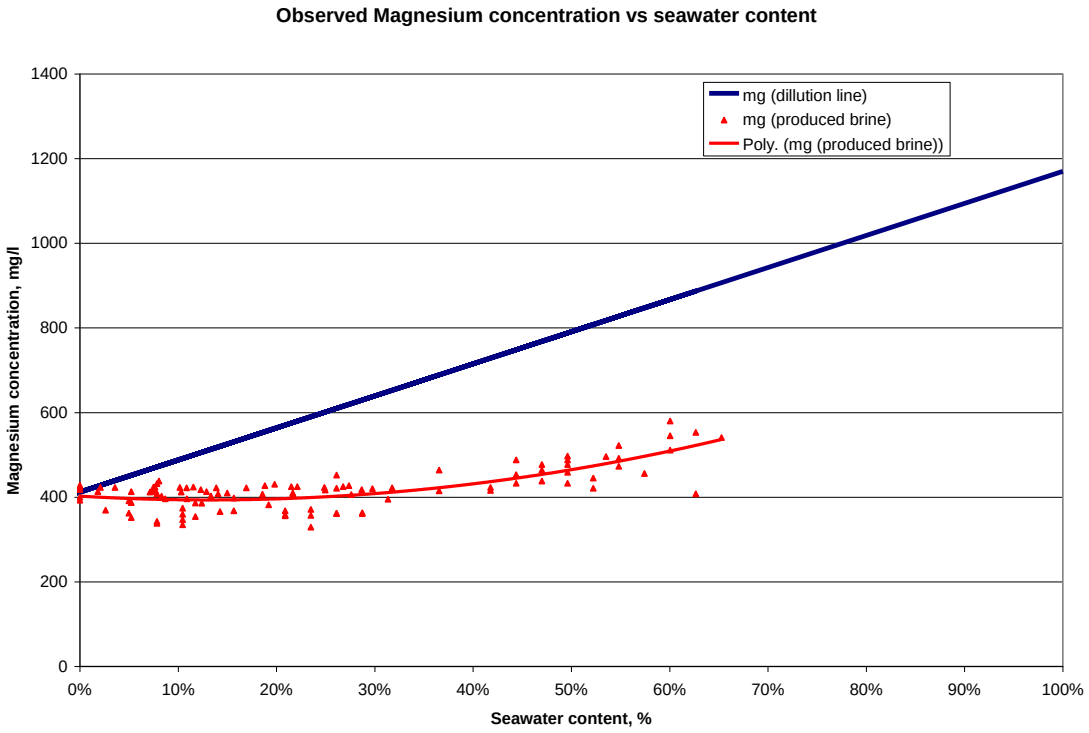


**Figure 25 - Observed magnesium concentration versus seawater content in Reservoir F**

Figure 26 compares different methods to estimate seawater content. Both cases, using either the chloride or the reacting ions method based on sulphate (equations 16 to 20) provide a similar result; on the other hand, if one only uses the sulphate, in this case, it will result in a large error in the calculation. The sulphate concentration increases more than one year after the seawater breakthrough, according to the chloride or the reacting ions method (sulphate corrected by the consumption of other ions, such as barium and calcium).

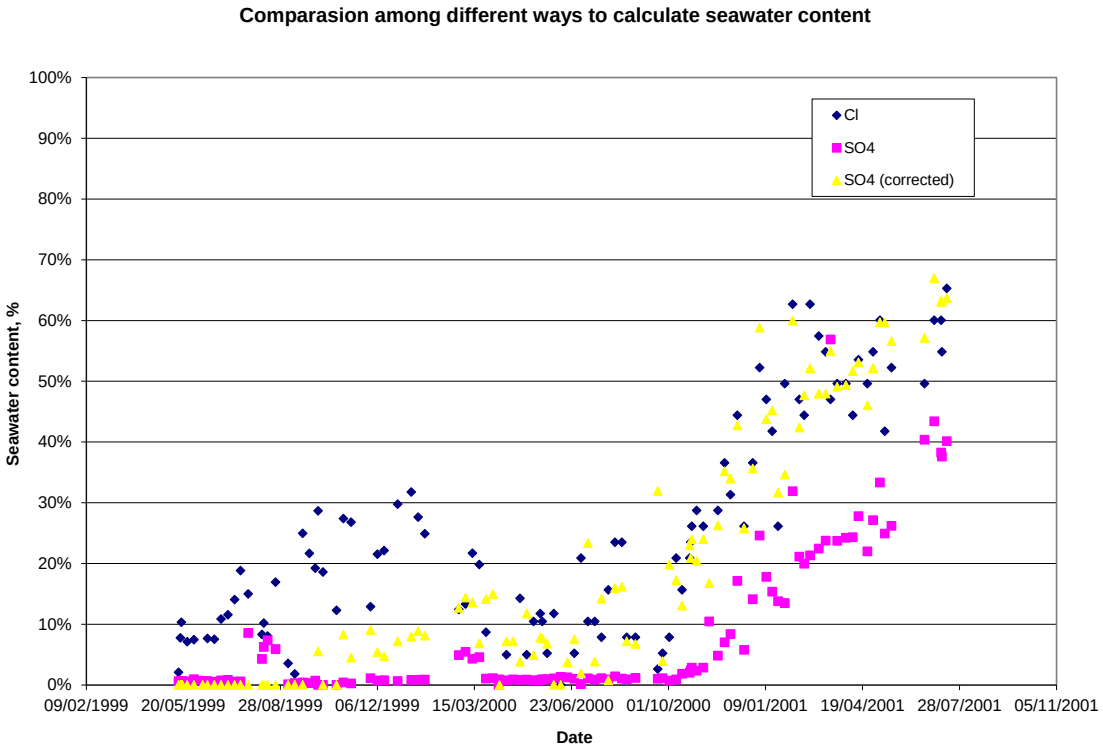


**Figure 26 – Seawater content with different methods**

## 2.8 RESERVOIR G

This reservoir is composed of high porosity (approximately 15-25%), low matrix permeability and naturally fractured chalk, oil density of 20º API, and connate water saturation around 20%. Pressure support in Reservoir G is provided by gas/water injection and the lifting method used is continuous gas lift. The water injected is standard seawater. The formation water composition is given in Table 9. The temperature of the reservoir is 131ºC and the reservoir pressure is approximately 500 kgf/cm².

**Table 9 – Representative Water Reservoir G**

| Water | $Na^+$ (mg/L) | $K^+$ (mg/L) | $Mg^{2+}$ (mg/L) | $Ca^{2+}$ (mg/L) | $Sr^{2+}$ (mg/L) | $Ba^{2+}$ (mg/L) | $Cl^-$ (mg/L) | $SO_4^{2-}$ (mg/L) | Salinity (mg/L) |
|---|---|---|---|---|---|---|---|---|---|
| Reservoir G | 55000 | 530 | 1700 | 22000 | 1600 | 1200 | 125000 | <10 | 207000 |

As expected, the calcium reacts with sulphate and also there is an exchange between magnesium and calcium. As a consequence, the produced brine has no sulphate content until high seawater fractions (Figure 27). No scale due to sulphate salts is expected in the wells until 70% seawater fraction.

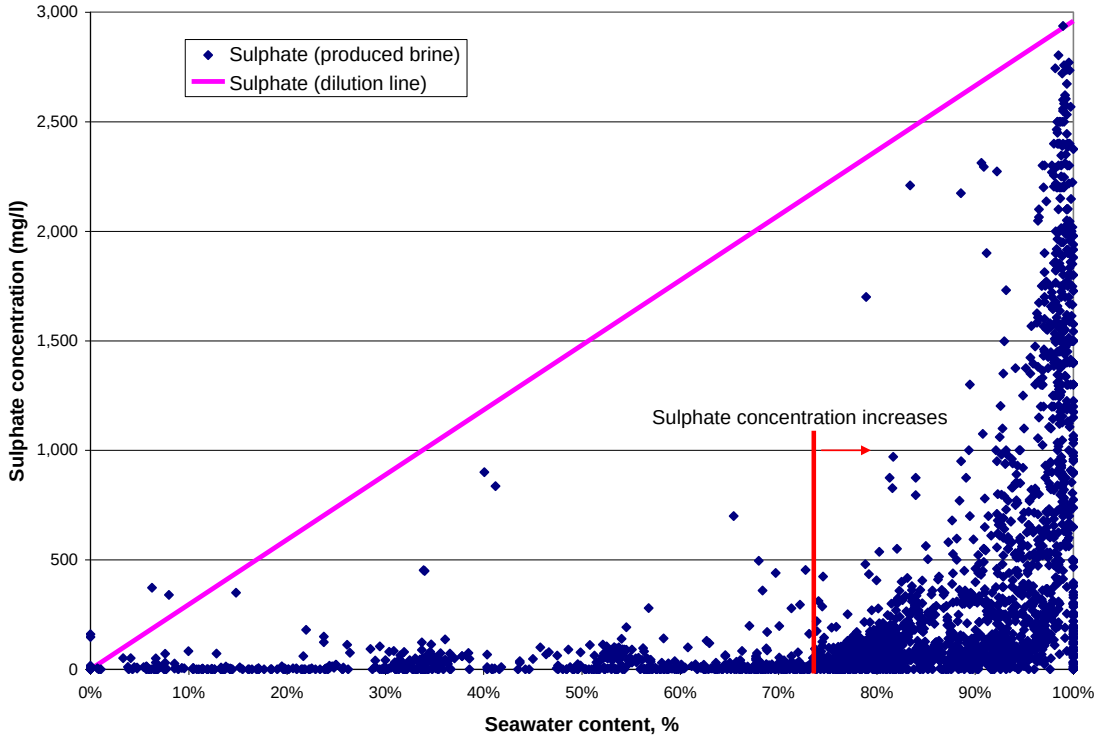


**Figure 27 – Sulphate concentration in the produced brine**

Figure 28 shows a comparison between the magnesium concentration in the produced brine and that expected by dilution. One can identify an exchange between calcium in the rock with magnesium in the brine when the seawater content is higher than 25%.

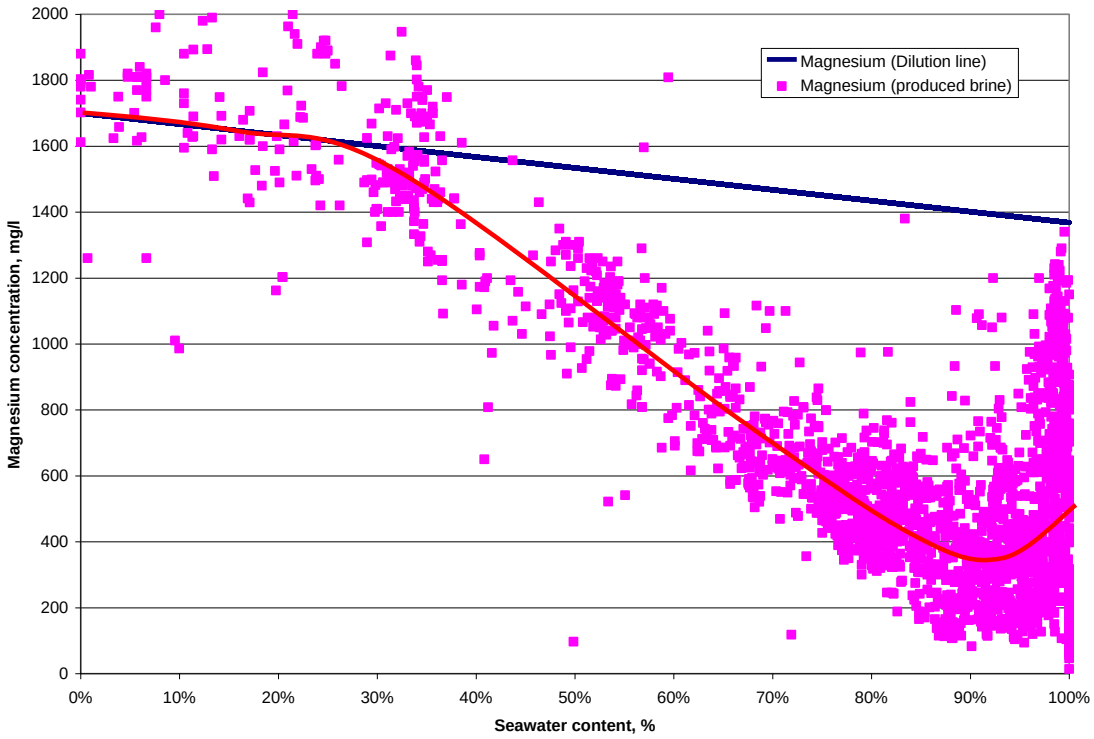


**Figure 28 – Comparison between the magnesium expected concentration by dilution and the concentration in the produced brine (the curve is an interpretation based on the data)**

## 2.9 RESERVOIR H

This is another example of a reservoir with high temperature (130 ºC) and high concentration of calcium in the formation brine. The reservoir pressure is around 175 kgf/cm². The formation water composition is given in Table 10.

**Table 10 – Representative Water Reservoir H**

| Water | $Na^+$ (mg/L) | $K^+$ (mg/L) | $Mg^{2+}$ (mg/L) | $Ca^{2+}$ (mg/L) | $Sr^{2+}$ (mg/L) | $Ba^{2+}$ (mg/L) | $Cl^-$ (mg/L) | $SO_4^{2-}$ (mg/L) | Salinity (mg/L) |
|---|---|---|---|---|---|---|---|---|---|
| Reservoir H | 37370 | 940 | 412 | 12300 | 785 | 160 | 82180 | 14 | 135240 |

Reservoir H is an excellent example of the importance of connate water saturation. In this case where the seawater is injected into the oil leg in areas without aquifers the produced brine has a high content of seawater, even in the first sample collected. Although in most of the wells the first sample collected has a high water cut, all the

wells that are supported by injection of water into the oil leg have high seawater content, even if the water cut is low. In this respect, this case is similar to Reservoir B.

Another point that should be considered is the fact that even if the reservoir has a small amount of formation water, in the areas without aquifers, it is easy to note the stripping of sulphate, calcium, strontium and barium. Therefore, one may notice a pattern of reaction between calcium and sulphate in reservoirs above 120º C which are rich in calcium. In fact, in all the cases studied in reservoirs with these features, there was a significant reduction of barium sulphate scale potential in the production wells. Figure 29 illustrates this phenomenon of ions stripped in a selected well in Reservoir H; the methodology that uses sulphate, barium, strontium, and calcium was used in order to calculate seawater percentage (equations 16 to 20 adapted).

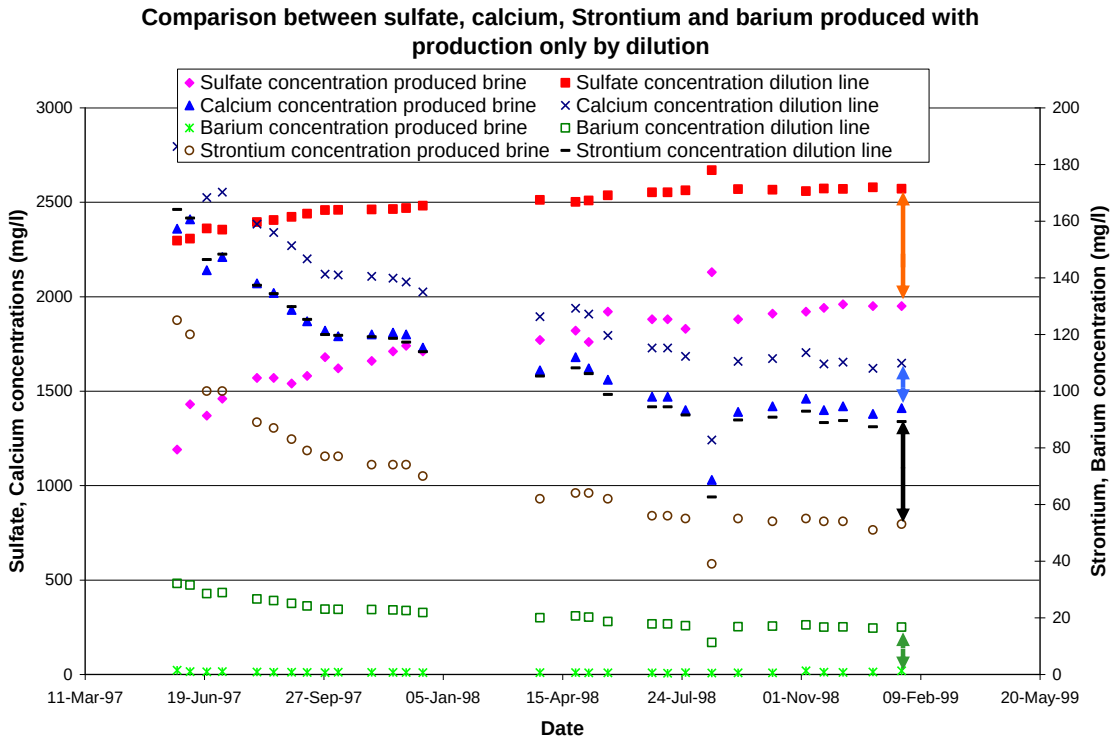


**Figure 29 – Comparison between sulphate, calcium, strontium and barium produced with the theoretical production without reactions (only dilution)**

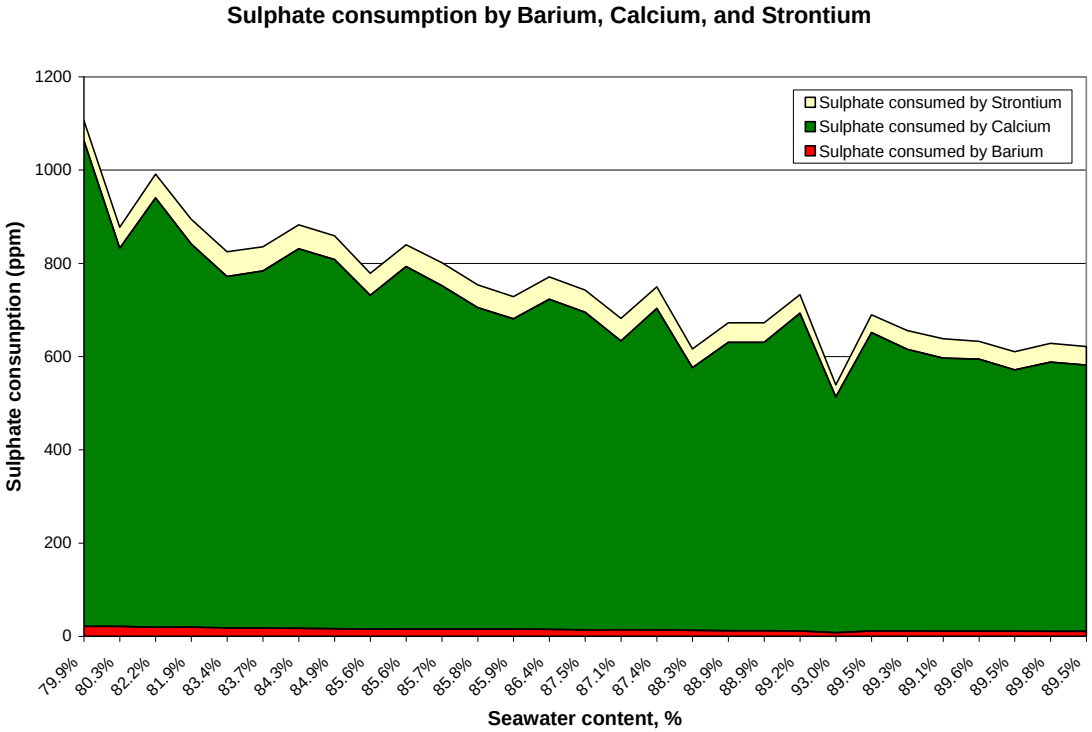


**Figure 30 – Sulphate consumption in the reservoir by barium, calcium and strontium**

As one can note (Figure 30), when the seawater content is higher than 80%, most of the sulphate consumption is caused by calcium and just a small amount is caused by barium and strontium. In part, this can be explained by the ion exchange between calcium and magnesium, but the high calcium concentration in the formation water alone will contribute very significantly to the sulphate stripping. Figure 31 shows the depletion in the magnesium when compared with the dilution line.

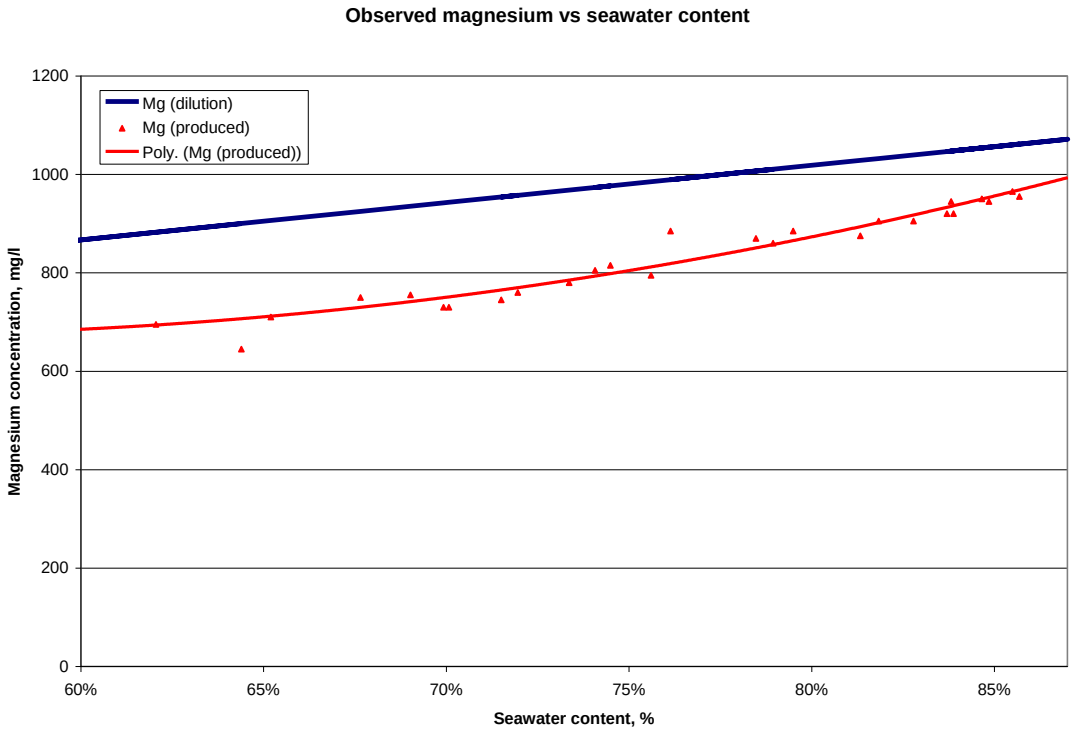


**Figure 31– Observed magnesium concentration versus seawater content in reservoir H**

Therefore, reservoirs E, F, G and H, as well as the Gyda field [35], show strong evidence that sulphate reacts with calcium deep in the reservoir. It is also essential to observe that in all the cases the reservoir temperature is above 120º C and the calcium concentrations in the formation water are higher than 7000mg/l. It is known that the solubility of calcium sulphate decreases with temperature, and thus the challenge is to determine the relationship between temperature, calcium concentration, sulphate concentration, and the impact of reactions in the reservoir. Further cases should be investigated in order to generate a representative model. For instance, cases with high concentration of calcium in a low temperature environment or the opposite case (high temperature and low calcium concentration in the formation brine) should be investigated. Figure 32, which was obtained based on North Sea seawater changing only the calcium concentrations (Multiscale® [31]), provides a good indication of the impact of concentration and temperature on the scaling tendency. It is evident that the scaling potential increases with the temperature, especially when the temperature is above 100ºC.

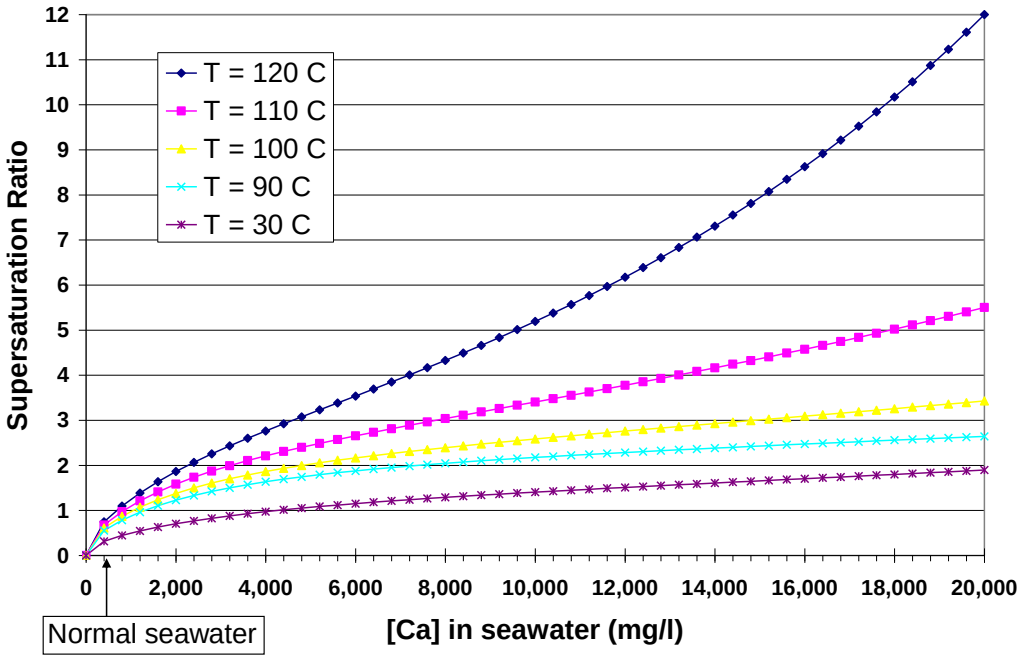


**Figure 32– Impact of calcium and temperature on the saturation ratio (seawater brine).**

Another fundamental point that was observed in these reservoirs is magnesium depletion. This may increase the availability of calcium in the system and consequently increase the extent of sulphate stripping.

Finally, three figures were prepared in order to show the main precipitation deep in the reservoir. It may be noticed that due to these reservoir effects, no well analysed in Reservoir H has a $BaSO_4$ scale potential due to the previous precipitation of sulphate salts. Figure 33 shows the barium sulphate precipitation in the reservoir versus seawater fraction. There is also a comparison with the Multiscale® [31] calculation. Thus, it is easy to observe that precipitation follows exactly the Multiscale® [31] prediction, and suggests a very quick reaction rate in the reservoir.

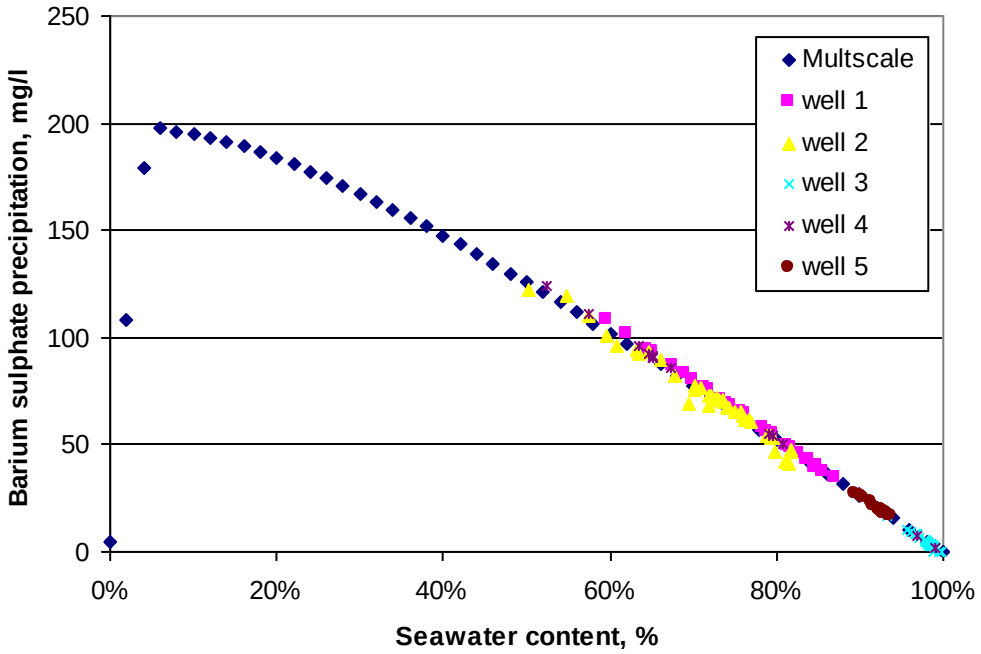


**Figure 33– Mass of barium sulphate precipitation in the reservoir versus seawater fraction for Reservoir H, compared with mass of precipitation predicted by Multiscale®.**

Figure 34 shows the same example; however, strontium sulphate is illustrated in this case. It can be noted that some wells follow the Multiscale® [31] tendency but with a reduction in the total amount precipitated, whilst other wells show a reduction in the strontium available in the produced brine far below the strontium stripping potential.

Figure 35 shows calcium sulphate precipitated deep in the reservoir. It is noted that some points are above the Multiscale® [31] prediction; these points can be explained by calcium and magnesium exchange between the rock and the fluid.

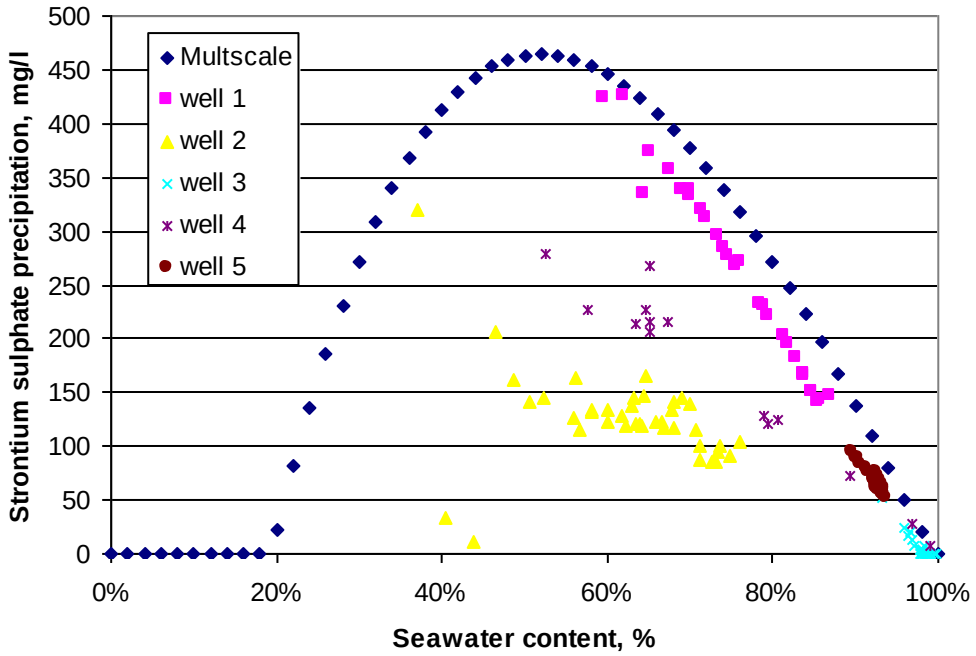


**Figure 34– Mass of strontium sulphate precipitation in the reservoir versus seawater fraction for Reservoir H, compared with mass of precipitation predicted by Multiscale® [31].**

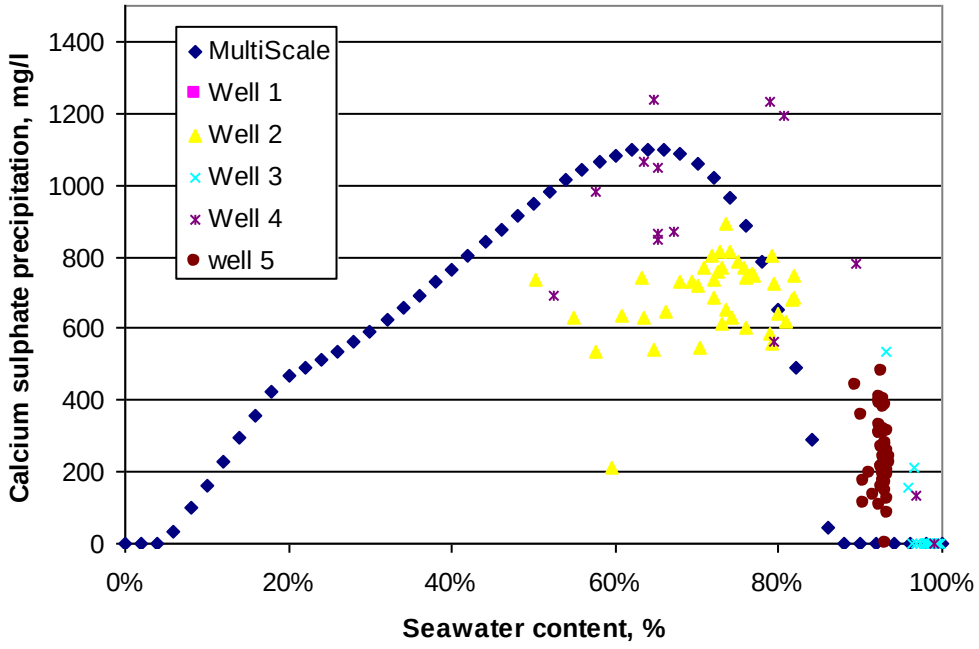


**Figure 35– Mass of calcium sulphate precipitation in the reservoir versus seawater fraction for Reservoir H, compared with mass of precipitation predicted by Multiscale® [31].**

The method used for estimating the ions stripped deep in the reservoir will be applied in all the cases analysed, and also for other cases not shown in this work, in order to calibrate better the reactions in the reservoir simulator.

## 2.10 RESERVOIR I

The spreadsheet provided by the operator of Field I has production brine analysis from some wells of the Field I platform. The data suggest some interesting conclusions as well as showing some evidence of ion stripping in the reservoir.

### 2.10.1 Data Supplied

First, all the raw data were inserted in a reacting ions spreadsheet (RI) in order to calculate the seawater fraction and to analyse the consistency of the data. The representative formation brine is detailed in Table 11. Reservoir conditions are 90$^{O}$C and 211 kgf/cm².

**Table 11 - Supplied formation brine composition Reservoir I.**

| Water | $Na^{+}$ (mg/L) | $K^{+}$ (mg/L) | $Mg^{2+}$ (mg/L) | $Ca^{2+}$ (mg/L) | $Sr^{2+}$ (mg/L) | $Ba^{2+}$ (mg/L) | $Cl^{-}$ (mg/L) | $SO_4^{2-}$ (mg/L) | Salinity (mg/L) |
|---|---|---|---|---|---|---|---|---|---|
| Reservoir I | 30117 | 301 | 364 | 1834 | 323 | 16 | 50700 | 53 | 83580* |

*Salinity based on chloride.

Based on the representative formation brine composition, the reacting ions spreadsheet is used to generate Figure 36, Figure 37 and Figure 38. As one can see, the figures show an inconsistent result, with in some cases the seawater fraction reaching -30%.

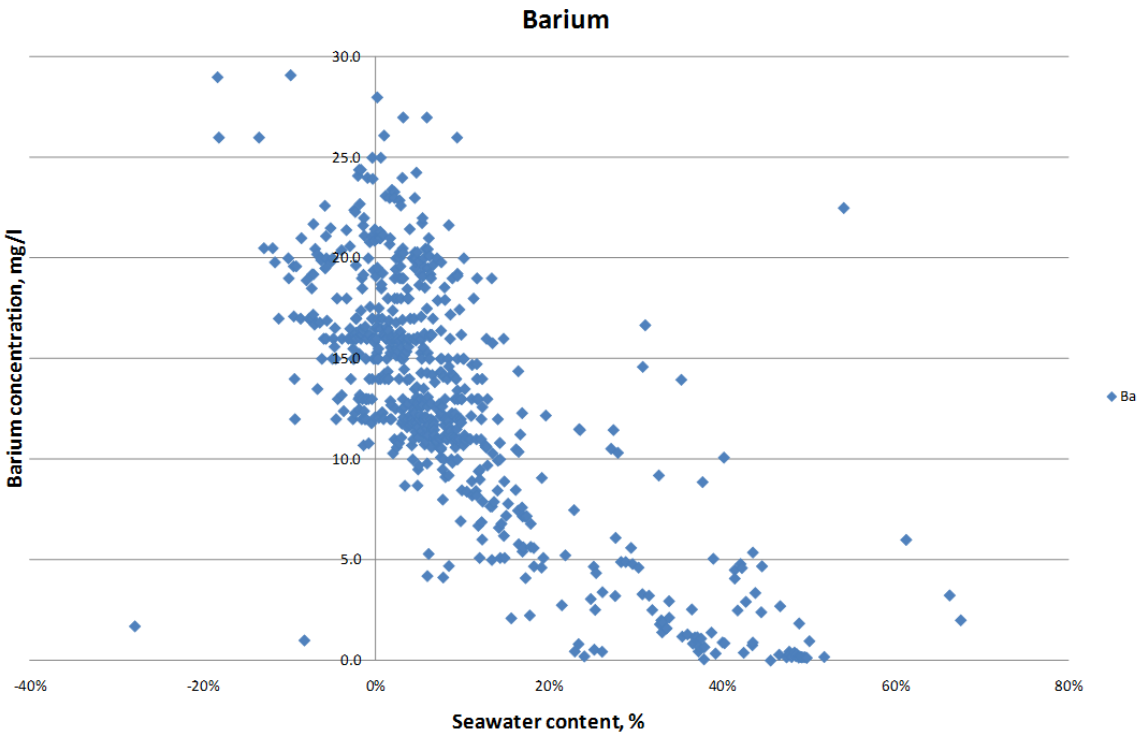


**Figure 36 - $Ba^{2+}$ concentration [mg/l] versus seawater fraction based on the representative formation brine, calculated using the reacting ions spreadsheet.**

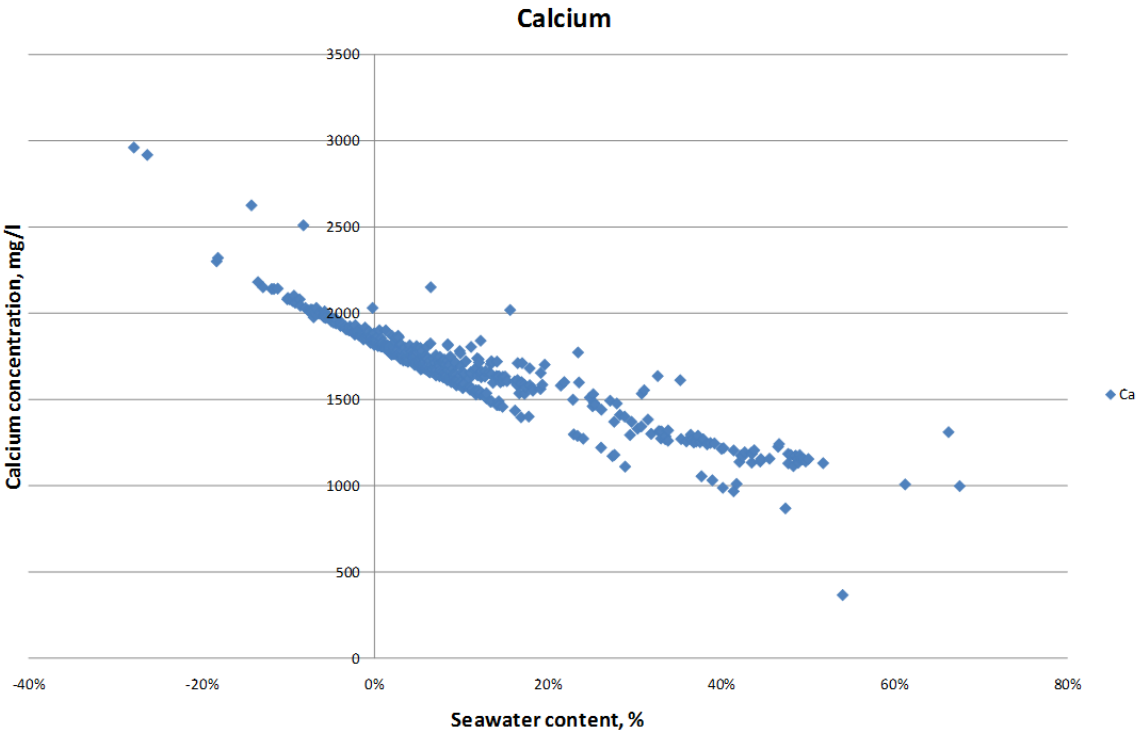


**Figure 37 - $Ca^{2+}$ concentration [mg/l] versus seawater fraction based on the representative formation brine, calculated using the reacting ions spreadsheet.**

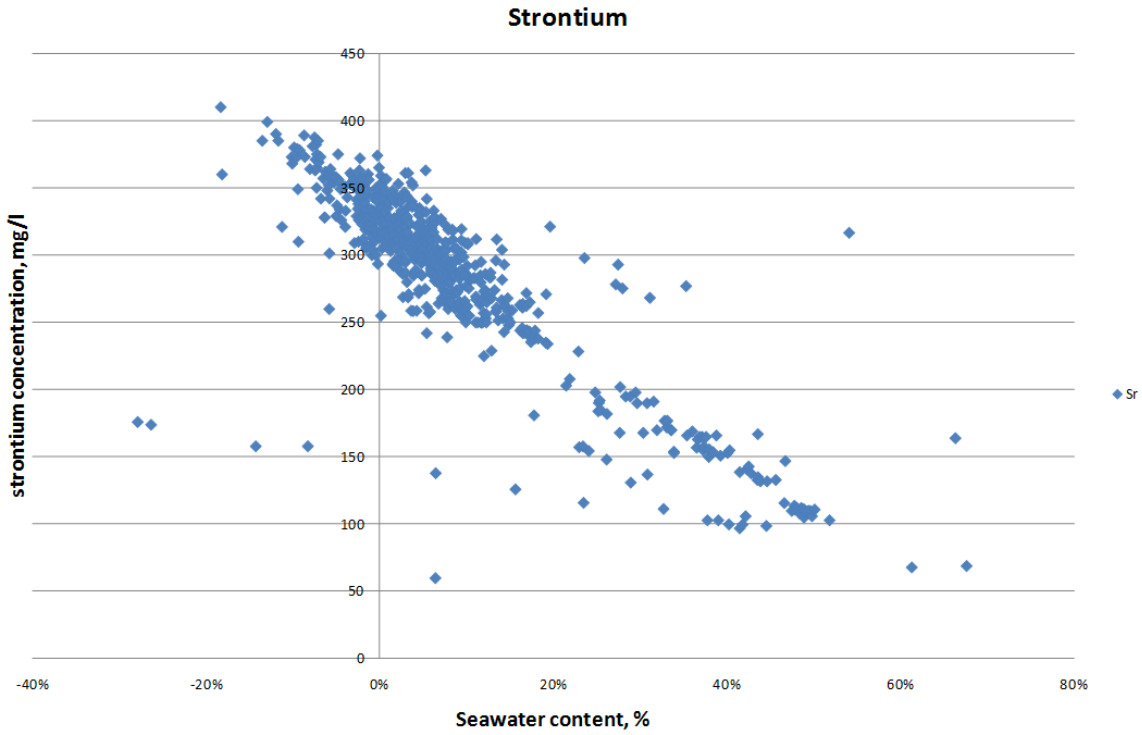


**Figure 38 - $Sr^{2+}$ concentration [mg/l] versus seawater fraction based on the representative formation brine, calculated using the reacting ions spreadsheet.**

As one can see, the resulting seawater fraction modelled is inconsistent. Hence, an initial production brine composition was used to identify a representative formation brine composition. As the model only uses a limited group of ions in the calculation, we initially just propose a change in the following ions: barium, strontium, calcium and sulphate. Table 12 shows the suggested concentration of this group of ions in the representative formation brine.

**Table 12 - Initial proposed change in the representative formation brine composition based on initial produced brine**

| Water | $Na^+$ (mg/L) | $K^+$ (mg/L) | $Mg^{2+}$ (mg/L) | $Ca^{2+}$ (mg/L) | $Sr^{2+}$ (mg/L) | $Ba^{2+}$ (mg/L) | $Cl^-$ (mg/L) | $SO_4^{2-}$ (mg/L) | Salinity (mg/L) |
|---|---|---|---|---|---|---|---|---|---|
| Reservoir I | 30117 | 301 | 364 | **2080** | **380** | **22** | 50700 | **60** | 83580 |

The proposed data that is partly shown in Table 12 was analysed using Multiscale® [31]. The saturation ratio of this brine at reservoir conditions (90°C and 207 bar) is slightly supersaturated with respect to barium sulphate (SR = 1.36). In this case, there

are two simple options. One option is to work directly with this proposed data because the reservoir may have natural inhibitors. The other option is to correct this brine composition so that the representative brine is not supersaturated. Normally, a good option is to alter slightly the sulphate concentration because it does not significantly impact the scaling tendency after seawater breakthrough and it is quite typical to count other sources of sulphur as a sulphate in the brine composition analysis. Thus, in this case the sulphate concentration to equilibrate the brine is 44 mg/l. In fact here both solutions lead to a similar result.

In order to validate the suggested data, the calculated seawater fraction with the "reacting ions" (RI) model was compared with the seawater fraction based on chloride ($Cl^-$) and also based on sodium ($Na^+$). Figure 39 shows the excellent consistency obtained with this comparison. It is important to observe that 96% (chloride) and 91% (sodium) of the calculated values were in a margin of +/-10% when compared with the "reacting ion" (RI) model.

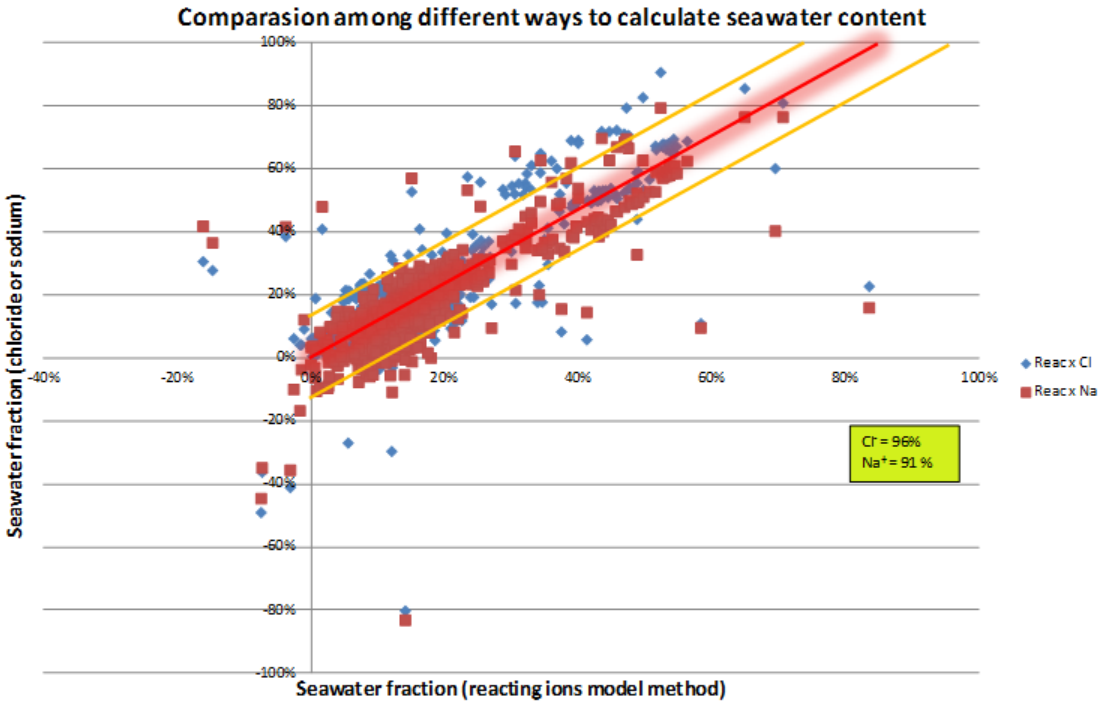


**Figure 39 - Seawater fraction calculation comparison (RI x $Cl^-$ and RI x $Na^+$)**

Figure 40, Figure 41 and Figure 42 were developed using the adapted data, where the representative formation brine composition had been altered. Figure 40 illustrates the barium concentration for different seawater contents as well as an interpretation of

barium stripping in the reservoir. Figure 41 represents the strontium concentration for different seawater contents and Figure 42 is a similar plot for calcium.

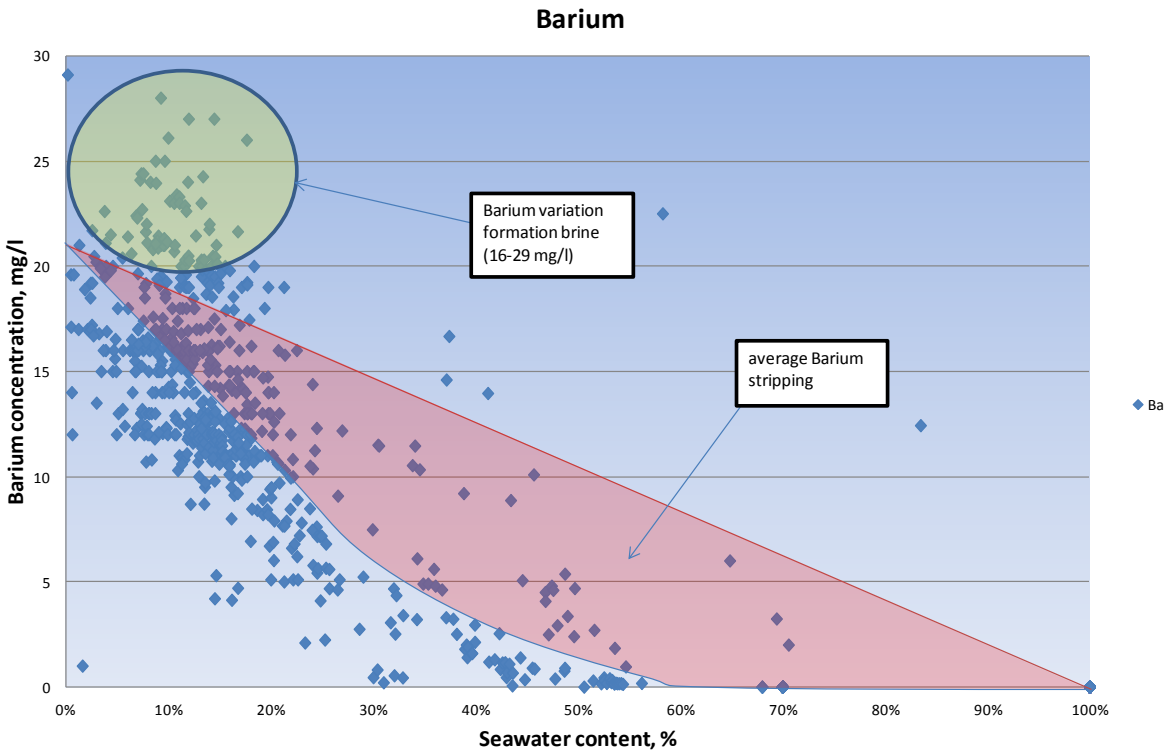


**Figure 40 - Barium concentration in the produced brine for different seawater contents.**

Figure 40 suggests that there is a variation in the barium concentration in the formation brine. This can be caused by an aquifer with a different brine composition or even a variation in the connate brine itself. In order to obtain more details regarding this phenomenon, it would be necessary to obtain more data that could help identify this variation as function of depth, or as an areal variation. Regardless, the data clearly illustrate barium stripping (a large proportion of these data were obtained with an adequate inhibitor concentration in the production brine) and a significant reduction in the possibility of barium sulphate precipitation occurring near the wellbore at elevated seawater fractions, especially above 65-70% seawater content. It would be interesting to confirm this interpretation with other production data, such as well productivities.

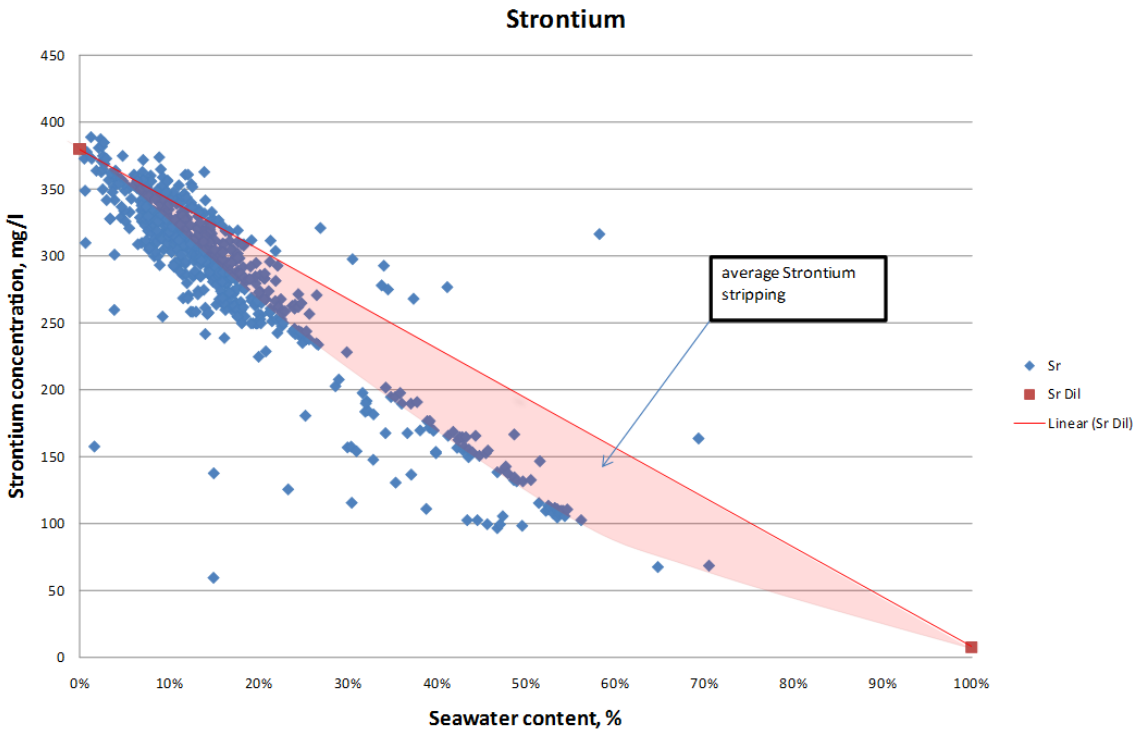


**Figure 41 - Strontium concentration in the produced brine for different seawater contents.**

Figure 41 also suggests some ion stripping, but in this case strontium stripping. The strontium stripping is less severe when compared with barium stripping. This is quite consistent, since strontium sulphate is much more soluble than barium sulphate.

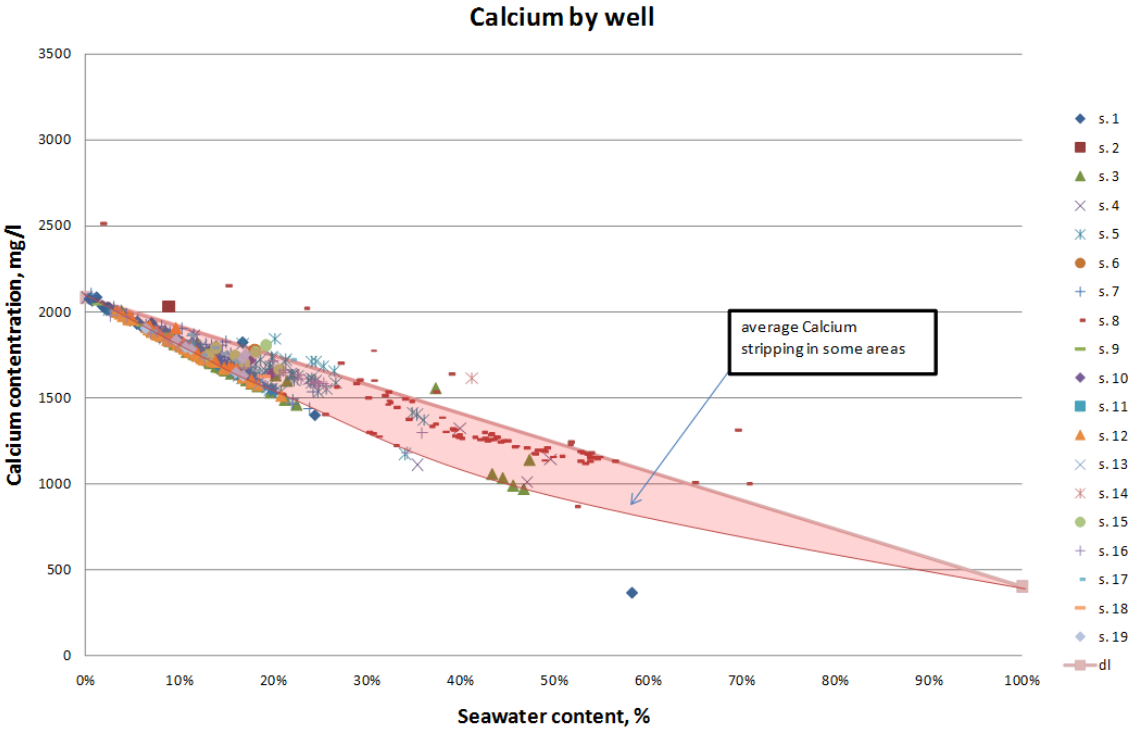


**Figure 42 - Calcium concentration (by well) in the produced brine for different seawater contents.**

In the case of calcium, the data was analysed well by well and a different colour was used for each well. According to the interpretation of Figure 42, in some wells (regions of the reservoir) there is calcium stripping while in other wells (areas) the ion concentrations follow the dilution line; this means that in some areas no calcium stripping was observed. In order to clarify the reasons why this phenomenon just occurs in some areas, further information about the reservoir would be required, such as pressure variations, differences in mineralogy, differences in sweep patterns, etc. The data do not suggest a calcium carbonate precipitation deep in the reservoir because the initial point in Figure 42 is the same for all the wells, and the shape of the curve shows interaction with the seawater and not only an isolated formation brine phenomenon.

### 2.10.2 OTHER OBSERVATIONS

The variation in ion concentrations of some wells as a function of time provides additional support for the interpretation previously mentioned that there is a variation in the formation brine compositions across this reservoir. Figure 43 shows the barium concentration versus time for well A2. It can clearly be observed that the barium concentration is increasing while there is no mixing with injected brine in the well i.e. before seawater breakthrough. Figure 44 illustrates the same phenomenon in the same well, this time in relation to strontium.

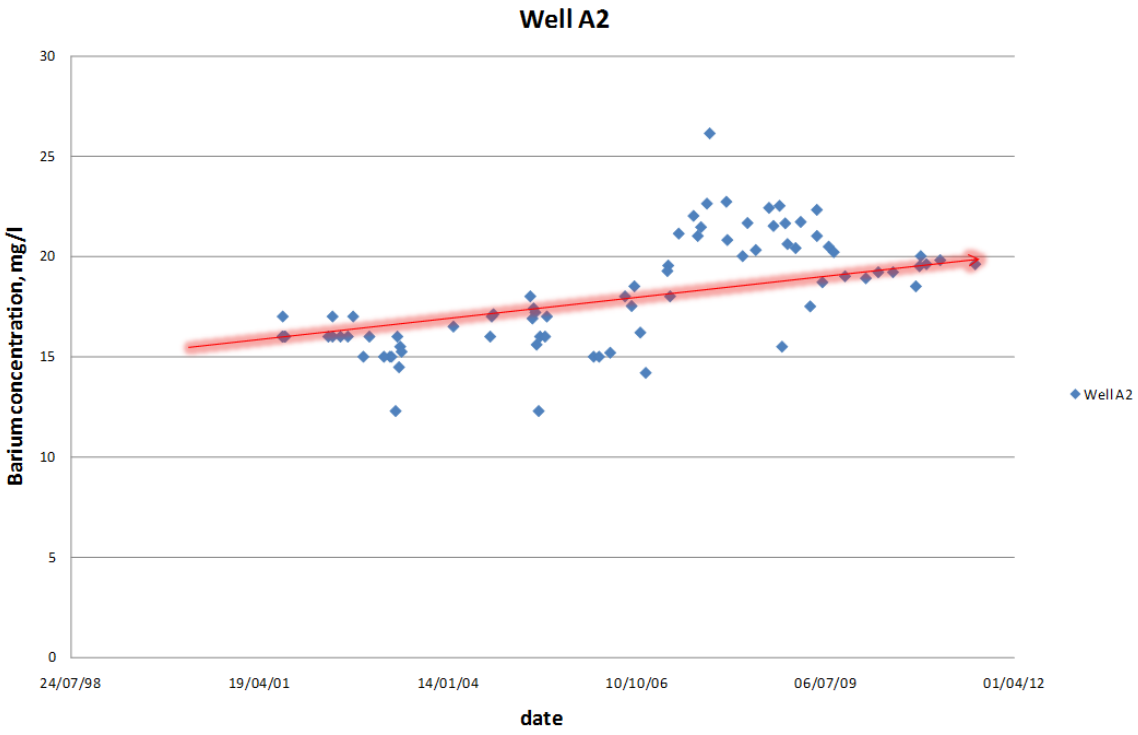


**Figure 43 - Barium production history in well A2**

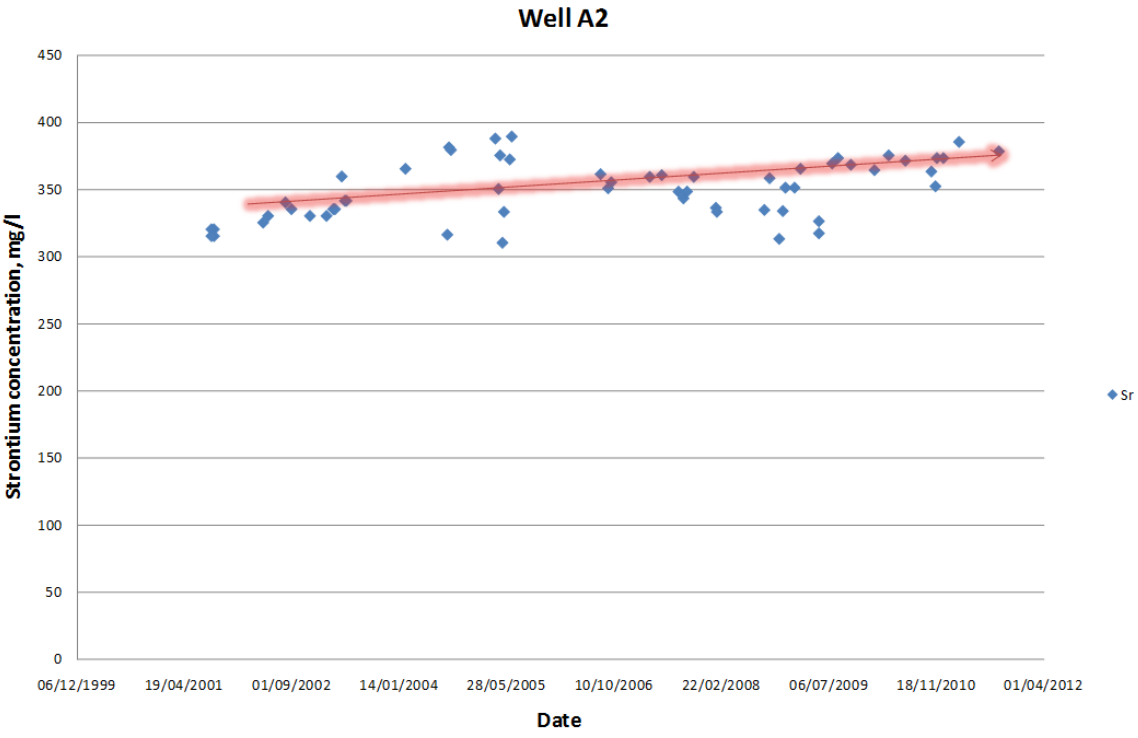


**Figure 44 - Strontium production history in well A2**

Another interesting observation is associated with the magnesium concentration, which is depleted when compared with the dilution mixing line (Figure 45). In fact this

phenomenon has been observed in various field cases. In Field I, this phenomenon can be partially explained by ion exchange between calcium and magnesium. However, further study is required for a complete understanding of the magnesium interactions inside the reservoir.

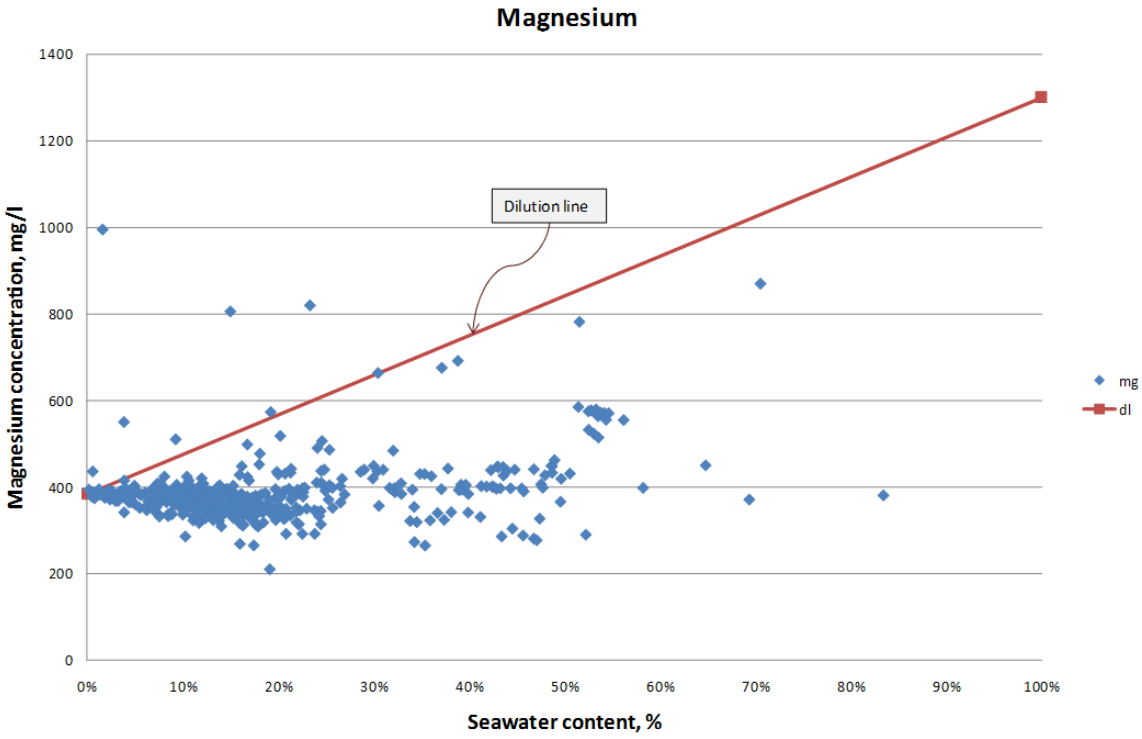


**Figure 45 - Observed magnesium concentration versus seawater content**

### 2.10.2.1 Further Analysis of Field I Data

Based on the suggested data and the Multiscale® [31] calculations, it is possible to develop a 3D scaling tendency surface for the field. Figure 46 shows a generic response surface of SR as a function of barium and sulphate concentrations of the mixing brines (injected and formation brines). In this new approach we consider the possibility of barium stripping deep in the reservoir. It is important to note that the red line in Figure 46 represents no reactions in the reservoir; as a consequence it shows the effect of the direct mix of brines. Figure 47 is an equivalent calculation of the situation where no in situ precipitation takes place (equivalent to the red line in Figure 46).

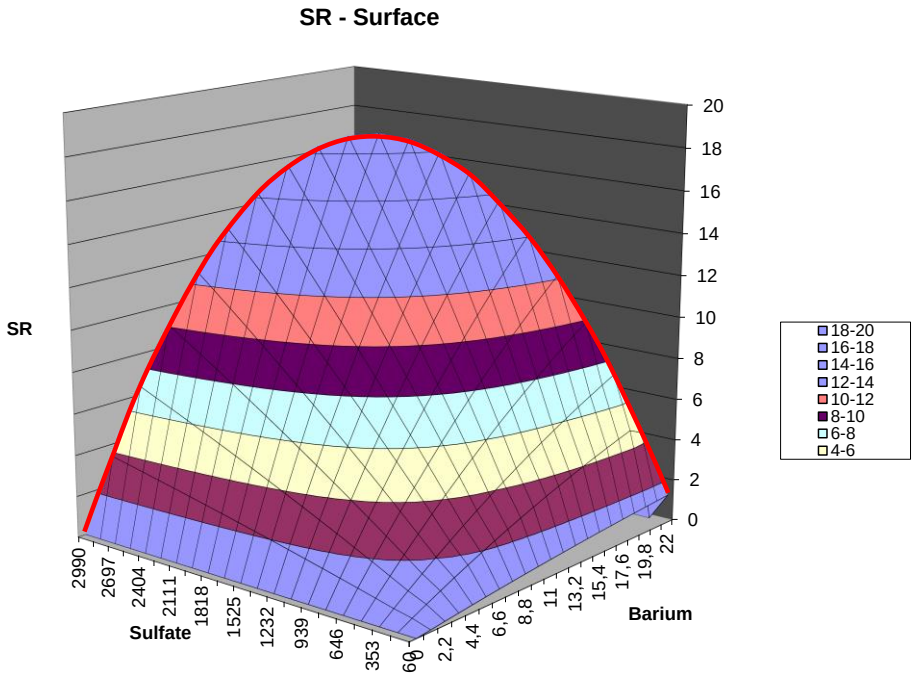


**Figure 46 - Surface response of SR for a mix of injected and formation brines, including the reservoir reaction effect on scale tendency.**

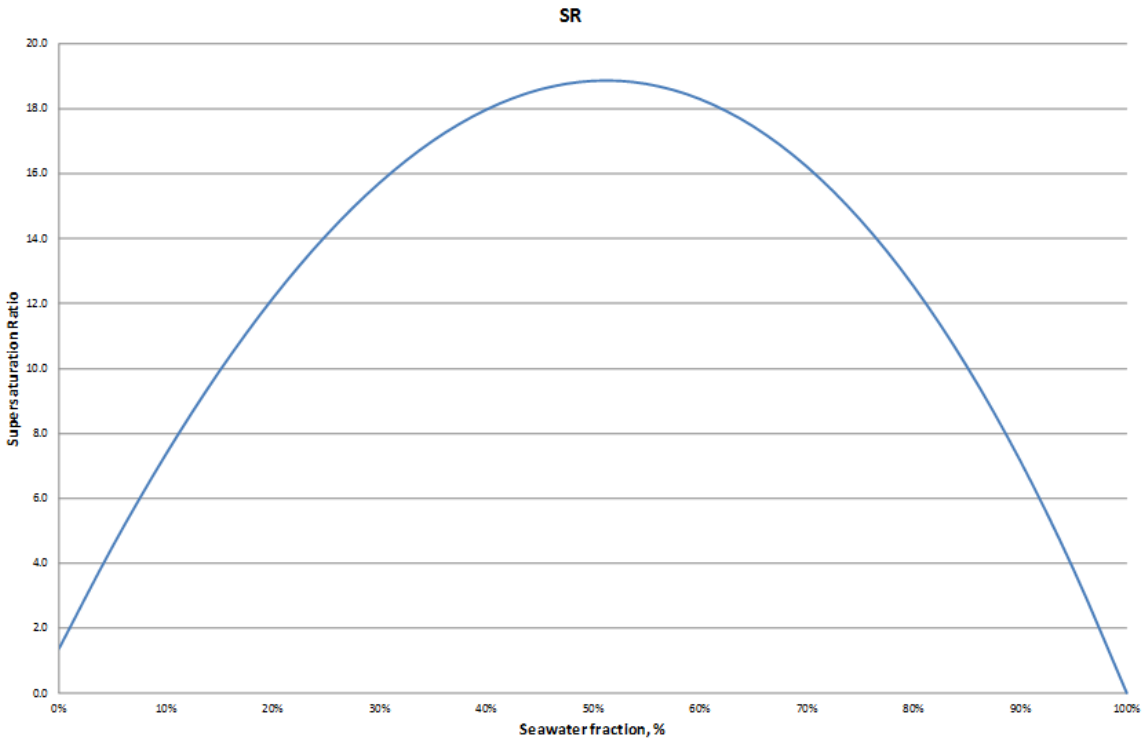


**Figure 47- Super saturation for a direct mix of brines (injected and formation), with no reservoir reactions.**

In order to simulate the data using Multiscale® [31], the formation brine was assumed to have a pH value of 7 and a generic seawater composition was used with a sulphate concentration of 2990 mg/l.

Another useful observation is the comparison between the barium and sulphate concentrations in the produced brine. Figure 48 shows this comparison, as well as a fitted curve that represents the average barium versus sulphate in the wells.

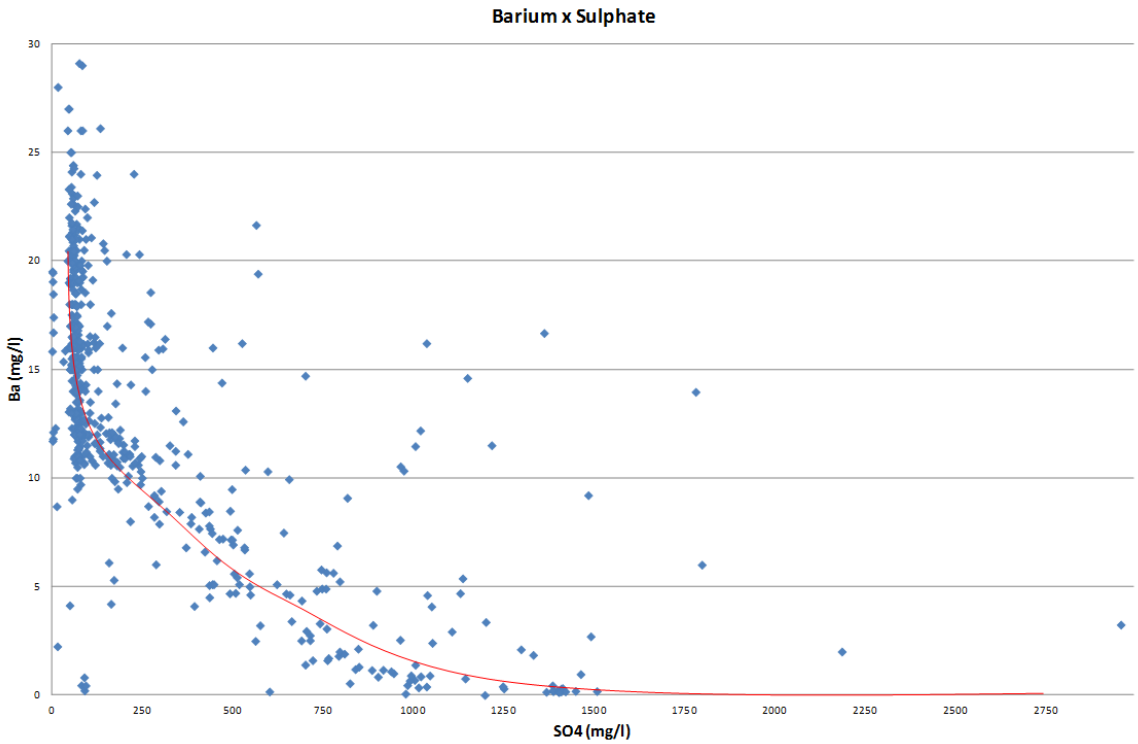


**Figure 48 - Barium versus Sulphate in the resulting production brine for all wells Field I.**

Based on the average curve (sulphate versus barium), and assuming that scale deposition in the near wellbore area was not very significant (because there is no evidence reported of significant productivity losses attributed to scale damage), one can estimate an average scale tendency in the wells and the maximum precipitation from the resulting production brine. Figure 49 illustrate this calculation.

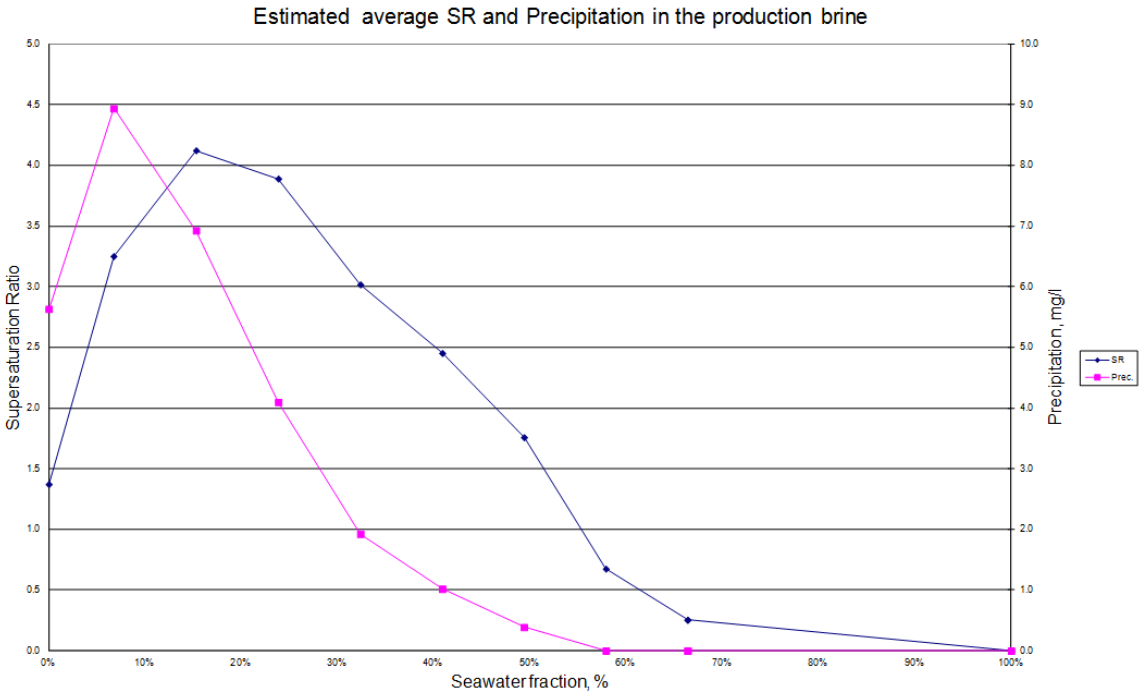


**Figure 49 - Saturation ratio and precipitation values for a well in this reservoir.**

Figure 49 shows how the reservoir behaviour can change the shape of the curves of saturation ratio and precipitation. When one does not consider the reservoir effect, these curves usually have the maximum saturation ratio between 50% and 60% seawater fraction. In this case, due to the effect of reactions in the reservoir, the maximum potential for scale is estimated around 20% seawater fraction.

Although the barium concentration is very low at seawater fractions above 50%, the calculation of saturation ratio shows that barium sulphate precipitation can occur at seawater contents of up to 70% (Figure 49). Thus, this well should be squeezed until 70-75% of seawater content (a conservative estimate because we work with average data). Moreover, the MIC is very low above 60% seawater content.

It is important to emphasize that brine production usually increases with the seawater content. Thus, although there is more precipitation per volume at small seawater fractions, in some cases the total mass of precipitation can be larger at intermediate seawater fractions. Therefore, Figure 49 has to be analysed in conjunction with other sources of information, such as water production rates.

## 2.11 OTHER RESERVOIRS

The behaviour of several other reservoirs was evaluated and the results, as well as in the examples shown throughout Chapter 2, indicated that the chemical reactions occurring inside the reservoir are relevant for the development of an optimized scale management strategy.

It is evident that, in a general manner, some of the ions do not follow the concentration expected from the dilution line, showing that several types of chemical reactions occur inside the reservoir, making it complex to forecast the resulting brine composition. The exceptions are the chloride and sodium ions that are less affected by chemical reactions and in a general manner, present a good correlation with the injected water content calculated by the reacting ions method [59,61].

## 2.12 MAGNESIUM BEHAVIOUR

Another observation from the data presented above is regarding magnesium behaviour. The results showed that magnesium participates in reactions inside the reservoir that affect its concentration significantly. There are also studies that correlate the substitution of calcium by magnesium in the chalk in order to explain enhanced oil recovery [62]. Hence, this ion cannot be used as a tracer to calculate injected water content.

To illustrate the observations, the magnesium behaviour is organized in groups, as will be seen in the following sections.

### 2.12.1 GROUP 1

In this group, the magnesium behaviour is characterized by concentrations below the dilution line for injected water contents of up to 60-70%, when magnesium concentrations become equal or even above the concentration expected by the dilution line. Figure 50 to Figure 53 show examples.

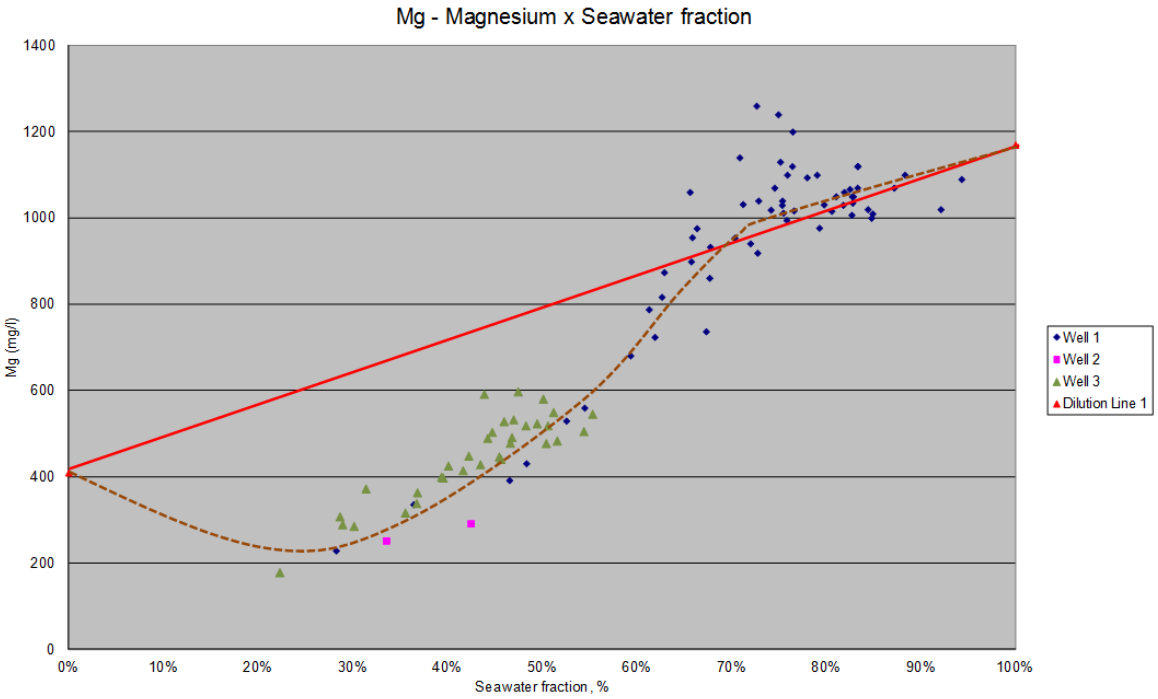


**Figure 50 - Magnesium versus seawater fraction (Example 1 – group 1).**

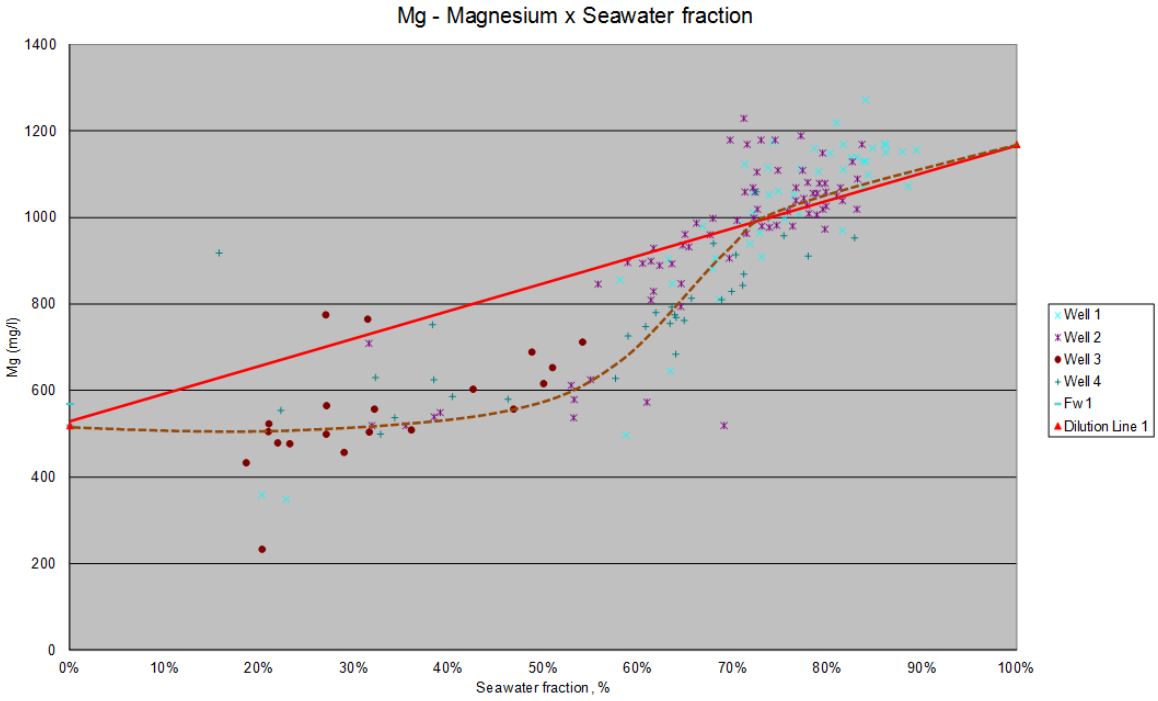


**Figure 51 - Magnesium versus seawater fraction (Example 2 – group 1).**

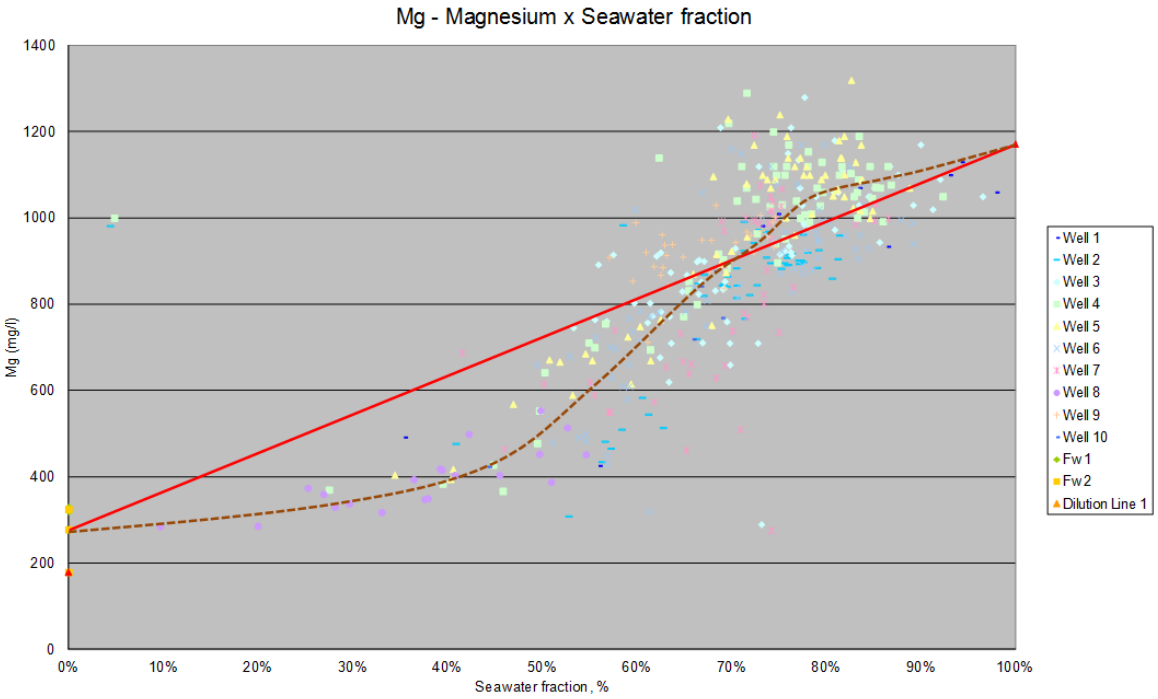


**Figure 52 - Magnesium versus seawater fraction (Example 3 – group 1).**

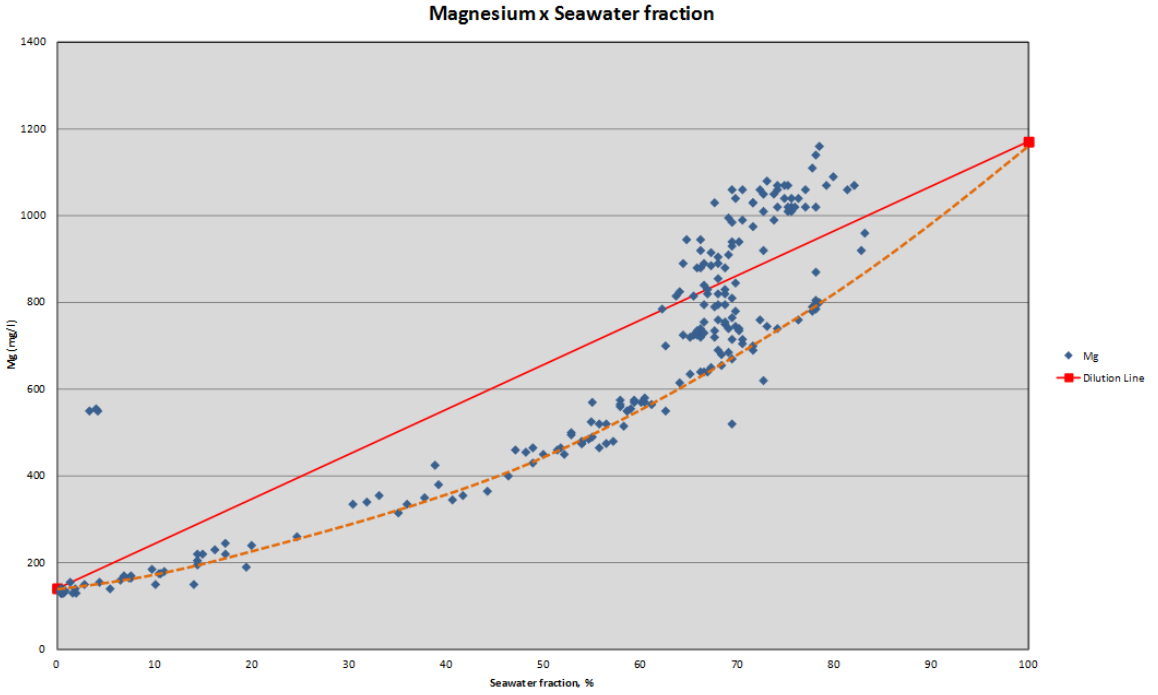


**Figure 53 - Magnesium versus seawater fraction (Example 4 – group 1).**

All the reservoirs used to collect data presented in Figure 50 to Figure 53 are unconsolidated sandstones, with porosities around 30%, water saturations ranging from 15 to 30% and permeabilities ranging from 1000-3000 mD with full sulphate seawater as the injected water. As can be seen, for seawater contents below 60-70% the

magnesium concentration clearly lies below the dilution line and there is a marked change in this behaviour when the seawater content increases to values above 70%.

### 2.12.2 GROUP 2

For a few cases, the magnesium concentration lies below the dilution line for injected water contents ranging from 0 to 100%. This kind of behaviour is defined as group 2 and Figure 54 shows an example of the magnesium behaviour for a reservoir that belongs to group 2.

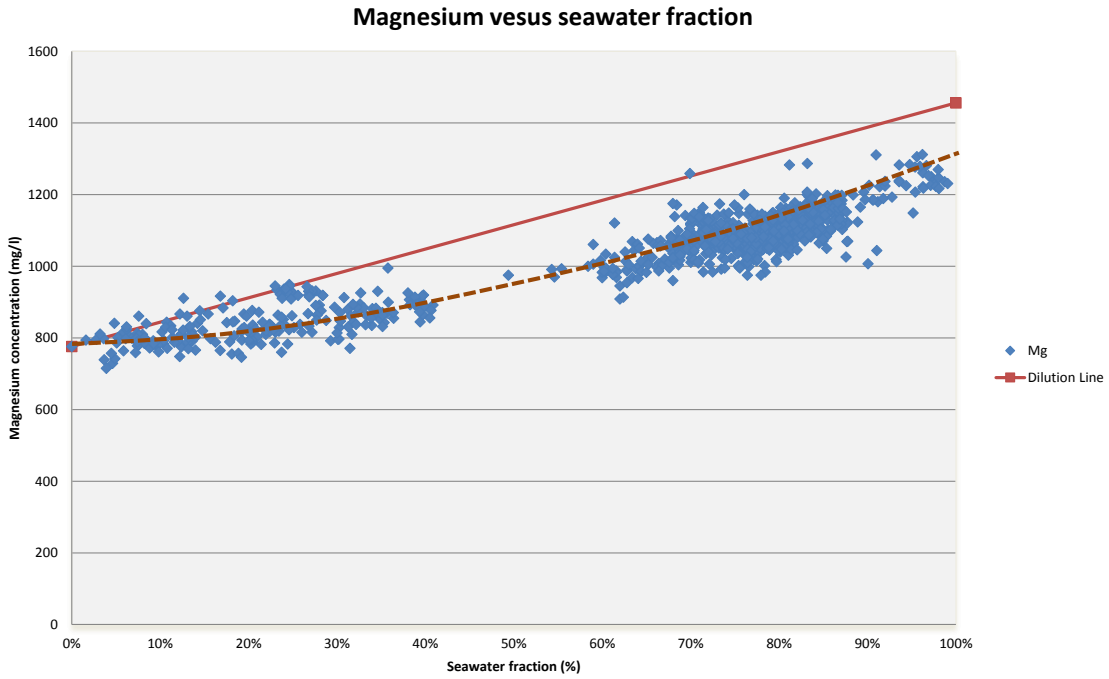


**Figure 54- Magnesium versus seawater fraction (Example 1 – group 2).**

The data presented in Figure 54 were collected from a sandstone reservoir, with porosity around 24% and very low water saturations (around 5%). As can be seen, the magnesium concentration lies below the dilution line for the entire range of seawater contents.

### 2.12.3 GROUP 3

Group 3 is formed by reservoirs that could fit in both groups 1 and 2; however, the history available did not reach the seawater content when magnesium concentration

changes the tendency, as presented in Figures 55-58. This behaviour is emphasized as a group because of the considerable number of reservoir cases that are in this situation.

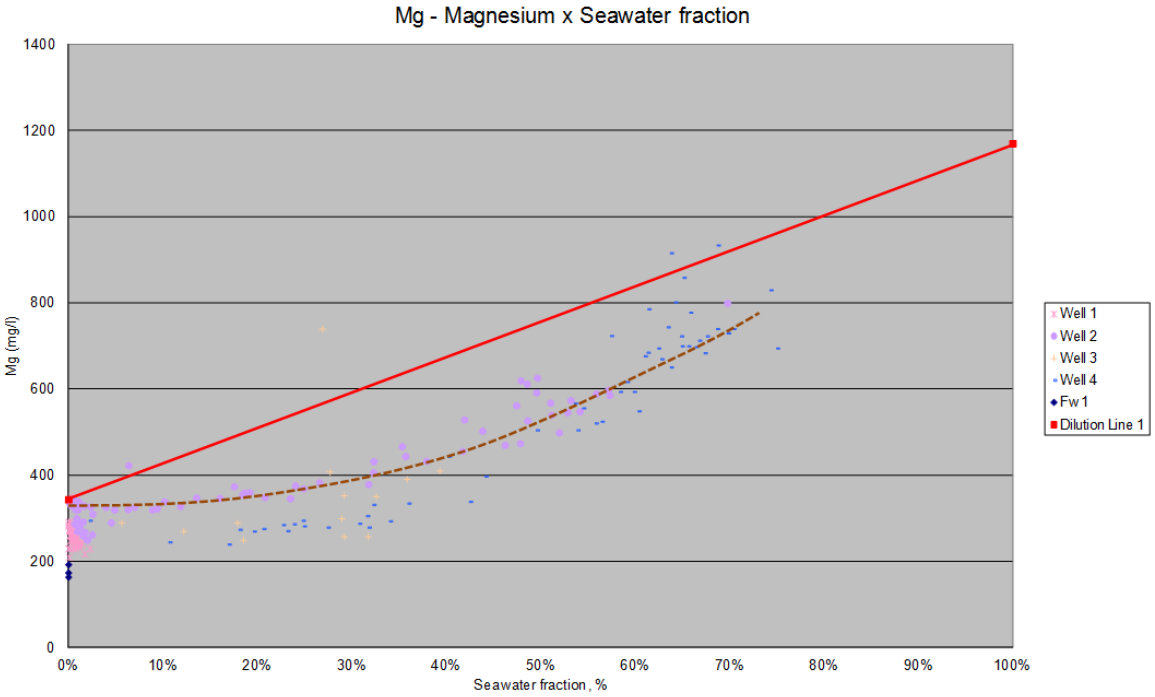


**Figure 55 - Magnesium versus seawater fraction (Example 1 – group 3).**

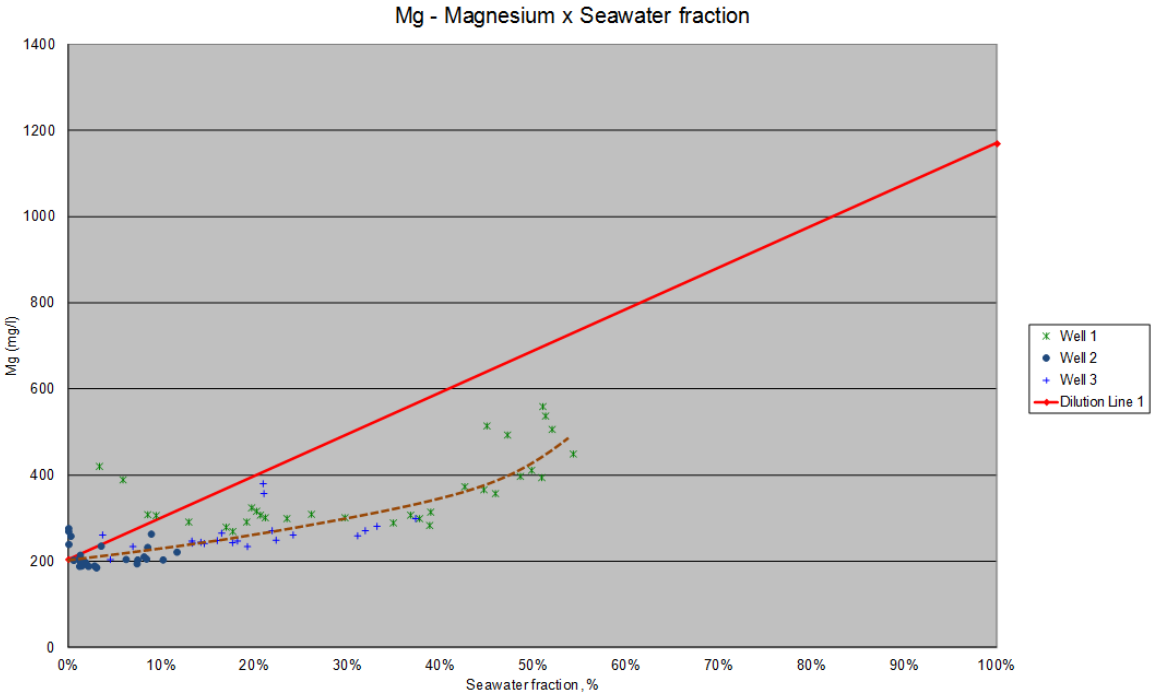


**Figure 56 - Magnesium versus seawater fraction (Example 2 – group 3).**

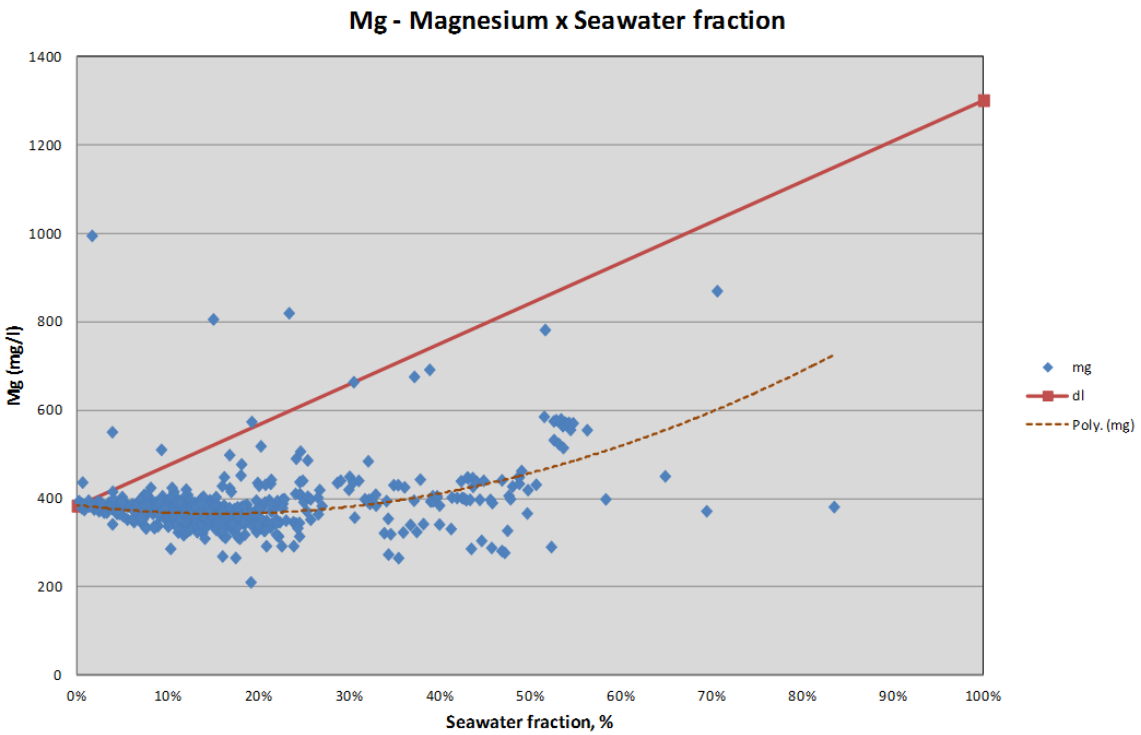


**Figure 57- Magnesium versus seawater fraction (Example 3 – group 3).**

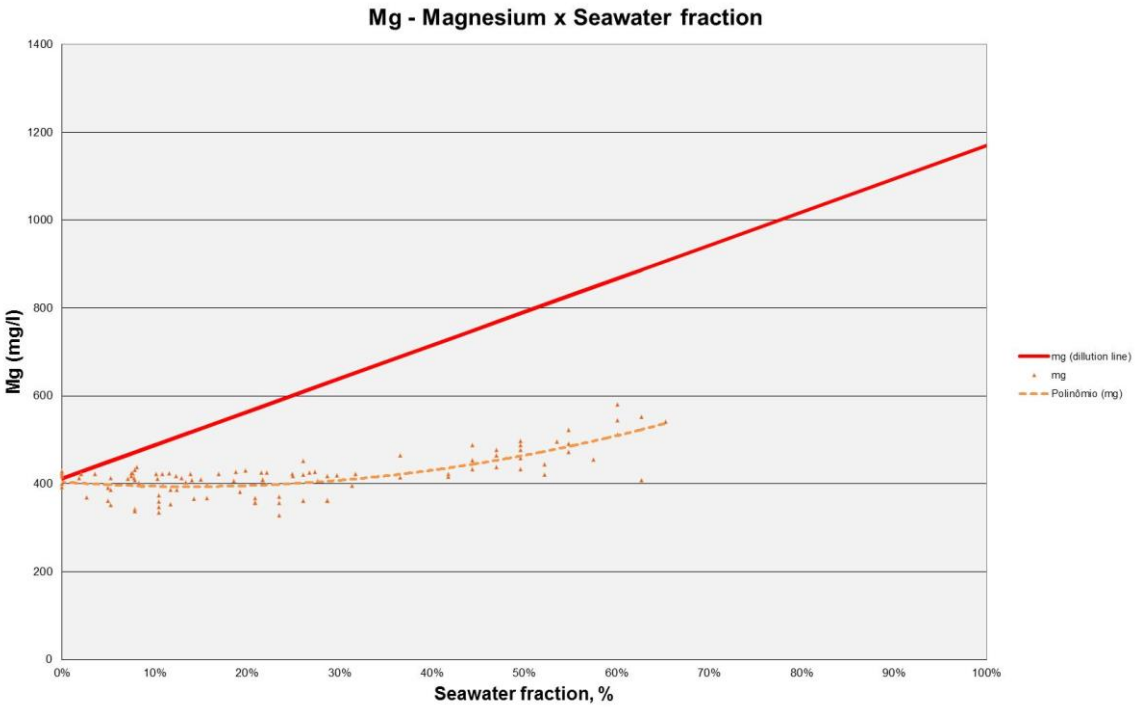


**Figure 58 - Magnesium versus seawater fraction (Example 4 – group 3).**

### 2.12.4 OTHER CASES

In all the reservoir data analyzed in this study apart from those shown Figure 50 to Figure 53, the magnesium concentrations were never above the dilution line. The dataset available for this study had one case in which the formation water magnesium concentration is higher than the seawater concentration. Even in this case, the magnesium concentration falls below the dilution line for seawater contents higher than 35%, as can be seen in Figure 28, indicating the occurrence of magnesium stripping.

## 2.13 COMPILED RESULTS

Table 13 shows a summary of the compiled results observed in chapter 2. It is important to emphasize that table 13 shows general results, however other results may occur depending on the reservoir conditions (pH, temperature, mineralogy, etc.) and initial brine compositions.

**Table 13 - Chapter 2 Compiled Results**

| Reservoir formation | Barium | Strontium | Calcium | Magnesium | Sulphate |
|---|---|---|---|---|---|
| Sandstone reservoirs | Generally significant stripping (due to very low solubility of $BaSO_4$) | Only minor stripping (due to higher solubility of $SrSO_4$) | Some stripping and/or ion exchange, but often in excess | Variable - May increase or decrease due to ion exchange | Generally in excess, so little deviation |
| Carbonate reservoirs | Extent of stripping dependent on amount of sulphate available after sulphate stripping | Little change | Stripping depends on temperature and initial concentration. | Significant stripping | Significant stripping (at high temperature) |

# CHAPTER 3: RESERVOIR SIMULATORS

In hydrologic systems reactive-transport simulation systems has evolved into a relatively mature set of techniques for modeling a variety of subsurface phenomena [78]. Unfortunately these simulators are not directly applicable to oil production, partly because of the lack of complex phase behavior of mixed hydrocarbon suitable treatment, and partly because of important options that are only available in commercial reservoir simulators (well management, interface with surface-network simulators, horizontal wells, complex phase behavior, enhanced oil recovery processes, etc.).

The building of a full field reservoir simulation model is a huge task. The goal is to build a model of the reservoir that represents the true system but it is impossible to know all static and dynamic multiphase flow properties of the reservoir. Consequently the model should be history matched so that, briefly, the simulator properly predicts the fluid outputs and pressures of the wells in the reservoir. Once a reasonably history match is obtained, the model can be used to predict production and injection profiles, infill wells, etc.). Based on a comparative economic analysis, the optimum development and producing strategy can be selected for implementation. History Matching is a time consuming process and depends greatly on a properly selected reservoir simulator. So, it would be advisable that the same selected simulator for history matching had the reaction capability for treating scale problems. If that is not the case, the chosen simulator with the reaction option should as close as possible as the latter. Therefore, there are not so many options for choosing a proper simulator considering all the relevant capabilities.

The focus in this thesis is not on mathematical modelling but on reviewing some representative reservoir simulators with respect to their reaction capabilities mainly for application to the scale problem in oil producing fields. The idea is to develop the basic motivating ideas, taking care to introduce only those mathematical notions that are absolutely essential.

This chapter presents the evaluation of reservoir simulators in terms of scale management. The positive and negative aspects of each simulator are discussed as well as examples of application. All the examples presented in this chapter are composed of

synthetic cases which are used to evaluate the simulators' capabilities to reproduce the occurrence of scale. If the simulator has the capability to model chemical reactions inside the reservoir, an attempt is made to represent ion stripping.

## 3.1 IMEX AND ECLIPSE 100

Commonly, operators use black-oil models for field predictions where hydrocarbon composition do not vary significantly, and these models, such as ECLIPSE 100 [63] and IMEX [64], do not have options to include chemical reactions and their effects on brine composition. Either of the commercial simulators mentioned have keywords only for tracking the injected brine or to calculate the resulting salinity. These models also do not have coupled energy equations, so they are isothermal. Therefore, both of these models are limited with regards to usefulness for scale analysis. Even if one only uses them for sulphate scales, the results should be interpreted carefully due to these limitations.

ECLIPSE 100 [63] has a very limited module to simulate scale in the wells, based on look up tables. The first table gives the rate of scale deposition as a function of seawater fraction, and the second table should provide a production index (PI) reduction as a function of scale deposition. These tables should be based on thermodynamic curves; however, this model does not consider any brine reaction deep in the reservoir and it is limited to a narrow range of scenarios. Hence, even this simplified model should be used carefully, because it can lead to larger errors due to its ignoring the changes in brine composition occurring in the reservoir. Other challenges include the difficulty to calibrate the PI reduction as function of scale deposition for each well. For these reasons, these keywords are very seldom used for scale management purposes.

As mentioned earlier, a possible use of IMEX [64] or ECLIPSE 100 [63] is to model tracer injection to estimate injected water content for each well. However, even in these cases it is necessary to be cautious when using the results provided due to numerical dispersion.

With the aim of illustrating the use of ECLIPSE 100 [63], in which the two tables (14 and 15) that allow one to reproduce productivity index losses due to scaling, one of the wells belonging to Reservoir A presented in Chapter 2 with permanent downhole gauge (PDG) data available, and in which scaling did occurs was modeled.

**Table 14 - ECLIPSE100 [63] Scale deposition table example**

| Sea water fraction | Scale deposition rate ($g/m^3$) |
|---|---|
| 0 | 0 |
| 0.001 | 0.2 |
| 0.1 | 1.2 |
| 0.2 | 2.4 |
| 0.3 | 2.8 |
| 0.4 | 3.2 |
| 0.5 | 2.4 |
| 0.6 | 2.0 |
| 0.7 | 1.07 |
| 0.8 | 0.8 |
| 0.9 | 0.53 |

**Table 15 - ECLIPSE100 [63] Scale damage table example**

| Scale deposition (g/m) | PI reduction multiplier |
|---|---|
| 0 | 1 |
| 10 | 0.99 |
| 20 | 0.8 |
| 30 | 0.7 |
| 40 | 0.6 |
| 50 | 0.5 |
| 60 | 0.4 |
| 70 | 0.3 |
| 80 | 0.2 |
| 90 | 0.1 |
| 100 | 0.000000001 |

Figure 59 shows ECLIPSE 100 [63] simulation results using tables 14 and 15.

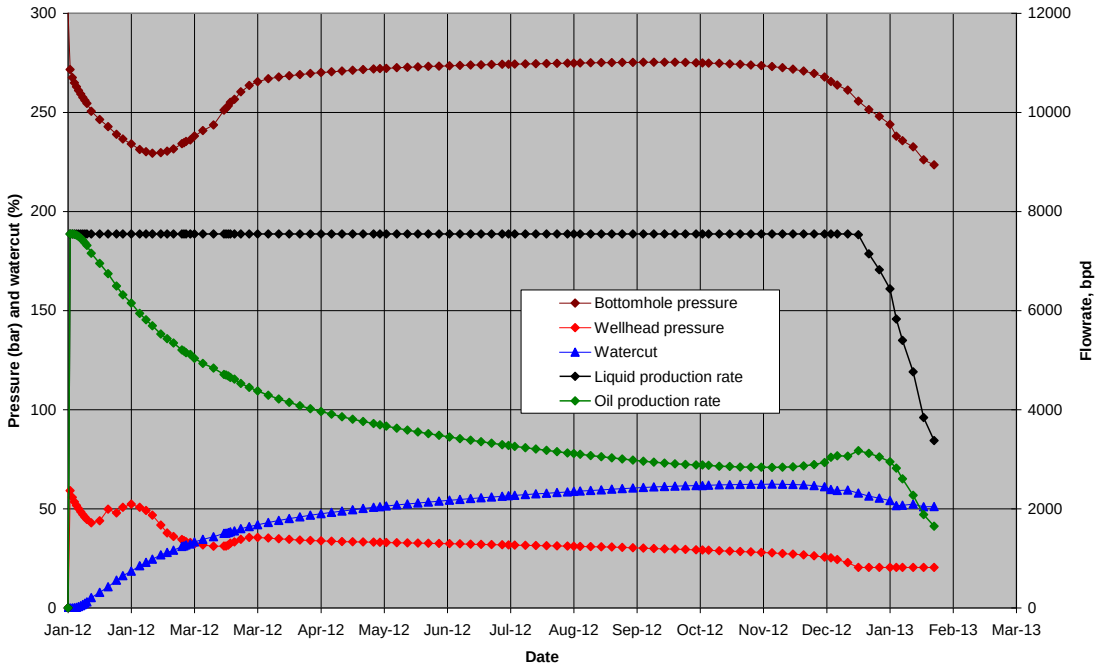


**Figure 59 – Production history of a well with scale occurrence beginning in nov/12**

As can be seen from Figure 59, the well starts production with a fluid flow rate of 7500 bpd. The watercut increases until it reaches the beginning of the scaling window in December 2012. Scaling window is the seawater fraction interval in which scaling may occur. From then on it is possible to observe a reduction in the bottomhole pressure, flowrate and also watercut. It is important to mention that in this simulation the well is started up and the maximum flow rate is set to 7500 bpd. The flow rate is kept constant until the scale precipitation reduces the productivity index such that it is no longer possible to sustain the flow rate of 7500 bpd and the well starts to be controlled by wellhead pressure.

An approach such as the one presented in Figure 59 can be used to history match wells with scale damage. The behavior of several wells was evaluated with this approach and the parameters needed to obtain the match varied significantly, even in wells belonging to the same reservoir. These results identify that it is not possible to extrapolate the results obtained in one well to other wells, giving evidence of the fragility of the predictive capability of these functions in ECLIPSE 100 [63].

## 3.2 STARS

STARS [65] is a finite difference simulator that models chemical reactions and changes in the permeability due to precipitation, and calculates temperature variations as well. As a result, it can be used to analyse compositional changes in the brine throughout the reservoir. However, the analysed version of this simulator does not have a thermodynamic prediction model; as a consequence, this does not provide an accurate result for chemical reactions.

The chemical reactions modelled are based on kinetic reactions; with the speed of the reactions an important parameter. Naturally, there is a conservation equation for each chemical component, as well as equations describing phase equilibrium between the phases. Indeed, there is a set of these equations for each block of the discretized grid. (22 represents the general heterogeneous mass transfer reaction.

$$\sum_{i=1}^{n_r} S_{ki}\, A_i \rightarrow \sum_{j=1}^{n_p} S_{kj}\, A_j + H_{rk} \tag{22}$$

The first and second terms of equation 24 represent, respectively, the reactants and the products of reaction k and the third term is the enthalpy of the reaction (energy/mol). The term "A" represents the same element that is present in the reactant ($A_{i,}$) and, as the reaction takes place, is also present in the product ($A_j$). $S_{ki}$ and $S_{kj}$ are respectively the stoichiometric coefficients of the reactant i and product j in reaction k. If $H_{rk}$ is positive the chemical reaction is exothermic; if it is negative the chemical reaction is endothermic.

Equation 23 illustrates the kinetic model in STARS [65] that is based on the Collision theory which is similar to the Arrhenius equation [66].

$$r_k = r_{rk} \times e^{\frac{-E_{ak}}{RT}} \times \prod_{i=1}^{n_c} C_i^{e_k} \tag{23}$$

Where $E_{ak}$ is the activation energy and $r_{rk}$ is the pre-exponential factor of the reaction k. R is the gas constant (R= 8.314472 J $\cdot$ $K^{-1}$ $\cdot$ $mol^{-1}$) and T is the absolute temperature.

The activation energy, $E_{ak}$, determines the temperature dependence of $r_k$. A positive value means an increase in the reaction rate as function of increasing temperature and a negative value means a decrease in the reaction rate as a function of increasing temperature. The enthalpies of reaction can be characterized between well defined limits and can be calculate by thermodynamic principles. The concentration factor for reacting component *i* is (equation 24):

$$C_i = \varphi_f \rho_j S_j x_{ji} \qquad j = w, o, g \qquad (24)$$

Where *j* is the phase in which component *i* is reacting, and $x_{ji}$ represents water, oil or gas mole fractions. $\varphi_f$ represents the fraction of the porous medium occupied by fluid phases (water, oil and gas). For the solid component, equation 25 is used:

$$C_i = (1 - \varphi_f) c_i \qquad (25)$$

Where $c_i$ is the concentration of component *i* in the solid phase.

The partial pressure form $C_i = y_i p_g$ is available also.

Where $y_i$ is the molar fraction of component *i* in the gas phase and $p_g$ is the pressure of the gas phase.

In STARS [65] the pre-exponential factor (equation 28) can be a function of fluid velocities, permeability or a constant factor. Another important point for modelling some chemical reactions is that there are five parameters used to calculate the partitioning of elements as a function of temperature and pressure. Equations 26 to (28 are used for the partitioning of gas to liquid (or liquid/liquid).

$$K = \left(\frac{K_{v1}}{p} + K_{v2} \times p + K_{v3}\right) \times e^{\frac{K_{v4}}{(T - K_{v5})}} \qquad (26)$$

$$K_{\left(\frac{gas}{liq}\right)} = \frac{gas\ mole\ fraction}{water\ mole\ fraction} = \frac{y}{w} \qquad (27)$$

$$K_{\left(\frac{liq}{liq}\right)} = \frac{oil\ mole\ fraction}{water\ mole\ fraction} = \frac{x}{w} \qquad (28)$$

As already mentioned, STARS [65] allows for chemical reactions, but it does not have a coupled thermodynamic prediction model, and it is also not possible to include solubility of the elements and a reaction rate as function of pressure and temperature. An advantage of this simulator is the easy way to include chemical reactions that the modeller may wish to specify and it is also easy to interpret the results, but the limitation is the inability to accurately model the kinetics of all the relevant reactions.

Although this software does not have a thermodynamic model, it is possible to obtain reasonable results for some sulphate reactions, such as barite precipitation, since barite has a very low solubility. In order to model other reactions it could be useful to include two equations for both dissolution and precipitation.

With the aim of evaluating the use of STARS [65], a reservoir in which the main scaling reaction is barium sulphate was modelled. The calcium concentration of the formation brine is lower than 2000 mg/l and the temperature is lower than 90ºC, such that reactions involving calcium were neglected. The parameter controlling the speed of the reaction is adjusted to match the wells, as can be seen in Figure 60. With this match, it is possible to evaluate the barium and sulphate concentrations vs the time and associate them with the saturation ratio 3D surface presented in Figure 17, giving the opportunity to estimate the duration of the scaling window, aiding the development of the scale management strategy. The main challenge to the use of this simulator is to obtain the parameter related to the speed of reaction during the project phase, since it is obtained by history matching. It is important to point out that the results of the STARS [65] simulations are very sensitive to this parameter.

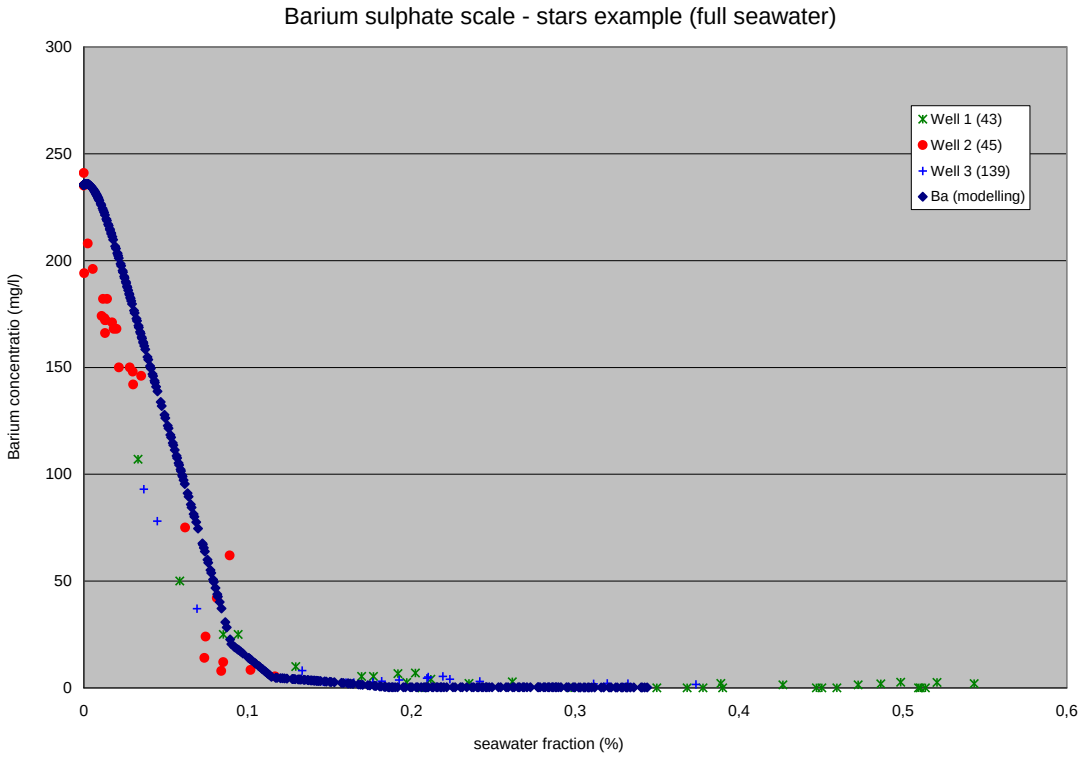


**Figure 60 – Stars simulation of barium concentrations compared with observed production data**

As one can see in Figure 60, it was possible to fit produced barium by well in Reservoir C using STARS [65].

## 3.3 GEM

GEM [67] is a fully compositional finite difference simulator that allows chemical reactions, changes in the permeability due to precipitation, and models temperature variation as well. As a result, it can be used for modelling aqueous phase chemical reactions and mineral precipitation/dissolution. This simulator also includes chemical equilibrium terms ($K_{eq}$) that can be a constant (equation 29) or a function of temperature in a polynomial equation (equation 30), where the temperature should be in ºC. Hence, it includes a simplified thermodynamic model. It is important to note that this simplified model neglects the effect of pressure on the equilibrium constant. For some components at reservoir conditions this approach can lead to large errors. In order to reduce this issue the modeller should adapt these parameters for reservoir conditions.

$$K_{eq} = const. \tag{29}$$

$$K_{eq} = a_0 + a_1 T + a_2 T^2 + a_3 T^3 + a_4 T^4 \quad (30)$$

There are two types of chemical reactions in GEM [67], the first one is recommended for aqueous components because these reactions are fast relative to mineral dissolution/precipitation. Therefore, these are chemical-equilibrium reactions, but are restricted to reactions not involving minerals. The second option is rate-dependent reactions, and this is specifically for mineral dissolution/precipitation.

a) Aqueous reaction (for species in the aqueous phase only):

The aqueous reactions are based on the thermodynamic equilibrium of the species (equations 31 and 32).

$$Q_\alpha - K_{eq} = 0, \alpha = 1,...,R_{aq} \quad (31)$$

$$Q_\alpha = \prod_{k=1}^{n_{aq}} a_{aq}^{\nu_{k\alpha}} \quad (32)$$

Where $K_{eq}$ is the chemical equilibrium (similar to solubility product mentioned in the literature review) for the aqueous reaction α, $a_k$ is the activity of component k, $\nu_{k\alpha}$ are the stoichiometry coefficients and $Q_\alpha$ is the activity product. The activities $a_k$ are related to the molality $m_k$ (moles per kg of $H_2O$) as follows (Equation 33):

$$a_i = \gamma_i \, m_i \text{ , i = 1,..,naq} \quad (33)$$

Where $\gamma_i$ is the activity coefficient. For an ideal solution, $\gamma_i$ = 1, and the activity is equal to the molality. However, it is possible to use a different model for ionic activity coefficients. The Debye-Huckel method calculates the activity coefficient of a species as a function of the species' size and the ionic strength of the solution. GEM uses an extension of this method that includes a Ḃ-dot parameter which depends on the electrical charge of the species, which varies with temperature (Equation 34) [68]. It is also possible to use the pure Debye-Huckel equation direct, in this case without the second term of the Equation 34 (+$\dot{B}$ $I$).

$$log\ \gamma_i = -\frac{A_\gamma z_i^2 \sqrt{I}}{1 + \mathring{a}_i B_\gamma \sqrt{I}} + BI \quad (34)$$

where A and B are parameters that depend on temperature, density and dielectric constant of water, $z_i$ is the ionic charge of the species i, å is the ion size parameter, $\dot{B}$ is the Ḃ-dot parameter, and I is the ionic strength of the solution defined in the equation 35.

$$I = \frac{1}{2}\sum_{i=1}^{naq} m_i z_i^2 \quad (35)$$

b) Mineral reaction (second approach)

As mentioned above the mineral equation is a rate-dependent reaction, and the dissolution/precipitation reaction is calculated from the Transition State Theory (TST). The reaction rate is based on three fundamental parameters: quantity of mineral available, reaction rate of the reaction, and the degree of super saturation. GEM [67] uses equation 36 that represents the kinetic rate [69]:

$$r_{fi} = \text{sgn}\left[1 - \frac{Q_i}{k_{eqi}}\right].A_i.S_w\left(k_{0i} + \sum_{m=1}^{nct} k_m a_m^x\right)\left\{1 - \left(\frac{Q_i}{k_{eqi}}\right)^y\right\}^z \quad (36)$$

(part 1) (part 2) (part 3)

where $r_{fi}$ is the final dissolution/precipitation rate for the mineral *i*, A is the reactive surface area of mineral *i*, $K_{eqi}$ is the equilibrium constant of the mineral i, and $Q_i$ is the ionic activity product for the mineral *i*. In GEM [67], the activities of all mineral components are set to one. $S_w$ is the water saturation in the cell. The parameters x, y, z are empirical powers. The reaction rates $K_{0i}$, are usually obtained from the literature for a specific temperature. Hence, GEM [67] uses the Arrhenius [66] equation to correct for the reservoir temperature (equation 37). The $a_m$ is the activity of the inhibiting or catalyzing species. In order to explain better (equation 36), it can be divided into three parts. The first part just represents the direction of the reaction, if it is positive there is precipitation, if it is negative there is dissolution, and if it is zero the components are in equilibrium. The second part controls the rate ("speed") of the reaction and the quantity

available for the reaction. Finally, the third part identifies how far from equilibrium the system is.

$$k_i = k_{0i} e^{\left(\frac{-E_{ai}}{R}\left(\frac{1}{T}-\frac{1}{T_0}\right)\right)} \tag{37}$$

Where $E_{ai}$ is the activation energy for reaction *i* [j/mol] and $k_o$ is the reaction rate for the reaction *i* on the reference temperature [mol/($m^2$s)]. The surface area changes with mineral precipitation/dissolution (equation 38).

$$A_i = A_{i0} \frac{N_i}{N_{i0}} \tag{38}$$

Where $A_{i0}$ is the reactive surface area at the initial time, $N_i$ is the mole number of mineral *i* per unit gridblock volume at current time and $N_{0i}$ is the mole number of mineral *i* per unit gridblock bulk volume at the initial time.

A weak point of GEM [67] is the fact that it is not possible to numerically equilibrate the formation brine composition before the start of the simulation. In addition, and associated with this, is the fact that it is not possible to model equilibrium mineral reactions. Thus GEM [67] requires data, such as mineral surface areas and reaction kinetics that often are simply not available. A positive point is the possibility to model the gas solubility in the aqueous phase with Henry's law and vaporization of $H_2O$ into the gas phase. This approach is very useful for modelling calcium carbonate scale or any other scale that depends on the partial pressure of $CO_2$ (i.e. is pH dependant).

Another weak point is that the Ḃ-dot model in the current version of GEM is accurate only for salinities up to approximately seawater salinity. Since many formation waters are more saline than seawater, the Pitzer formulation would be preferred.

In order to present an example of the application of GEM, an analysis of the impact of calcium concentration and reservoir temperature over the concentration of sulphate in the produced brine is going to be presented.

### 3.3.1 Influence of calcium concentration and temperature on produced brine composition

The model used in this example consists of a rectangular reservoir containing a pair of wells, as can be seen in Figure 61.

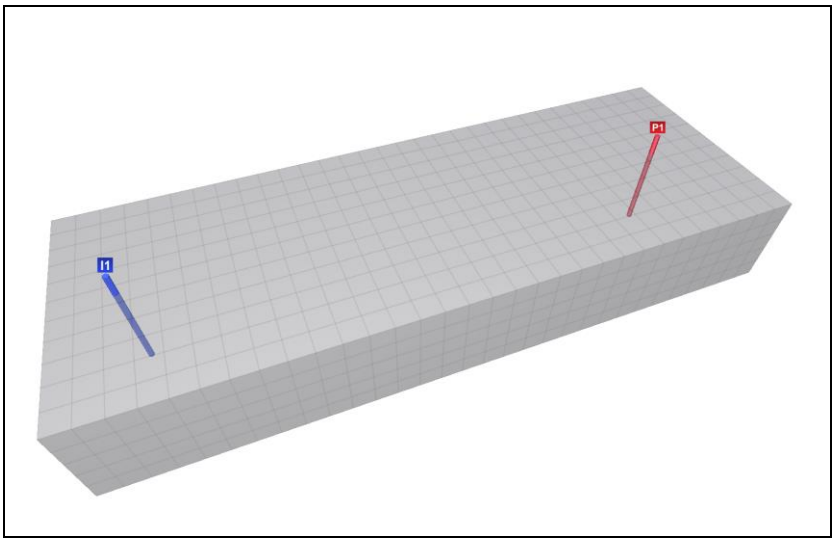


**Figure 61 - Reservoir model.**

The reservoir properties are homogeneous and Corey relative permeability curves were used. Table 16 shows the main reservoir and model properties.

**Table 16 – Main reservoir properties**

| | | | |
|---|---|---|---|
| Φ | 30% | dx | 50 m |
| hor. permeability | 2000 mD | dy | 50 m |
| vert. permeability | 200 mD | dz | 4 m |
| μo | 1,7 | cells in x direction | 31 |
| μw | 1,7 | cells in y direction | 11 |
| krw max | 1 | cells in z direction | 5 |
| kro max | 1 | Initial pressure @-2800 m | 40000 kPa |
| Sor | 0,3 | pore compressibility | $7.2x10^{-7}$ $kPa^{-1}$ |

Both the injector and producer wells are considered to have perforations in the layer placed in the center of the reservoir (layer 3). The wells are placed 1200 m apart from each other, which is typical of offshore reservoirs.

The pressures applied during the whole study are such that during all the simulations there is no free gas inside the reservoir, these being flow of only oil and water.

The geochemical reaction modeled in this study is (Equation 49):

$$CaSO_{4-solid} \leftrightarrow Ca^{++}_{aqueous} + SO^{2-}_{4-aqueous} \tag{39}$$

Reactions involving solids are modeled in GEM [67] as dissolution reactions and the rate of reaction is calculated by Equation 40:

$$r_i = \hat{A} \cdot k_i \cdot \left(1 - \frac{a_i}{K_{eq,i}}\right) \tag{40}$$

Where $r_i$ is the rate, $A_i$ is the reactive surface area for mineral i, $k_i$ is the rate constant for mineral I, $K_{eq,i}$ is the chemical equilibrium constant and $Q_i$ is the activity product of mineral reaction i. The equilibrium constants are considered to be temperature dependent, calculated by the following 4$^{th}$ order polynomial (Equation 41):

$$\log(K_{eq}) = a_0 + a_1 \cdot T + a_2 \cdot T^2 + a_3 \cdot T^3 + a_4 \cdot T^4 \tag{41}$$

The parameters of the polynomials presented in Table 17 were obtained by fitting them to the data published by Kharaka [70].

**Table 17 – Coefficients for calculating the chemical equilibrium constants**

| $a_0$ | $a_1$ | $a_2$ | $a_3$ | $a_4$ |
|---|---|---|---|---|
| -4.2019 | 0.00184827 | -0.000230964 | 1.08082E-06 | -1.76423E-09 |

Figure 62 presents the dependency of the chemical equilibrium constants with temperature.

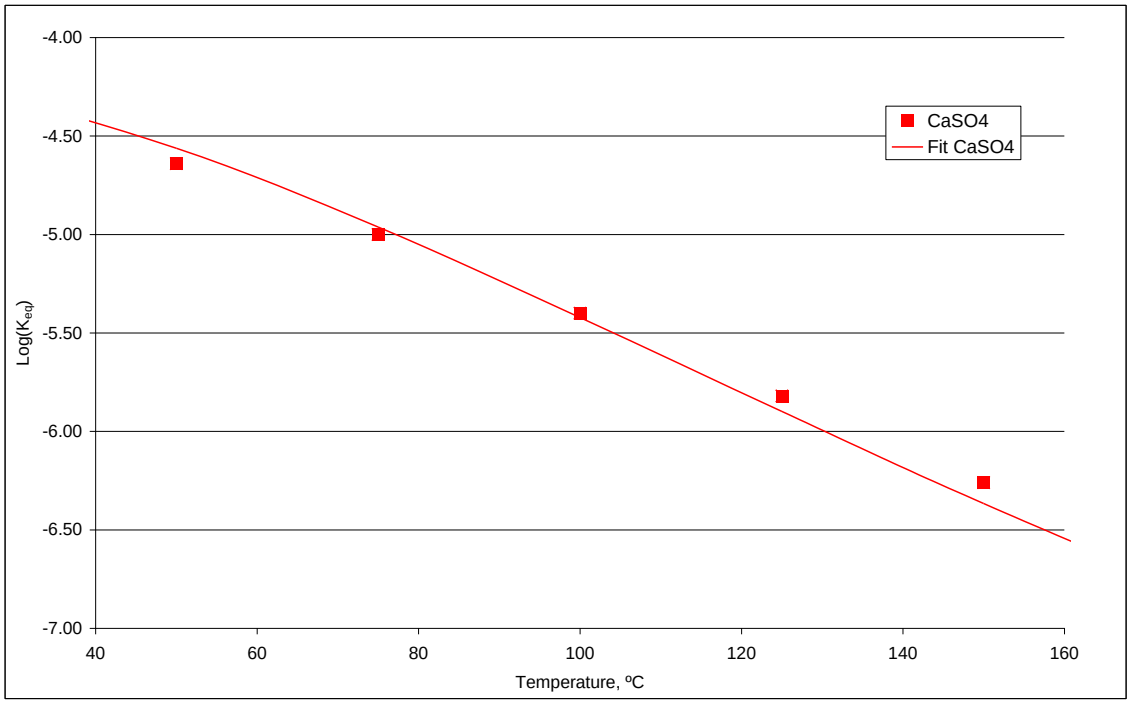


**Figure 62 – Chemical equilibrium constants of $CaSO_4$.**

The activity coefficients, necessary to calculate the activity product, were calculated by the Ḃ-dot model [68]. In order to properly calculate the activity coefficients, we include $Na^+$ and $Cl^-$ as inert components in the formulation.

The reaction rate constants are calculated according to the Arrhenius law [66] (Equation 42):

$$k_i = k_{0i} \cdot e^{-\frac{E_{ai}}{R}\left(\frac{1}{T}-\frac{1}{T_0}\right)} \tag{42}$$

Where $E_{ai}$ is the activation energy and $k_{0i}$ is the reaction rate constant (mol/(m².s)) at the reference temperature $T_0$. In this study, the activation energy for anhydrite ($CaSO_4$) precipitation/dissolution reaction is considered to be 61000 J/mol, according to Kontrec [71]. In a work published by Serafeimides [72], the reaction rate constants in temperatures near 25ºC were in the range of $4 \cdot 10^{-6}$ to $4 \cdot 10^{-5}$ mol/(m$^2$·s), they also presented estimates for the reactive surface area, leading to a value of $1.11 \cdot 10^{7}$ m²/m³. These data by Serafeimides [72] were adopted in the simulations presented below.

The concentrations of calcium, sulphate, sodium and chloride in the injected water (seawater) were 410, 2700, 10800 and 19400 mg/L, respectively. Due to the dependency of $CaSO_4$ solubility upon temperature (Figure 62), it was necessary to model the temperature variations caused by seawater injection at a temperature different from reservoir temperature, otherwise, a significant amount of $CaSO_4$ precipitation would occur in the immediate vicinity of the injector well.

To avoid the undesirable occurrence of mineral reactions upon model initialization, the initial volume fraction of $CaSO_4$ in the reservoir and the sulphate concentration in the formation brine were considered to be zero. By doing this, it is necessary to adopt a minimal reactive surface area, otherwise there would be no mineral reactions occurring during the whole simulation. Sensitivity analysis performed indicated low dependency of the produced water composition on the minimal reactive surface area. The value adopted was 10 $m^2/m^3$.

As can be seen from Figure 63, there is a great dependency of $CaSO_4$ solubility upon temperature, in such a way that it is expected that temperature may play an important role on sulphate stripping caused by $CaSO_4$ precipitation inside the reservoir. Figure 63 presents the sulphate concentration in the produced brine as a function of injected water percentage on the produced brine for different temperatures. For this case, the initial concentrations of calcium, sodium and chloride in the formation brine were set to 22000, 55000 and 125000 mg/L, respectively.

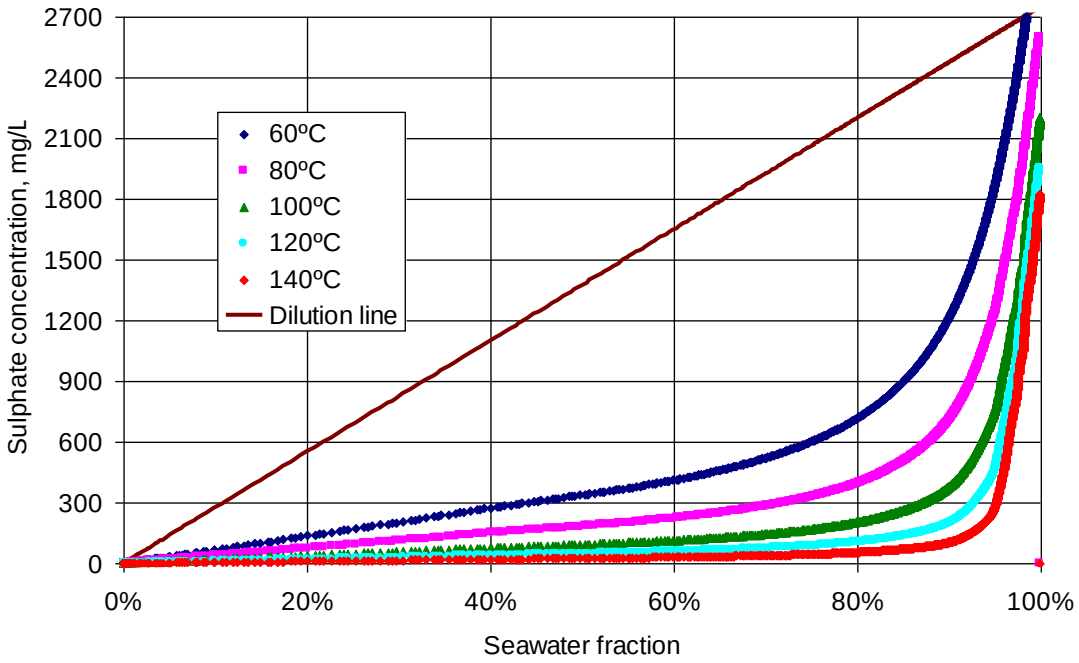


**Figure 63 – sulphate concentration in produced brine for different reservoirs temperatures**

As can be seen from Figure 63, the higher the temperature, the more significant is the sulphate stripping caused by $CaSO_4$ precipitation inside the reservoir. It is also possible to observe that for reservoirs containing high calcium concentrations in the formation brine, the simulations indicate that sulphate stripping occurs even for reservoirs with temperatures as low as 60ºC. Figure 64 presents field data from reservoir G, which has a temperature of 131ºC and a calcium concentration in the formation brine of 22000 mg/L, and the results of simulation under these conditions.

The solubility of $CaSO_4$ is lower at higher temperatures, and temperature will influence which mineral phase is dominant. At 131º C the precipitate will be mainly anhydrite ($CaSO_4$). At 60º C the main phase will be gypsum ($CaSO_4.2H_2O$).

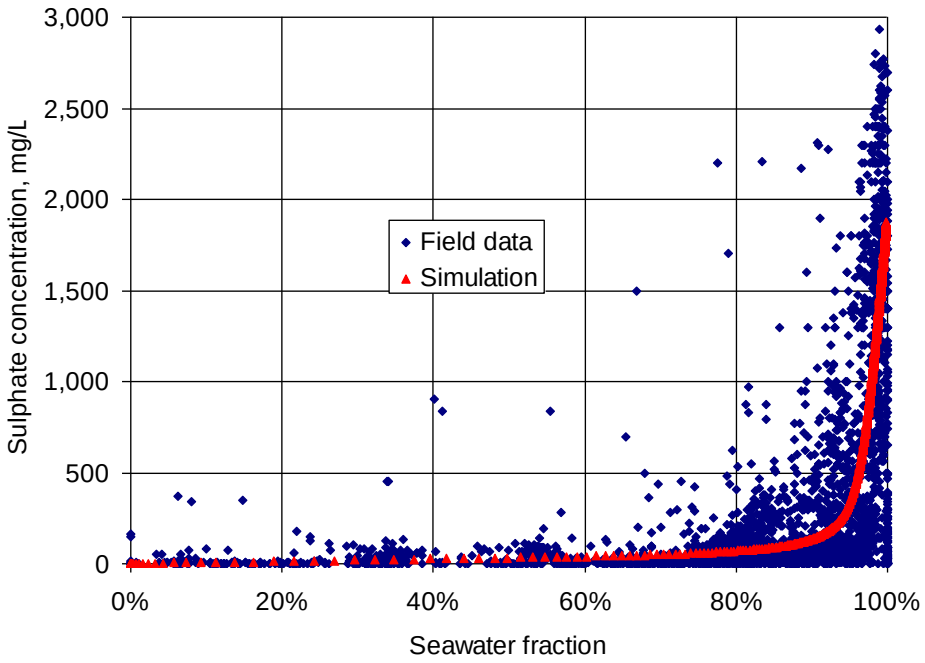


**Figure 64 – GEM simulated sulphate concentration compared with production data**

As can be seen from the Figure 64, there is a good agreement between simulated and field data, indicating that calcium sulphate precipitation is the main reaction responsible for sulphate stripping observed in the field data of reservoir G.

In order to evaluate the impact of calcium concentration on sulphate stripping, simulations were carried out at 80ºC, varying the formation brine calcium concentration. The sodium and chloride concentrations were 40000 and 60000 mg/L, respectively. The results are presented in the Figure 65.

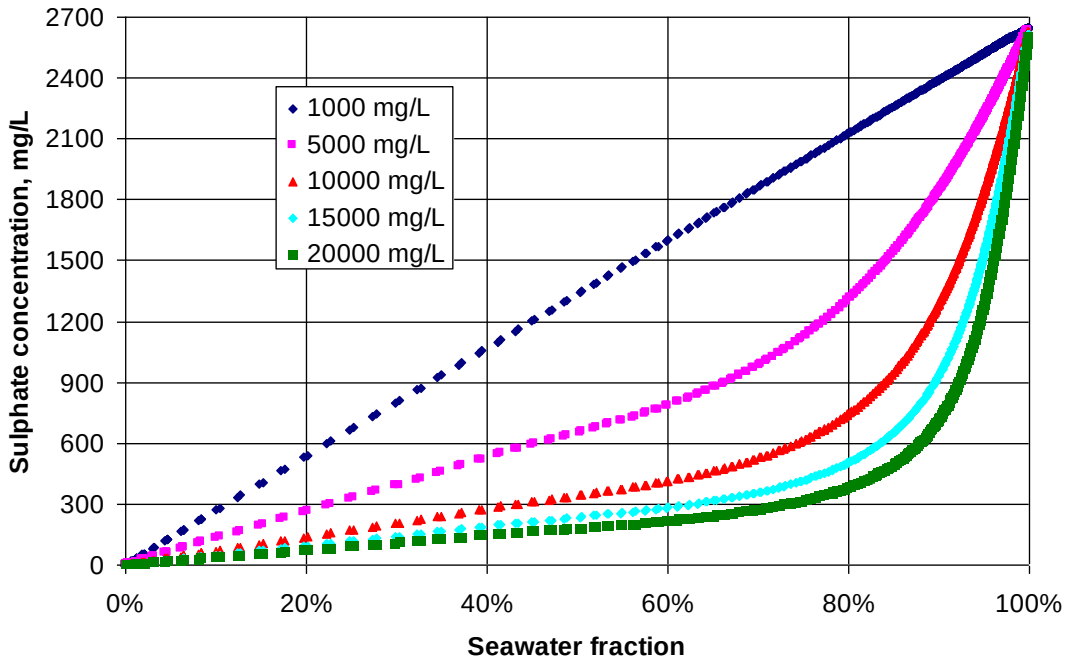


**Figure 65 – sulphate concentration for different calcium concentrations in the formation brine**

As can be observed in Figure 65, the simulation indicates that for calcium concentrations higher than 5000 mg/L, it is already possible to observe significant sulphate stripping.

The analysis presented in this section shows that for calcium sulphate precipitation has great impact on produced water composition, hence, to develop a scale management strategy for a field with formation brines containing high calcium concentrations, one should take into account sulphate stripping. It is important to mention that sulphate stripping inside the reservoir can delay, or even avoid the occurrence of sulphate scales in the production wells and the incorporation of geochemical reactions in the reservoir simulator can lead to an improved and more cost effective scale management strategy.

### 3.3.2 Precipitation inside the reservoir and in the near wellbore region

To evaluate the capability of the simulator to represent scale deposition around the production wells, a test case was simulated using data from Reservoir A (section 2.2). The grid used for the simulation is composed of cells with dimensions of 20x20x4 meters, consisting of a grid more refined than the one used in section 3.3.1, in order to capture effects occurring in the surroundings of the wellbore. The distance between

producer and injector well is of 1360 meters and the grid is composed of five vertical layers. The wells P1 and I1 are vertical wells fully penetrating the reservoir.

The geochemical reaction modeled in this study are (equation 43 to equation 45):

$$BaSO_{4-solid} \leftrightarrow Ba^{++}_{aqueous} + SO^{2-}_{4-aqueous} \quad (43)$$

$$SrSO_{4-solid} \leftrightarrow Sr^{++}_{aqueous} + SO^{2-}_{4-aqueous} \quad (44)$$

$$CaSO_{4-solid} \leftrightarrow Ca^{++}_{aqueous} + SO^{2-}_{4-aqueous} \quad (45)$$

The chemical equiblirium constant are represented by Equation 43. The parameters presented in Table 18 were obtained by fitting them to data published by Kharaka [70].

**Table 18 – Coefficients for calculating the chemical equilibrium constants**

| Reaction | $a_0$ | $a_1$ | $a_2$ | $a_3$ | $a_4$ |
|---|---|---|---|---|---|
| $CaSO_4$ | -4.2019 | 0.00184827 | -0.000230964 | 1.08082E-06 | -1.76423E-09 |
| $SrSO_4$ | -6.5216 | 0.00719088 | -0.000163447 | 5.76331E-07 | -8.53891E-10 |
| $BaSO_4$ | -10.5059 | 0.02799850 | -0.000270185 | 9.35558E-07 | -1.28636E-09 |

Figure 66 presents the dependency of the chemical equilibrium constants with temperature.

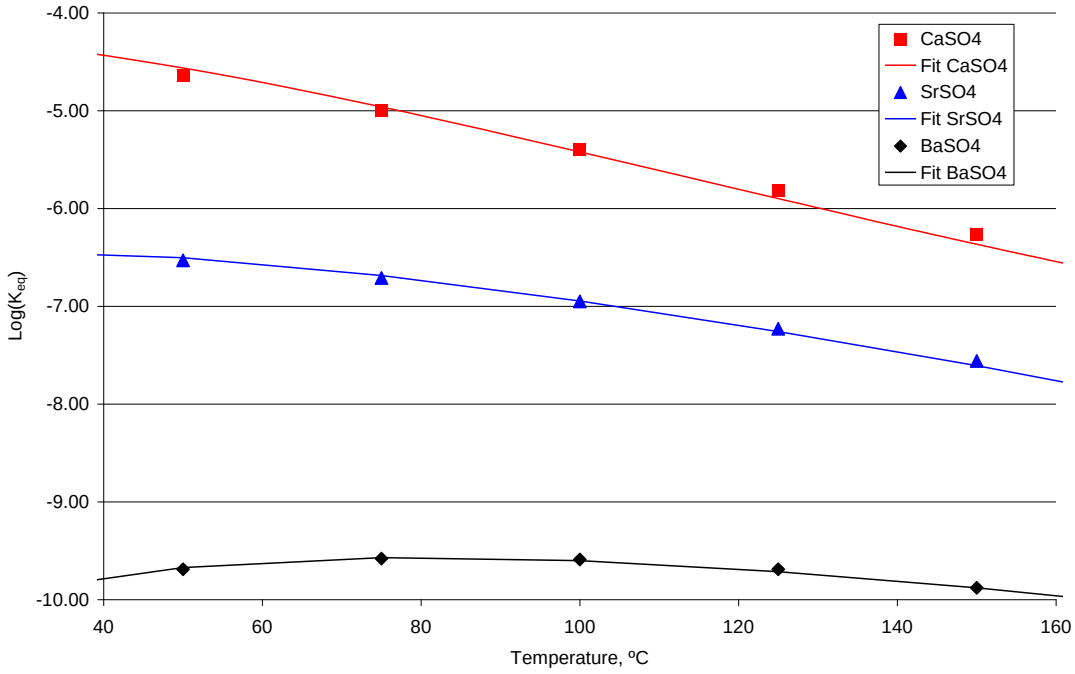


**Figure 66 - Chemical equilibrium constants.**

Due to the uncertainty in the kinetic parameters for barium and strontium sulphate precipitation, a sensitivity analysis was conducted to evaluate the impact of the kinetic parameters, namely, activation energy and reaction rate constant. The results of the sensitivity analysis indicated that for the grid used in this study, changes in the kinetic parameters caused no significant changes in the concentrations of ions and salts inside the reservoir.

Figure 67 and Figure 68 present the barium sulphate precipitation (gmol) inside the reservoir. Both pictures use the color scale presented in Figure 67. As the dimensions of the cells are the same, the amount of barium sulphate precipitation in the cell can be used to evaluate the intensity of precipitation inside the reservoir. Figure 67 presents a picture of the barium sulphate concentration in the base of the reservoir when the well reaches a watercut of 85%. It is important to mention that, for this example case, beyond this point, there are no significant variations in barium sulphate deposition inside the reservoir. As can be seen from Figure 67, the point of highest scale precipitation occurs around the producer well.

From Figure 68, which presents a section between wells I1 and P1, it is possible to observe that most of the precipitation happens at the base of the reservoir. This

phenomenon can be explained by gravitational effects that lead to greater water throughput in the base of the reservoir, leading to greater barium sulphate precipitation.

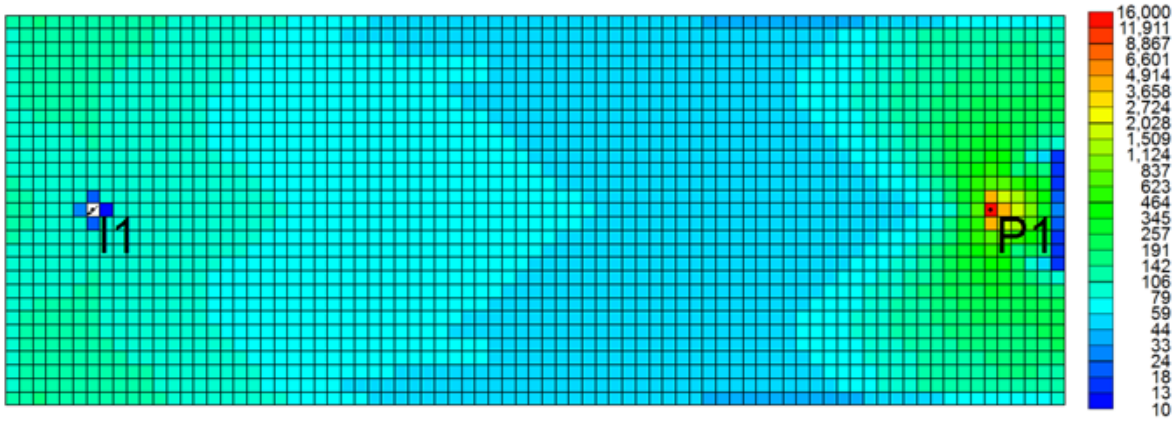


**Figure 67 – Plan view of the reservoir base, showing barium sulphate deposition in gmol.**

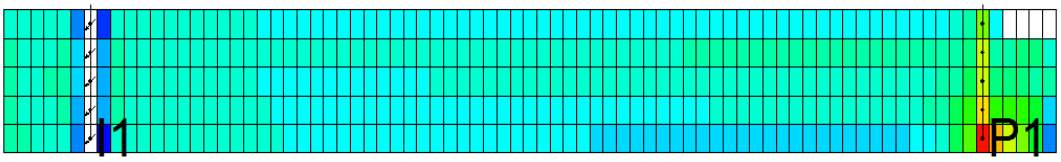


**Figure 68 – Section view of the reservoir between the wells, showing barium sulphate deposition in gmol.**

In order to better understand why most of the precipitation happens around the producer well, Figure 69 illustrates the stream-lines of water flow inside the reservoir. As expected, there is a significant convergence of the stream-lines around the producer well, that leads to a mixing of brines containing different concentrations of barium and sulphate, causing the scale deposition. The closer to the production well, the greater the convergence of the stream-lines, then the greater the tendency for to incompatible brines to mix. In addition the brine volume throughput per unit volume of rock increases as the stream-lines convergence, and for these two reasons scale build up increases as fluids approach produces wells. The corollary is that is the stream-lines diverge away for the injection well, mixing reduces. Scale damage to a pure seawater injector well has never been reported.

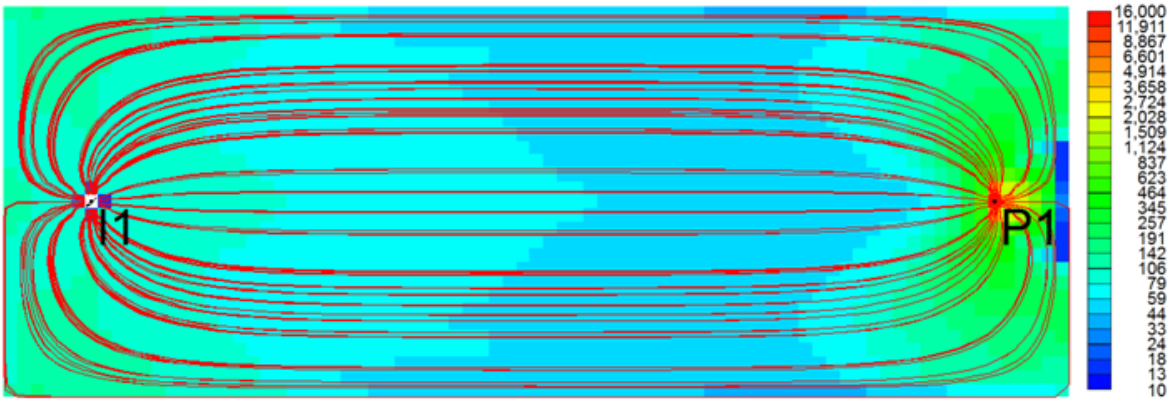


**Figure 69 – Plan view of the reservoir base, showing the stream lines and barium sulphate deposition in gmol.**

The precipitation of strontium sulphate was similar to barium sulphate, the main difference being the fact that over long times, there is dissolution of the precipitaded SrSO4 around the injector well. This dissolution can be seen in Figure 70 and was caused by contact of the scale with undersaturated injected water. This dissolution is also influenced by higher solubility constants at lower temperatures (Figure 66); the simulations indicate a reduction of temperature around the injector well with time.

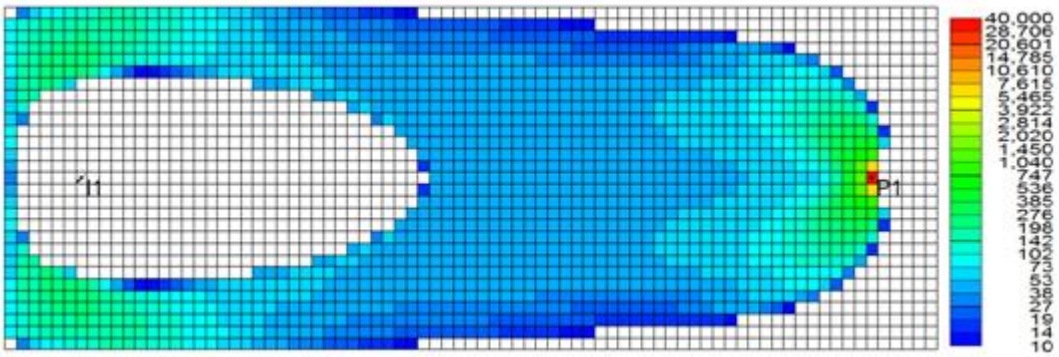


**Figure 70 – Plan view of the reservoir base, showing the strontium sulphate precipitation (gmol) and dissolution.**

## 3.4 ASPECTS REGARDING THE CONSTRUCTION OF MODELS

In this section, the main difficulties regarding the use of reservoir simulators to forecast scale deposition as well as the uncertainties related to reservoir characterization are going to be discussed.

First of all, kinetic data are rarely available for oilfield scaling reactions, and thus laboratory experiments must be conducted to generate them. It must then be identified if the rock/fluid interactions under the reservoir conditions are rate limited. Second, it is important to mention the difficulties arising from modeling the kinetics of precipitation of insoluble salts. All these aspects only add more uncertainty in the already complicated reservoir simulation.

The validation of models is complicated due to the difficulty in obtaining observed data, either from the laboratory or from the field. The starting point for the validation of any option available in the reservoir simulator is that it there is a reliable geological characterization of the reservoir. In the case of historical data from the wells, it is essential that the simulation results show a reasonable fit for the fluids produced or injected, especially water. The pressure in the wells also needs to be adjusted, for instance, the pressure in the PDG (permanent downhole gauge). In the case of scale, the problem is worse because the concentrations of ions in the produced brine also need to be adjusted. These ions act as tracers that can undergo complex reactions as they move through the reservoir or when they are near the wellbores. In the case of adjusting the produced brine composition, it may require a more detailed geological characterization, with a consequent refinement of the reservoir simulation, which can cause a significant increase in processing time of the simulation.

It is also important to mention that for most fields, black-oil models are used. This model was not designed for reactions. Therefore, there is an additional complicating factor in scale simulation, because it is necessary, in most of the cases, to convert the reservoir models from one simulator to another (for example, from ECLIPSE [63] to GEM [67]). Thus, the modeling of the phenomena can also be compromised by the conversion of models.

Finally, taking into account chemical reactions in the simulations may make it difficult to obtain numerical convergence, mainly when the volume of the cells is reduced. In very refined models, the porosity variations in the vicinity of the wellbore can be large, making it necessary to use very small time steps to avoid the occurrence of numerical errors and obtain accuracy in the solution. This is another challenge in the simulation of scale deposition and chemical reactions in petroleum reservoirs.

Hence, how can one use simulation to predict scale in a specific field, especially in fields in the project phase? The idea presented here to address this question is broken down into certain steps. First of all, it is important to review data from fields with similarities regarding scale potential and, if possible, build one robust and refined model in a reaction simulator. It is fundamental to calibrate the reactions with data from the analogue field or from a group of similar fields; an important point here is to prioritize the match of the phenomenon in deferment of the production rates.

In the following chapter, reservoir properties beyond the scale potential predicted by thermodynamical models will be discussed, as well as the incorporation of scale history in the scale management strategy, aiming to establish analogies between the reservoir that can be useful for predictions of scale potential at the producer wells.

# CHAPTER 4: FIELD DATA INCORPORATION ON THE SCALE MANAGEMENT STRATEGY

Despite of a large number of softwares available as scale predicting tools, the prognostic of sulphate scale proved to be a difficult task in oilfield operations. This occurs mainly due to many chemical and hydrodynamic factors such as temperature, pressure, ionic strength, flow velocity, brine composition, etc. Lack of information about the whole problem associated to uncertainty noticeably complicate the facing situation. Despite of these problems if the reservoir simulator is properly selected it will insure a better integration with processes that involve chemical reactions providing better predictions and ways of optimizing the scale management process.

In this chapter, some possibilities to incorporate field data into scale management strategy are proposed. This activity can be useful for decision making in the project execution phase (equipment and well design) as well as during production, allowing for improvements to the scale management approach.

The incorporation of field data can be done in two ways: (1) using an analogue reservoir; (2) using data from the actual field.

## 4.1 USE OF AN ANALOGUE RESERVOIR

Evidently, the first step in the development of a scale management strategy that takes into account analogue reservoirs is to choose a representative analogue that is able to represent the main aspects related to the in situ precipitation of salts.

According to the Society of Petroleum Engineers [81], "an analogous reservoir is one in the same geographic area that is formed by the same, or very similar geological processes as, a reservoir in question (or under study for reserves evaluation) as regards sedimentation, diagenesis, pressure, temperature, chemical and mechanical history, and structure. It also has the same or similar geologic age, geologic features, and reservoir rock and fluid properties". Analogous features and characteristics can include approximate depth, pressure, temperature, reservoir drive mechanism, original fluid

content, oil gravity, reservoir size, gross thickness, pay thickness, net-to-gross ratio, lithology, heterogeneity, porosity and permeability. The development scheme for a reservoir (e.g. as reflected by well spacing) can also be important in establishing the relevance of the analogy. Analogue Reservoir should be identified by a properly selected multidisciplinary team (Petroleum Engineer, Geologist and Geophysicist).

The results presented in Chapter 2 showed that the SR obtained by direct mixing of formation and injection brines is insufficient to compare the scale potential of different reservoirs, in such a way that other parameters need to be established to determine a representative analogue.

With the aim of illustrating a case in which the comparison of only the SR leads to erroneous conclusions, Figure 71 presents two fields in which the SR indicates a similar barium sulphate scale potential.

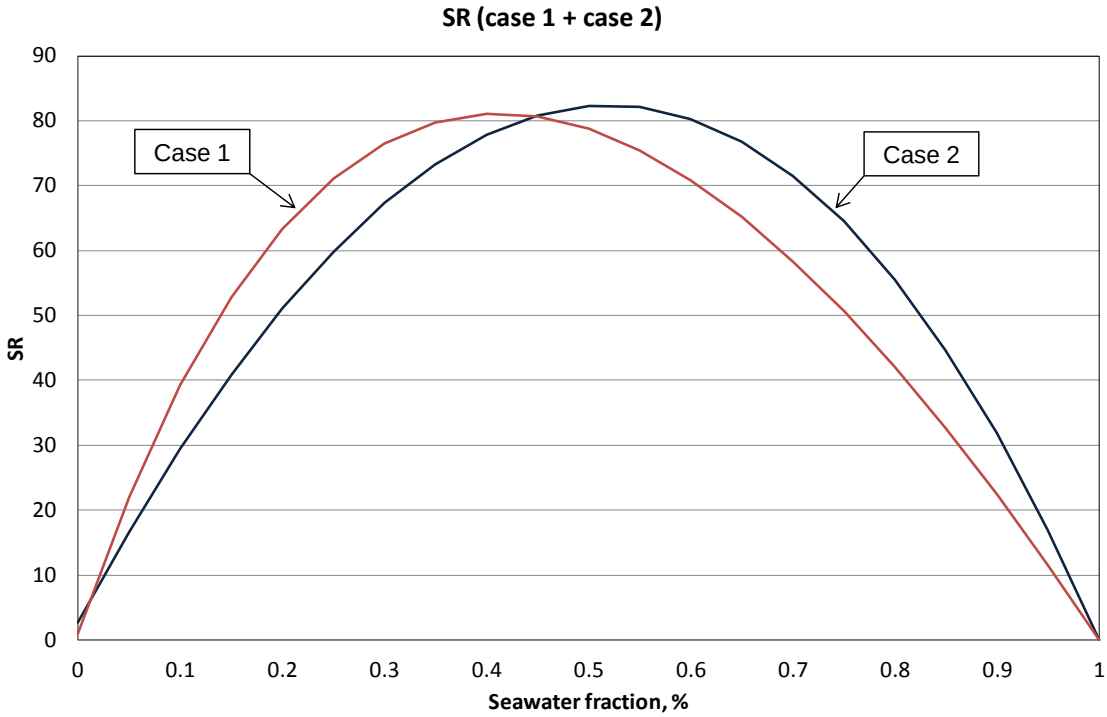


**Figure 71- Comparison of saturation ratio between two reservoirs.**

The two reservoirs in question in Figure 71 have long production histories. However, Case 1 (red line) experienced production losses due to barium sulphate precipitation and in Case 2 (black line) production losses due to scaling were not observed, despite the absence of any scale prevention technique. Such different behaviors for reservoirs with similar SRs occurs because of the reactions deep inside the reservoir, pointing to the

fact that other characteristics of the reservoir should be considered when selecting an analogue reservoir. Other parameters that may be evaluated are:

a) Connate water saturation and aquifer presence

Taking into account that the injection water continuously provides the same ion concentration throughout the entire reservoir production time, generally, there is a large availability of ions present in the injected water, in such a way that the ions present in the formation brine (e.g. Ba, Sr, Ca, etc) are in many cases the limiting reagents for precipitation of salts within the reservoir. The amount of formation water present in the reservoir (connate water saturation and presence of aquifers) has a good correlation with the duration of co-production of incompatible brines, which determines how long the producer well will be susceptible to scale damage. From these considerations, it is clear that the connate water saturation plays an important role in the scaling potential definition of oilfields. Considering this, for reservoirs similar in all other aspects except the connate water saturation, it is expected that the reservoir with higher connate water saturation will face a higher scaling risk.

It is important to remember that these considerations do not apply in cases where the ions present in the formation water are not the limiting reagents, for example, where the aquifer is the main recovery mechanism and in some cases where there is significant produced water re-injection.

To illustrate the aspects mentioned previously, a compositional reservoir simulation was performed using GEM, considering a producer/injector pair in reservoirs where the only difference is the connate water saturation ($S_{wi}$ = 15, 20, 25, and 30%). Figure 72 shows the cumulative mass of $BaSO_4$ precipitated inside the whole reservoir for different values of $S_{wi}$.

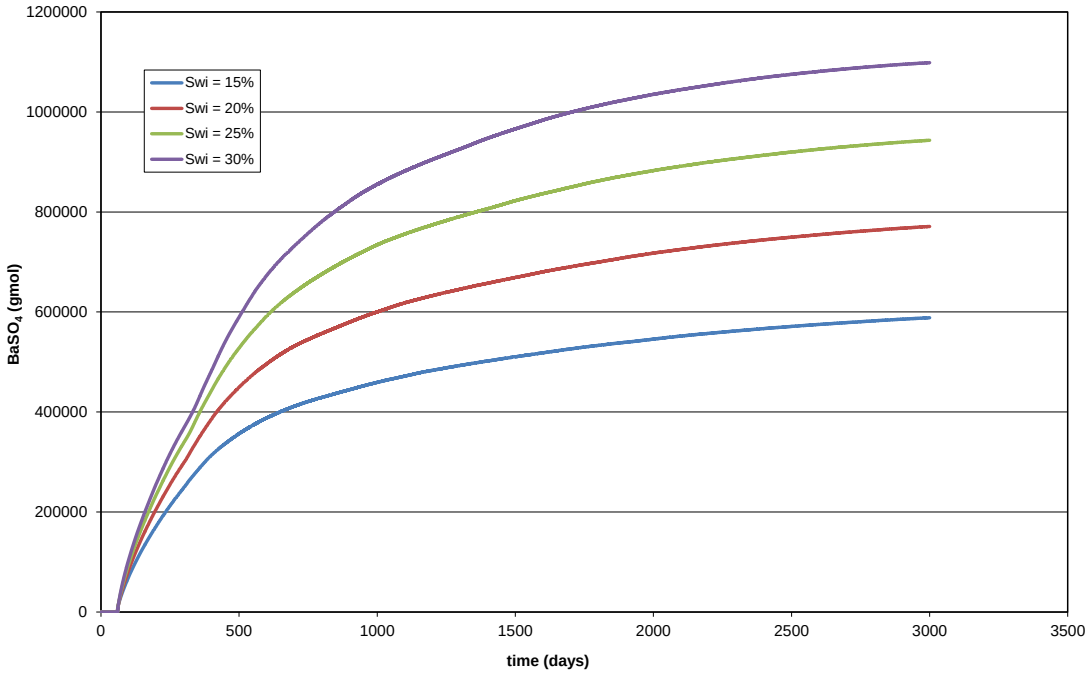


Figure 72 – Cumulative mass of $BaSO_4$ precipitated inside the whole reservoir.

The analysis of Figure 72 indicates an approximately linear relationship between the connate water saturation ($S_{wi}$) and the total mass of $BaSO_4$ precipitated inside the reservoir. On the other hand, this linear relationship is not observed in the well, as can be seen from Figure 73, which presents the mass of $BaSO_4$ precipitated in the base cell of the producer well as a function of time for different values of $S_{wi}$.

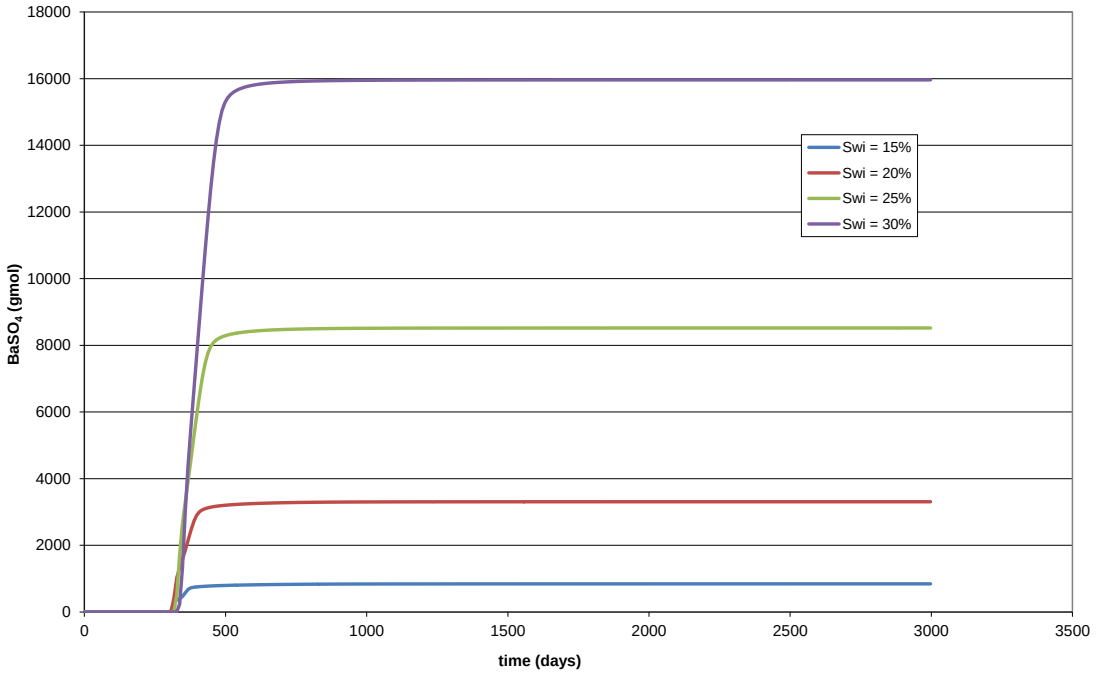


Figure 73 – Cumulative mass of $BaSO_4$ precipitated in the base cell of the producer well

It is clear from Figure 73 that the mass precipitated increases with increasing $S_{wi}$, but, the influence of $S_{wi}$ is stronger than the linear relationship found in Figure 72. These observations show that it is very important to properly evaluate the impact of the connate water saturation on the development of the scale management strategy. This is an expected result since the formation water is rich in barium, and the seawater injection is a continuous sulphate supplier.

b) Reservoir drainage strategy (well placement)

The placement of the wells inside the reservoir can completely change the scaling potential in the producer wells. In a drainage strategy in which many injectors support the same producer, the scale risk will be different than if the drainage strategy is based upon producer/injector pairs. In the first case there is a higher chance that brines with different composition will reach the producer well at the same time, increasing the scale precipitation risk.

Another relevant situation related to the impact of well placement on scale risks occurs when the injection wells are placed inside the aquifer. In these cases, the mixing of incompatible brines near the producer well can be considerably delayed, thus,

prolonging the production time without scale precipitation around or in the producer well. On the other hand, if a producer well is supported by two injectors, one being placed in the oil zone and the other in the aquifer, the scaling potential can be greatly increased because of the mixing of large amounts of incompatible waters near the producer well for prolonged periods of time.

To properly establish this analogy, it is necessary to evaluate the situation of each well individually, and in some cases, it can be necessary to use reservoir simulators to identify the similarities. For example, in section 3.1 (Figure 59), it is shown that the size of the transition zone for wells in the same reservoir can be completely different, this difference being caused by well placement.

c) Vertical heterogeneities

Reservoirs that have significant vertical stratification are proned to have an increased scaling potential in the producer well, due to the mixing of brines with different compositions directly in the well. To evaluate the analogy, it is recommended to analyze wells logs and cores.

To illustrate the impact of vertical heterogeneities in the scale potential at the producer well, simulations were performed with GEM considering synthetic reservoirs with different vertical permeabilities. The flowrates of both wells (producer and injector) were the same in all simulations and the reservoir was composed of three homogeneous layers. Both wells are completed in the three layers of the reservoir. The permeabilities of the layers were (from top to bottom): 1, 3 and 5 Darcy. Figure 74 shows the saturation ratio in the well for the three hypothetical cases described previously. Figure 74 was elaborated using the output of molar concentration given by GEM and the SR was calculate based on a Multiscale simulation and the 3D surface methodology described in chapter 2.

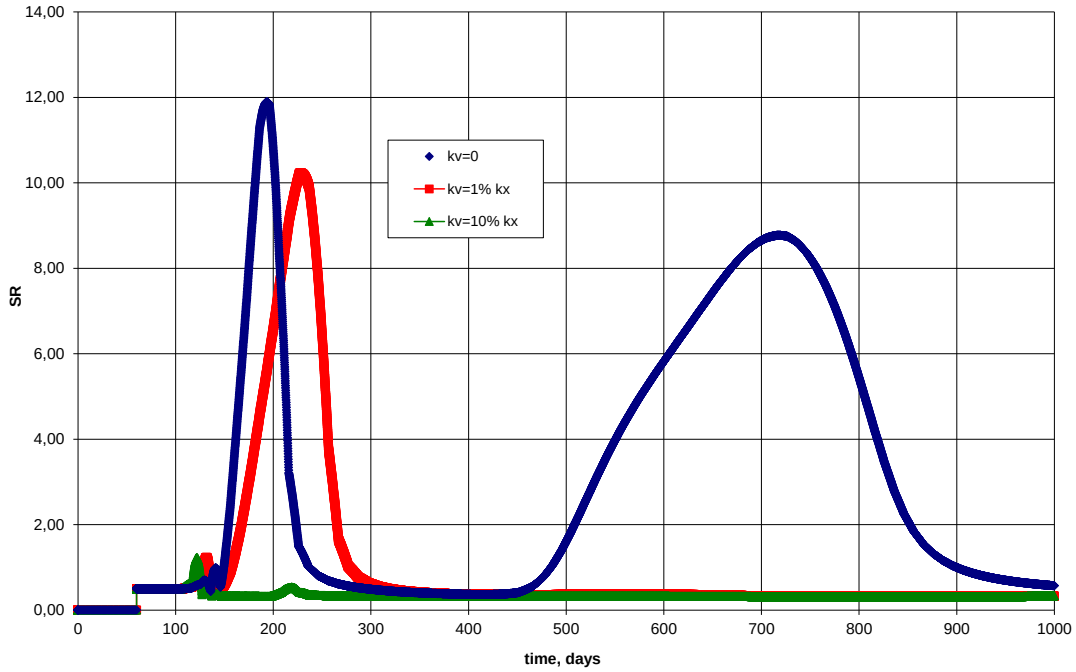


**Figure 74 – Impact of vertical permeability on the $BaSO_4$ Saturation Ratio at the producer well.**

As can be seen in Figure 74, the vertical permeability has a remarkable effect on the saturation ratio in the produced brine. The reservoirs with lower vertical permeability present the higher SR, leading to higher risk of scale damage, due to the breakthrough of brines with different compositions during the well´s lifetime. It can also be observed in this example that when the vertical permeability is zero, there are two critical moments for scaling due to the different times for water breakthrough on each layer.

d) Reservoir temperature and Calcium concentration;

As mentioned in Chapter 2: and in section 3.3.1, the reservoir temperature plays an important role in calcium sulphate precipitation. Figure 62 shows the dependence of the CaSO4 equilibrium constant with temperature. For high temperature reservoirs with a high calcium concentration in the formation brine, CaSO4 precipitation causes significant sulphate stripping, reducing the scaling potential.

e) Reservoir permeability, porosity and mineralogy:

Reservoir mineralogy may have a significant impact on the brine composition. Some reservoirs tend to be more reactive than others, for instance, a sandstone with high

feldspar content or a carbonate reservoir interact more with the brine than a very clean quartzitic sandstone. Thus, the reservoirs which interact more with the brine tend to attenuate the variations in brine composition over time.

Regarding the impact of permeability on the scaling potential, it is difficult to establish a direct relationship. In theory, variations in permeability and the presence of fractures can affect the contact surface between the rock and the fluid, the degree of turbulence and pressure variations experienced by the fluids.

Ideally, to select an analogue field or well, all the issues mentioned above should be considered. It is clear that this is a difficult task and the team responsible for the scale management strategy should establish simplifications in order to select representative analogues, resorting to reservoir simulations when necessary.

After the selection of one or more analogue reservoirs, one can incorporate these data to elaborate the scale management strategy and attain a more realistic forecast of the scale potential in each well. A straight forward approach is to use reservoir simulators (Chapter 3) to fit the produced brine composition from the analogue field and obtain the main parameters related to the chemical reactions. This strategy was employed in section 3.2. After matching the data, fitted parameters can be used to forecast the scale risk, estimate the scale occurrence window for each well, and develop an optimized scale management strategy for the field being studied.

An example of the use of the proposed methodology is presented below. The objective of this study was to develop the scale management strategy of Field C (section 2.4) based on historical data and flow characteristics of Reservoir X, which was considered an appropriate analogue. Both fields are managed by seawater flooding.

Table 19 shows a comparison of some characteristics of Reservoirs X and C.

**Table 19 – Reservoirs X and C parameters.**

| | Reservoir X | Reservoir C |
|---|---|---|
| Temperature | 78ºC | 75ºC |
| Reservoir type | Unconsolidated sandstone | Unconsolidated sandstone |
| Initial reservoir pressure | 305 kgf/cm$^2$ | 302 kgf/cm$^2$ |
| Swi | 30% | 30% |
| aquifer | insignificant | insignificant |
| Lay-out of wells | Injector x productor pair (1 front) | Injector x productor pair (1 front) |
| Vertical Heterogeneities | Sandstone interbedded with clay comprising several layers | Sandstone interbedded with clay composing several layers |

Reservoir X suffered severe production losses due to $BaSO_4$ deposition. Beyond the similarities observed in Table 19, it is fundamental to evaluate the SR of both reservoirs. Reservoir C presents a $Ba^{2+}$ concentration higher than Reservoir X, leading to a higher SR, confirming the elevated risk of scale occurrence in Reservoir C

The simulator STARS [65] was used to fit the history of produced brine composition from Reservoir X and obtain the parameters related to the chemical reactions. After doing this, the Reservoir C flow model was set up with these parameters to evaluate the scaling tendency. The results indicated that ion stripping inside the reservoir is significant, reducing the scale potential at the producer well. Another result observed in the analogue, Reservoir C, is that the critical period for scaling is immediately after water breakthrough, when the seawater content is still low (as can be seen in Figure 75). Taking this into account, an optimized scale management strategy was developed. This strategy entailed the periodic deployment of scale inhibitor squeeze operations immediately after water breakthrough, and the MIC would be higher at the beginning of the period of water production and would then be reduced with increasing seawater content in the produced brine. Another recommendation of this study was to evaluate the application of scale inhibitor impregnated proppant in the gravel pack for new wells

in Reservoir C, with the aim of preventing production losses immediately after water breakthrough. Continuous inhibitor injection via umbilical and capillary tubing in the downhole completion was also evaluated. To develop a proper scale management plan, it is important to evaluate, in addition to the scale inhibitor efficiency, other aspects such as those presented by Bezerra [73], which include a list of requirements that the inhibitor needs to meet for continuous injection in deepwater satellite wells.

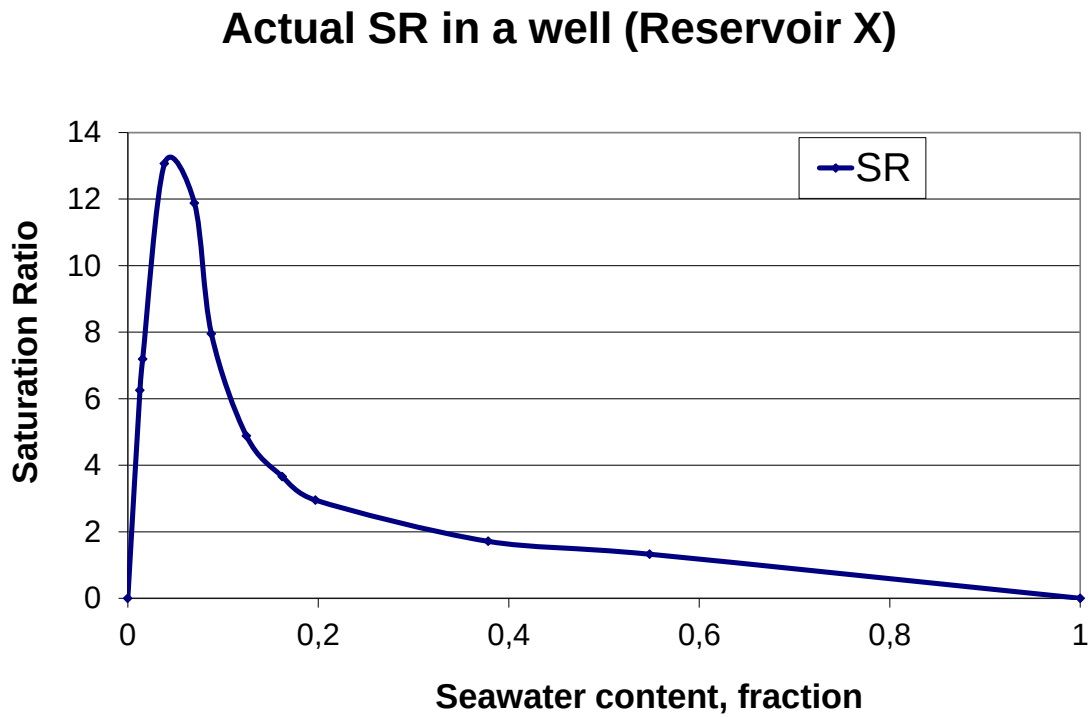


**Figure 75- Saturation ratio versus seawater content after the effect of sulphate stripping.**

The choice of Reservoir X as an analogue proved to be a good choice. The production history that is being observed in Reservoir C is in good agreement with the forecasts realized based upon data from Reservoir X. As a consequence, the scale management strategy employed is successful, prevents the production losses that occurred in Reservoir X from happening in Reservoir C, due to the systematic application of an appropriate scale inhibition plan as will be described in the next section.

## 4.2 INCORPORATION OF HISTORY DATA ON SCALE MANAGEMENT

Rather than using data from an analogue field, it is better to use, if available, data from the field itself for which the scale management strategy is being developed.

A good example of the use of these data is Reservoir X, presented in the last section. At the beginning of production, severe production losses were caused by $BaSO_4$ precipitation. Aiming to mitigate these losses, a clear scale inhibition plan was implemented, with the result that production losses were avoided.

Initially, aiming to operate in a conservative way, the MIC was determined by considering the maximum SR obtained by mixing the formation and injected brines, which led to a high frequency of scale inhibitor squeezes. Based on analysis of the produced water composition, it was verified that the ionic composition was very different from what would be expected only by dilution of the brines. These results were used to match the parameters related to chemical reactions in STARS [65] and a good fitting of the produced brine composition was obtained. Using these results, the MIC was recalculated based upon the verified produced brine compositions, leading to a more realistic value, which led to a lower frequency of scale inhibitor squeezes, reducing operational costs and avoiding production losses due to temporarily well shut-in. Figure 76 presents the inhibitor concentration on the produced brine as a function of time.

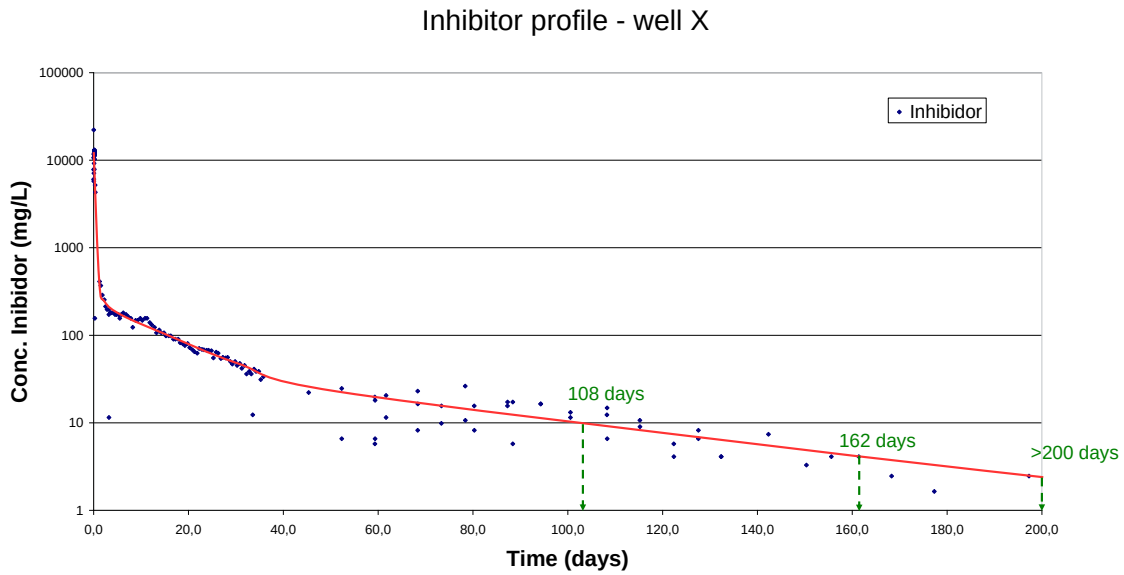


**Figure 76 – Inhibitor profile in the well X**

The noteworthy consequence of the applied reservoir management plan is that the reduction in the SRs causes a reduction in the MIC, hence the squeeze lifetime increases. Figure 76 shows that if one uses the MIC of 10 ppm, which is obtained by

ignoring the reservoir effect in the brine composition, the squeeze lifetime is approximately 110 days; on the other hand, after reservoir stripping, the squeeze lifetime may be longer than one year. The reservoir management team has conservatively been applying inhibitor squeeze treatments every six months, taking into account the reservoir effect on the produced brine composition, but also recognizing that scale inhibitor placement may not always be ideal, and hence allowing some contingency. Since 2006, when this technique was implemented, the number of treatments was reduced by half because of this approach. It is important to state that no production loss attributable to scale was observed during this time, even when the inhibitor concentration was below 10 ppm. Downhole pressure data collected by the PDG reinforce that no well has experienced loss of productivity.

# CHAPTER 5: CONCLUSIONS AND RECOMMENDATIONS

Good monitoring associated with a careful analysis of the produced brine composition, especially after inhibitor squeezes, can provide interesting insights into the chemical reactions that occur inside the reservoir. In all the cases studied in this work, the geochemical processes occurring in the reservoir cause a reduction in the scaling potential in the near wellbore area; in some cases the reduction was dramatic and it was shown that some inhibitor squeezes were possibly unnecessary for sulphate scale prevention.

It was also observed that because of the reservoir effect described, the MIC can be reduced, increasing the squeeze lifetime and reducing operational costs. The representative brine composition, after passing through the reservoir, can be used in order to determine a more realistic value for the MIC. This study can have a positive impact on reservoir management, reducing operational costs, minimizing the damage risk and increasing production by reducing the shut in time of the producer wells. This technique has been used successfully in reservoirs A and C.

The effect of reservoir reactions on the produced brine can completely change the timing of when highest risk occurs in terms of scaling tendency as a function of seawater content. Thus, the maximum scale potential can be found at seawater fractions different than those predicted by direct mixing of brines. Depending on the type of reactions that are taking place inside the reservoir, the peak of SR may be earlier (eg Reservoirs A and C) or later (cases presented with calcium sulphate precipitation deep in the reservoir).

It was observed in all the reservoirs studied with temperatures above 120ºC and calcium concentration in the formation brine above 7000 mg/l, that the potential for sulphate scale precipitation in the near wellbore is dramatically reduced because of calcium sulphate precipitation deep in the reservoir. This is an important phenomenon, at least until high seawater fractions are observed in the produced brine. However, the real limits of calcium concentration/reservoir temperature should be better determined with further field data - i.e. the thresholds may be lower than 120ºC and 7000 mg/l. The author considers that for reservoirs with these characteristics, the use of sulphate

reduction plant (SRP) needs to be carefully evaluated in order to avoid unnecessary expenses.

Although reactive flow simulation in reservoirs is a big challenge, the author believes that some of these issues can be overcome by studying a wide range of reservoir types. Understanding of specific reservoir patterns can improve the scale predictions, or at least, can generate scale predictions that are better than only using thermodynamic simulation based on a direct mix of brines. The authors also understand that this is an important step to be taken in order to obtain more realistic scale prediction for the oil industry.

This work introduced the use of a 3D surface to obtain estimates of SR taking into account different degrees of ion stripping in the reservoir. The 3D surface can help the reservoir management team to understand the impacts of ion stripping on the scaling tendency, and also simplifies studies where a large number of simulations are necessary. This approach facilitates the automation of SR calculation when several simulations are necessary, and allows one to compare the impact of different reservoir reaction processes.

The results presented in this dissertation clearly show the importance of reviewing produced brine composition data in mature oilfields; this is especially valuable when the same field has wells at different stages of maturity. Thus, it is possible to use data from the mature wells to obtain an optimized scale management plan for the new wells. Hence, analyzing the produced brine composition data is the key to understanding the main chemical reactions inside the reservoir allowing the scale management strategy to be optimized.

The data also emphasize that magnesium should not be used as tracer to identify seawater fraction, since it is involved in reactions.

The results obtained by the numerical simulations, mainly when using GEM [67], presented extremely consistent results, indicating an increase in the precipitation of inorganic salts in places where there is a convergence of the flowlines. Simulations made with cell dimensions of 20 x 20 x 4 meters showed that the brine reaches the well

in chemical equilibrium and the scaling is caused by mixing of waters with different compositions coming from different directions in the reservoir.

Reservoir numerical simulation, mainly using GEM [67], proved to be a useful tool to evaluate the scale potential in the production wells and these results suggest that numerical simulation can be used to perform uncertainty analysis regarding the scale risks, by changing the parameters related to the chemical reactions.

It is important to emphasize that an integrated team, including chemists, engineers, and geoscientists is fundamental for successful scale management.

In all the cases studied, the more evident stripping was that of the barium ion, and the magnitude of the stripping varied from field to field but clearly occurred in all of them. Strontium was another ion that underwent stripping in most of the cases. In reservoirs with a temperature above 90ºC and significant calcium concentrations, it was observed that the calcium ion plays an important role in the chemical reactions inside the reservoir, causing significant sulphate stripping when full seawater was injected. Sulphate stripping was only significant in these cases or when the formation brine has a concentration of Ba/Sr that, in terms of molarity, is comparable to the sulphate concentration in the seawater.

## 5.1 RECOMMENDATIONS FOR FUTURE WORK

The recommendations that come from the observations and conclusions obtained in this work are summarized below:

- Develop a database with produced brine compositions from various fields to increase the knowledge of the factors governing scale precipitation and to provide a wider variety of data from which to choose the analogue reservoirs.
- Due to the lack of availability of information regarding the kinetic parameters, it is recommended lab experiments be performed with the aim to evaluate these parameters under reservoir conditions. These data are important for the numerical simulations;

- Evaluate the results of other fully compositional simulators in order to compare advantages and disadvantages amongst them;
- Realize studies in order to evaluate the interactions that happen between magnesium and the brine/rock, as the results identified that it is clear that further developments are necessary to understand the factors governing magnesium behavior;
- It is recommended to deepen the studies using GEM [67] with a higher grid refinement around the wellbore in order to assess the near wellbore behavior of the ionic concentration and precipitation of salts.

# CHAPTER 6: REFERENCES

[1] – “The water Supply of London”. Journal the Lancet (31 July 1869) - volume 94, issue 2396, pages 160-161.

[2] – “Some points in the London water Supply”. Journal the Lancet (1 October 1898) - volume 152, issue 3918, page 886.

[3] – Washburne, C. W.: “Chlorides in Oil-Field waters”. Paper number 915687-G. Published in Transactions, AIME, Volume 48, 1915, pages 687-694.

[4] – Panyity, L. S.: “Valuation of properties in the Bradford District”, Petroleum Transactions, AIME, Volume G-26, 1926, pages 235-240.

[5] – Umpleby, J. B.: “Increasing the Extraction of Oil by Water Flooding”. Petroleum Development and Technology in 1925. 112. AIME, Pamphlet No. 1570-G.

[6] – Schilthuis, R.J.: “Connate water in oil and gas sands”. In: Petroleum Development and Technology, AIME, pp 199-214, 1938.

[7] – Stiff, H. A., Davis, L. E.: “A Method for Predicting the Tendency of Oil Field Waters to Deposit Calcium Sulphate,” Petr. Trans. AIME, 195, (1952), 25-28.

[8] – Crawford, P. B.: “Scale Forming Waters, Part I,” Producers Monthly, (October 1957), 15.

[9] – Featherson, A. B., Mihram, G. R., Waters, A. B.: “Minimization of Scale Deposits in Oil Wells by Placement of Phosphates in Producing Zones,” J. Petr. Tech., 11, (1959), 29-32.

[10] – https://sites.google.com/site/petroleumhistoryresources/Home/offshore-oil-history (accessed 11 May 2011).

[11] – http://www.em.gov.bc.ca/OG/offshoreoilandgas/Pages/OffshoreOilandGasAroundtheWorld.aspx (accessed 20 May 2011).

[12] – Glater, J., York, J. L., Campbell, K. S.: “Principles of Desalination, Second Edition, Part B” Chapter 10 – Scale formation and Prevention, pg 627. 1980.

[13] – Poetker, R. G. and Stone, J.D.:” Squeeze Inhibitor into Formation”, Pet. Eng. (1956) 28, No. 5, B-29.

[14] – Kerver, J. K., Heilhecker, J. K.: “Scale Inhibition by the Squeeze Technique”. The Journal of Canadian Petroleum Technology, January-March, 1969, Montreal.

[15] – Sorbie, K. S.: “A General Coupled Kinetic Adsorption / Precipitation Transport Model for Scale Inhibitor Retention in Porous Media: I Model formulation”, SPE 130702 presented at the SPE International Conference on Oilfield scale held in Aberdeen, United Kingdom, 26-27 May 2010.

[16] – Vazquez, O., Sorbie, K. S., Mackay, E.J.: “A General Coupled Kinetic Adsorption / Precipitation Transport Model for Scale Inhibitor Retention in Porous Media: II Sensitivity Calculations and Field Predictions”, SPE 130703 presented at the SPE International Conference on Oilfield scale held in Aberdeen, United Kingdom, 26-27 May 2010.

[17] – Liburkin, V.G., Kondratev, B.S., Pavlykoa, T.S.: “Action of Magnetic Treatment of water on the Structure Formation of Gypsum”. Glass and Ceramics. 1986.

[18] – Donaldson, J., Grimes, S.: “Control of Scale in Sea Water Applications by Magnetic treatment of Fluids”, SPE 16540, SPE Offshore Europe, 8-11 September 1987, Aberdeen, United Kingdom.

[19] – Higashitani, K., Kage, A., Katamura, S, Imai, K., Hatade, S.: “Effect of a Magnetic Field on the Formation of CaCO3 Particles”. Journal of Colloid and Interface Science. Volume 156, 1993, pp 90-95.

[20] – Barrett, R.A., Parsons, S.A.: “The influence of Magnetic fields on Calcium Carbonate Precipitation”. Water research. 1998. Vol. 32, pp 609-612.

[21] – Farshad, F. F., Linsley, J., Kuznetsov, O., Vargas, S.: “The effects of Magnetic Treatment on Calcium Sulfate Scale Formation”. SPE 76767. SPE Westem Regional/AAPG Pacific Section. Anchorage, Alaska, U.S.A., 20-22 May 2002.

[22] – Plummer, M. P.: “Preventing Plugging by Insoluble Salts in a Hydrocarbon-Bearing Formation and Associated Wells”. U.S. Patent No. 4723603 (1988), U.K. Patent No. 2221700.

[23] – Khatib, Z., Verbeek, P.: “Water to Value – Produced water Management for Sustainable Field Development of Mature and Green Fields”, SPE 73853, SPE International Conference on Health, Safety and Environment in Oil and Gas Exploration and Production, Kuala Lumpur, Malaysia, 20-22 March 2002.

[24] – Veil, J.A., Clark, C.E.: “Produced Water Volumes and Management Practices”. SPE 125999. SPE International Conference on Health, Safety and Environment in Oil and Gas Exploration and Production, Rio de Janeiro, Brazil, 12-14 April 2010.

[25] – Mackay, E. J.; Jordan, M. M.; Feasey, N. D.; Shah, D.; Kumar, P.; Ali, S. A.: “Integrated Risk Analysis for scale management in deepwater developments”, SPE 87459, SPE International Symposium on Oilfield Scale, Aberdeen, U.K., May 2004.

[26] – http://www.merusonline.com/in-general/water-containing-calcium-carbonate, (accessed 07 May 2011).

[27] - http://www.quantummicromet.co.uk/images/calcium_carbonate_crystals.jpg, (accessed 07 May 2011).

[28] – Souza, A. L. S.: “Relatório Interno Petrobras”. Rio de Janeiro, Brasil. 2006.

[29] – Puntervold, T., Austad, T.: “Injection of seawater and mixtures with produced water into North Sea chalk formation: Impact of fluid-rock interactions on wettability and Scale formation”. Journal of Petroleum Science and Engineering (July 2008) 63 - 23-33.

[30] – Collins, I. R.; Duncum, S.D.; Jordan, M.M.; Feasey, N.D.: “The Development of a Revolution Scale-Control Product for the Control of Near-Well Bore Sulphate Scale

Within Production Wells by the Treatment of Injection Seawater", SPE 100357, SPE International Oilfield Scale Symposium, 31 May-1 June 2006, Aberdeen, UK

[31] – Kaasa, B. 1998. Prediction of pH, Mineral Precipitation and Multiphase Equilibria During Oil Recovery. Program presented at the Norwegian University of Science and Technology.

[32] – Yuan, M.D., Todd, A.C.: "Prediction of Sulphate Scaling Tendency in Oilfield Operations", Journal of Petroleum Science and Engineering (February 1991) - volume 6, Number 1 pages 63-72.

[33] – Webb, P.J., Kuhn, O.: "Enhanced Scale Management through the Application of Inorganic Geochemistry and Statistics" paper SPE 87458 presented at the SPE 6th International Symposium on Oilfield Scale, Aberdeen, Scotland, 26-27 May 2004.

[34] - Li, Y.H., Crane, S.C., Scott, E.M., Braden, J.C., Lelland, W.G.: "Waterflood Geochemical Modeling and Prudhoe Bay Zone 4 Case Study". Journal of Petroleum Science and Engineering (March 1997) - volume 2 58-69.

[35] - Mackay, E.J., Sorbie, K.S, Kavle, V., Sørhaug, Melvin, Sjursaether, Jordan, M., 2006, "Impact of In-Situ Sulphate Stripping on Scale Management in the Gyda Field", paper 100516 presented at the SPE International Symposium on Oilfield scale, Aberdeen, Scotland, 30 May-1 June 2006.

[36] – Korsnes, R. I., Strand, S., Hoff, Ø., Petersen, T., Madland, M. V., Austad, T., 2006. DOES the Chemical Interaction between Seawater and Chalk Affect the mechanical properties of Chalk? EUROCK 2006 – Multiphysics Coupling and Long Term Behaviour in Rock Mechanics. Taylor & Francis Group, London0 41541001 0.

[37] – Zenger, D.H , Dunham, J.B. : "Concept and Models of Dolomitization – An introduction 1-9 in Concepts and Models of Dolomitization". SEPM Spec. Pubn, No.28, Tulsa, 1980.

[38] – Houston, S. J., Yardley, B. W. D., Smalley, P. C., Collins, I.: "Precipitation and issolution of Minerals During Waterflooding of a North Sea Oil Field", SPE 100603, SPE International Oilfield Scale Symposium, 30 May-1 June 2006, Aberdeen, UK.

[39] – Puntervold, T., Austad, T., Journal of petroleum Science and Engineering 63 (2008) 23-33.

[40] – Dyer, S. J., Graham, G. M.: "The effect of temperature and pressure on oilfield scale formation", Journal of Petroleum Science and Engineering 35 (2002) 95-107.

[41] – Vetter, O.J., Philips, R.C.: "Prediction of Calcium sulphate Scale Under down hole Conditions". J. Pet. Tech 1299-1308. October 1970.

[42] – Atkinson, A., Mecik, M.: "The Chemistry of Scale Prediction". Journal of Petroleum Science and Engineering 17 pp. 113-121 (1997).

[43] – Onyenezide, P. B.: "Evaluation of the Influence of Brine Composition of Mixed scaling Brine Systems". MSc Petroleum Engineering, Project Report 2009/2010, Heriot Watt University.

[44] – Waage, P., Guldberg, C. M.: "Studies Concerning Affinity". Forhandlinger: Videnskabs - Selskabet i Christinia (Norwegian Academy of Science and Letters): 35, 1864.

[45] – Bedrikovetsky, P. G., Lopes Jr., R. P., Rosario, F. F., Bezerra, M. C., Lima, E. A.: "Oilfield Scaling – Part I: Mathematical and Laboratory Modelling". SPE 81127, SPE Latin American and Caribbean Petroleum Engineering conference, Port-of-Spain, Trinidad, 27-30 April 2003.

[46] – Perkins, T.K., Johnston, O.C.: "A Review of Diffusion and Dispersion in Porous Media". SPE 480. SPE Journal Volume 3, Number 1 pages 70-84, March 1963.

[47] – Lake, L. W.: "Enhanced Oil Recovery". Englewood Cliffs, New Jersey: Prentice hall, 1989.

[48] – Mackay, E.J.: "Predicting In-Situ Sulphate Scale Deposition and the Impact on Produced Ion Concentrations", Trans IChemE (March 2003) 81 (A) 326-332.

[49] - Mackay, E.J. and Sorbie, K.S.: "Brine Mixing in Waterflooded Reservoirs and the Implications for Scale Prevention" paper SPE 60193 presented at the SPE 2nd International Symposium on Oilfield Scale, Aberdeen, Scotland, 26-27 January 2000.

[50] - Sorbie, K. S. and Mackay, E.J.: “Mixing of injected, connate and aquifer brines in waterflooding and its relevance to oilfield scaling”, Journal of Petroleum Science and Engineering (july 2000) 27 (1-2) 85-106.

[51] - Paulo, J., Mackay, E.J., Menzies, N.A. and Poynton, N.: “Implications of brine Mixing in the Reservoir for Scale Management in the Alba Field” paper SPE 68310 presented at the SPE 3rd International Symposium on Oilfield Scale, Aberdeen, Scotland, 30-31 January 2001.

[52] – Fawzy, T., Mackay, E.J.: “The Application of Streamline Reservoir Simulation Calculations to the management of Oilfield Scale” paper SPE 119605 presented at the SPE Middle East Oil & Gas show and conference, Bahrain, 15-18 March 2009.

[53] - Mackay, E.J.: “Modelling of In-Situ Scale Deposition: the Impact of Reservoir and Well Geometries and Kinetic Reaction Rates” paper SPE 81830, SPE Prod. & Facilities (February 2003) 18 (1) 45-56.

[54] – Tahmasebi, H. A., Azad, U., Kharrat, R.: “Prediction of permeability Reduction Due to Calcium Sulfate Scale Formation in Porous Media”. SPE 105105, 15th SPE Middle East Oil & Gas Show and Conference, Bahrain, Kingdom of Bahrain, 11-14 March 2007.

[55] - Mackay, E.J., Jordan, M.M. and Torabi, F.: “Predicting Brine Mixing Deep within the Reservoir, and the Impact on Scale Control in Marginal and Deepwater Developments” paper SPE 85104, SPE Prod & Facilities (Aug 2003) 18 (3) 210-220.

[56] – Jordan, M.M., Johnston, C.J., O’Brien, T.M., Hopwood, P.: “Integrate Field Management to allow Effective Scale Control during the Water cycle in Mature Oil Field”. Paper 06394 presented at the NACExpo Corrosion 61st annual conference & exposition, Houston, USA, 2006.

[57] – Mackay, E. J., Jordan, M. M., Torabi, F.: “Predicting Brine Mixing Deep Within the Reservoir, and the impact on Scale Control in Marginal and Deepwater Developments”, SPE 73779, SPE International Symposium and Exhibition on Formation Damage Control, Lafayette, Louisiana, U.S.A., February 2002.

[58] – Paulo, J., Mackay, E. J.: “Modelling of In-Situ Scale Deposition” presented at 12th International Oil Field Chemical Symposium, Geilo, Normay, 1-4 April 2001.

[59] - Gomes, R.M., Deucher, R.H., Aniceto, P.H.S., Silva, F.A.M., Prais, F., Skinner, R.: “Scale Management Strategy and its Results in a Giant Deepwater Oilfield in Capos Basin”. Paper SPE 131013 presented at the SPE International Symposium on Oilfield Scale, Aberdeen, Scotland, 26-27 May 2010.

[60] – Bertero, L., Chierici, G. L., Gottardi, G., Mesini, E., Mormino, G.: “Chemical equilibrium models: their use in simulating the injection of incompatible waters”. SPE Reservoir Engineering 288-294, February 1988.

[61] - Ishkov, O., Mackay, E.J., Sorbie, K. S.: “Reacting Ions Method to Identify Injected Water Fraction in Produced Brine”. Paper SPE 121701 presented at the SPE Oilfield Chemistry Symposium, The Woodlands, Texas, 20-22 April 2009.

[62] – Austad, T., Strand, S., Madland, M. V., Puntervold, T., & Korsnes, R. I.: “Seawater in Chalk: An EOR and Compaction Fluid”. Society of Petroleum Engineers. doi:10.2118/118431-PA. August 1, 2008.

[63] – ECLIPSE, reservoir simulation software, reference manual, Schlumberger, 2010.

[64] – IMEX, Advanced Oil/Gas Reservoir Simulator, User’ guide, CMG – Computer Modeling Group Ltd, 2010.

[65] – STARS, Advanced process and thermal reservoir simulator, User’ guide, CMG – Computer Modeling Group Ltd, 2010.

[66] – S. Arrhenius, Z. Phys. Chem., 4, 226(1889).

[67] – GEM, Advanced Compositional and GHG Reservoir Simulator, User’s guide, CMG – Computer Modeling Group Ltd, 2010.

[68] - Helgeson, H.C.: “Thermodynamics of hydrothermal systems at elevated temperatures and pressures”. Am J Sci, 267: 729-804. 1969.

[69] – Steefel, C.I., Lasaga, A.C.: “A coupled model for transport of multiple chemical species and kinetic precipitation/dissolution reactions with application to reactive flow in single phase hydrothermal systems”. Am J Sci, 294(5): 529-592. 1994.

[70] – Kharaka, Y. K., Gunter, W. D., Aggarwal, P. K., Perkins, E. H., DeBraal, J. D.: “A Computer Program for Geochemical Modeling of Water-Rock Interactions”, U.S. GEOLOGICAL SURVEY, Water-Resources Investigations Report 88-4227. Menlo Park, California 1988.

[71] – Kontrec, J., Kralj, D., Brecevic, L.: “Transformation of anhydrous calcium sulphate into calcium sulphate dihydrate in aqueous solution”, Journal of Crystal Growth 240 (2002) 203-211.

[72] – Serafeimidis, K., Anagnostou, G.: “On the kinetics of the chemical reactions underlying the swelling of anhydritic rocks”, ETH Zurich Eurock 2012.

[73] – Bezerra, M. C. M., Rosario, F. F., & Rosa, K. R. S. A.: “Scale Management in Deep and Ultradeep Water Fields”. Offshore Technology Conference. doi:10.4043/24508-MS. (October 29, 2013).

[74] – OLI. 2013. OLI ScaleChem , http://www.olisystems.com/new-scalechem.shtml. (Accessed 21 Jan 2016).

[75] – Kan, A.T., X. Wu, G. Fu, and M.B. Tomson. "SPE 93264 Validation of Scale Prediction Algorithms at Oilfield Conditions", Proc., 2005 SPE International Symposium on Oilfield Chemistry, Houston, TX (2005).

[76] – Pitzer, K.S. 1980. “Thermodynamics of Aqueous Electrolytes at Various Temperatures, Pressures and Compositions”, ACS Symposium Series 133, S.A. Newman (ed.)

[77] – Pitzer, K.S. 1983. “Thermodynamics of Electrolyte Solutions over the Entire Miscibility Range”, Chem. Eng. Thermodynamics, S.A. Newman (ed.), Butterworths, England.

[78] – Xu, T., Spycher, N., Pruess, K. . TOUGHREACT user’s guide: A simulation program for non-isothermal multiphase reactive geochemical transport in variably saturated geologic media. Lawrence Berkeley National Laboratory Report LBNL-55460, 2004.

[79] – Bethke, C.M.: “Geochemical and Biogeochemical reaction modeling” Cambridge University Press, 2008.

[80] – Pitzer, K. S, Brewer, L. Lewis, G.N., Randall M., Thermodynamics 2nd ed., (1961), McGraw-Hill

[81] – https://definedterm.com/analogous_reservoir (accessed 18 Oct 2016).